

2-9-2011

Investigations into late transition metal pincer complexes as possible direct partial oxidation catalysts

Raymond B. Lansing Jr

Follow this and additional works at: https://digitalrepository.unm.edu/chem_etds



Part of the [Physical Chemistry Commons](#)

Recommended Citation

Lansing, Raymond B. Jr. "Investigations into late transition metal pincer complexes as possible direct partial oxidation catalysts." (2011). https://digitalrepository.unm.edu/chem_etds/7

This Dissertation is brought to you for free and open access by the Electronic Theses and Dissertations at UNM Digital Repository. It has been accepted for inclusion in Chemistry ETDs by an authorized administrator of UNM Digital Repository. For more information, please contact disc@unm.edu.

Raymond B. Lansing Jr.

Candidate

Chemistry and Chemical Biology

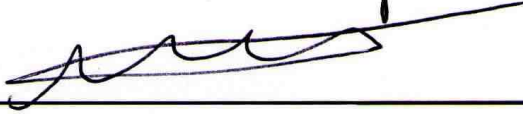
Department

This dissertation is approved, and it is acceptable in quality and form for publication:

Approved by the Dissertation Committee:



, Chairperson



Robert J. Paine Jr.

John B. Cunn

**Investigations Into Late Transition Metal Pincer Complexes as Possible
Direct Partial Oxidation Catalysts**

BY

Raymond B. Lansing Jr.

B.S., Chemistry, The University of New Mexico, 2002

DISSERTATION

Submitted in Partial Fulfillment of the
Requirements for the Degree of

**Doctor of Philosophy
Chemistry**

The University of New Mexico
Albuquerque, New Mexico

December, 2010

**Investigations Into Late Transition Metal Pincer Complexes as
Possible Direct Partial Oxidation Catalysts**

BY

Raymond B. Lansing Jr.

ABSTRACT OF DISSERTATION

Submitted in Partial Fulfillment of the
Requirements for the Degree of

**Doctor of Philosophy
Chemistry**

The University of New Mexico
Albuquerque, New Mexico

December, 2010

**INVESTIGATIONS INTO LATE TRANSITION METAL Pincer COMPLEXES
AS POSSIBLE DIRECT PARTIAL OXIDATION CATALYSTS**

BY

Raymond B. Lansing Jr.

B.S., Chemistry, The University of New Mexico, 2002
Ph. D., Chemistry, The University of New Mexico, 2010

ABSTRACT

This investigation examined aspects of a potential catalytic route for the partial oxidation of organic substrates using molecular oxygen as the oxidant. The proposed cycle begins with the insertion of molecular oxygen into a metal hydride bond to generate a metal hydroperoxide. The next step involves the transfer of an oxygen atom to an acceptor substrate to generate an oxidized species and a metal hydroxide. The starting metal hydride can then be regenerated in two viable ways, either through use of CO or H₂. The experimental plan involved the syntheses and characterization of new inorganic and organometallic complexes, and it focused on PCP and related pincer ligand systems bound to Group 9 and 10 transition metal hydrides as the potential catalyst. A prominent feature of these pincer complexes is the opportunity for modification of their electronic and steric properties.

The first part of the research involved the generation of pincer metal hydrides based on a neutral ligand (PNP) as compared to its anionic counterpart

(PCP). Several new PNP-Rh-H complexes were prepared and their reactions with molecular oxygen were investigated. Unfortunately, the isolation of a rhodium hydroperoxide was not achieved. The investigation reveals that these Rh(I) species are unstable and decompose immediately when allowed to react with molecular oxygen.

Another PNP system was investigated in order to expand options for the potential catalytic cycle. In this case, an Ozerov-type anionic PNP ligand was used to synthesize Group 10 pincer metal hydrides. Several new symmetric PNP-M-H (M = Ni, Pd, Pt) complexes were prepared and characterized. Modification of these PNP ligands was accomplished, resulting in new unsymmetric and racemic chiral ligands and metal complexes. Several of these PNP-Pd-H complexes have been shown to react with molecular oxygen to generate palladium hydroperoxides. The oxygen atom transfer ability of these complexes was investigated through reaction with several organic substrates. As yet, however, no evidence has been observed to indicate partial oxidation via oxygen atom transfer.

TABLE OF CONTENTS

List of Figures	viii
List of Tables	xi
List of Schemes	xii
List of Abbreviations	xiv
Chapter 1	1
1.1 Potential Catalytic Route for Partial Oxidation of Organic Substrates..	1
1.2 Pincer Ligands	7
1.3 Applications of Pincer Ligands.....	9
1.3.1 Heck Reaction.....	10
1.3.2 Suzuki-Miyaura Coupling	14
1.3.3 Hydrogen Transfer Catalyst	16
1.3.4 Alkane Dehydrogenation.....	18
1.3.5 Asymmetric Allylic Alkylation Catalysts	20
Chapter 2	21
2.1 Attempted Synthesis of PNP-Rh-H with Commonly-Used Hydrides ..	21
2.2 Alternative Route to PNP-Rh-H Complexes.....	33
2.3 Reactions with O ₂	42
2.4 Concluding Remarks.....	46
2.5 Experimental.....	47
2.5.1 General Experimental	47
2.5.2 Crystallographic Determination	48
2.5.3 Synthesis of Rhodium Compounds.....	49

Chapter 3	54
3.1 Syntheses of Symmetric PNP Free Ligands and Complexes	54
3.2 Syntheses of Unsymmetric PNP Free Ligands and Complexes	67
3.3 Oxidative Addition Reactions	84
3.4 Racemic Chiral PNP ligands and complexes	92
3.5 Reactions with O ₂ and Attempted Oxygen Transfer Reactions	106
3.6 Concluding Remarks	112
3.7 Experimental	113
3.7.1 General Experimental	113
3.7.2 Crystallographic Determination	114
3.7.3 Synthesis of PNP ligands and complexes	115
Final Remarks	132
Appendix	135
References and Notes	142

List of Figures

Figure 1. Examples of Pincer Ligands	8
Figure 2: Modification Options of Pincer Ligands	9
Figure 3. Heck Coupling Catalysts	12
Figure 4. Pd-SCS Heck Catalysts.....	13
Figure 5. PNP-based Heck Catalysts	14
Figure 6. Suzuki-Miyaura Catalysts	16
Figure 7. Hydrogen Transfer Catalysts.....	17
Figure 8. Thermal Ellipsoid Plot of 29 Shown at 50% Probability Level with Hydrogens Omitted for Clarity.....	28
Figure 9. Thermal Ellipsoid Plot of 30 Shown at 50% Probability Level with Hydrogens Omitted for Clarity.....	30
Figure 10. Thermal Ellipsoid Plot of 31 Shown at 50% Probability Level with Hydrogens Omitted for Clarity.....	35
Figure 11. Ball and Stick Plot of 34 Shown at 50% Probability Level with Hydrogens Omitted for Clarity.....	38
Figure 12. Examples of PNP-based Ligands.....	55
Figure 13. Thermal Ellipsoid Plot of 45 Shown at 50% Probability Level with Hydrogens Omitted for Clarity.....	57
Figure 14. Thermal Ellipsoid Plot of 48 Shown at 50% Probability Level with Hydrogens Omitted for Clarity.....	61
Figure 15. Thermal Ellipsoid Plot of 53 Shown at 50% Probability Level with Hydrogens Omitted for Clarity.....	66

Figure 16. Thermal Ellipsoid Plot of 56 Shown at 50% Probability Level with Hydrogens Omitted for Clarity.....	69
Figure 17. Thermal Ellipsoid Plot of 58 Shown at 50% Probability Level with Hydrogens Omitted for Clarity.....	72
Figure 18. Thermal Ellipsoid Plot of 60 Shown at 50% Probability Level with Hydrogens Omitted for Clarity.....	75
Figure 19. Thermal Ellipsoid Plot of 59 Shown at 50% Probability Level with Hydrogens Omitted for Clarity.....	77
Figure 20. Thermal Ellipsoid Plot of 61 Shown at 50% Probability Level with Hydrogens Omitted for Clarity.....	79
Figure 21. Thermal Ellipsoid Plot of 63 Shown at 50% Probability Level with Hydrogens Omitted for Clarity.....	83
Figure 22. Thermal Ellipsoid Plot of 67 Shown at 50% Probability Level with Hydrogens Omitted for Clarity.....	88
Figure 23. Thermal Ellipsoid Plot of 68 Shown at 50% Probability Level with Hydrogens Omitted for Clarity.....	90
Figure 24. Examples of Chiral NCN Complexes.....	92
Figure 25. Examples of Chiral P-based Ligands	93
Figure 26. Thermal Ellipsoid Plot of 73 Shown at 50% Probability Level with Hydrogens Omitted for Clarity.....	95
Figure 27. Thermal Ellipsoid Plot of 74 Shown at 50%Probability Level with Hydrogens Omitted for Clarity.....	96

Figure 28. Thermal Ellipsoid Plot of 75 Shown at 50%Probability Level with Hydrogens Omitted for Clarity.....	98
Figure 29. Thermal Ellipsoid Plot of 76 Shown at 50% Probability Level with Hydrogens Omitted for Clarity.....	100
Figure 30. Thermal Ellipsoid Plot of 77 Shown at 50% Probability Level with Hydrogens Omitted for Clarity.....	103
Figure 31. Thermal Ellipsoid Plot of 78 Shown at 50% Probability Level with Hydrogens Omitted for Clarity.....	105
Figure 32. Ball and Stick Plot of ⁱ PrPNP-Pd-OOH	108

List of Tables

Table 1. Selected Bond Lengths and Angles for Compound 29	29
Table 2. Selected Bond Lengths and Angles for Compound 30	31
Table 3. Selected Bond Lengths and Angles for Compound 31	36
Table 4. Selected Bond Lengths and Angles for Compound 34	39
Table 5. Selected Bond Lengths and Angles for Compound 45	57
Table 6. Selected Bond Lengths and Angles for Compound 48	62
Table 7. Selected Bond Lengths and Angles for Compound 53	66
Table 8. Selected Bond Lengths and Angles for Compound 56	69
Table 9. Selected Bond Lengths and Angles for Compound 58	73
Table 10. Selected Bond Lengths and Angles for Compound 60	75
Table 11. Selected Bond Lengths and Angles for Compound 59	78
Table 12. Selected Bond Lengths and Angles for Compound 61	80
Table 13. Selected Bond Lengths and Angles for Compound 63	84
Table 14. Selected Bond Lengths and Angles for Compound 67	88
Table 15. Selected Bond Lengths and Angles for Compound 68	90
Table 16. Selected Bond Lengths and Angles for Compound 73	95
Table 17. Selected Bond Lengths and Angles for Compound 74	97
Table 18. Selected Bond Lengths and Angles for Compound 75	98
Table 19. Selected Bond Lengths and Angles for Compound 76	100
Table 20. Selected Bond Lengths and Angles for Compound 77	104
Table 21. Selected Bond Lengths and Angles for Compound 78	105

List of Schemes

Scheme 1. Direct Epoxidations Using Heterogeneous Catalysts	2
Scheme 2. Attempted Direct Oxidation of PO.....	3
Scheme 3. Commercial Production Routes to Propylene Oxide.....	5
Scheme 4. Proposed Catalytic Cycle for the Partial Oxidation of Organic Substrates.....	6
Scheme 5. Heck Reaction	10
Scheme 6. Suzuki-Miyaura Coupling.....	15
Scheme 7: Hydrogen Transfer Reaction	17
Scheme 8. Alkane Dehydrogenation Catalyst	19
Scheme 9. Asymmetric Allylic Alkylation Catalyst	20
Scheme 10. Preparation of PNP-based Ligands	22
Scheme 11. Preparation of PNP-based Ligands	23
Scheme 12. Preparation of PNP-based Ligands	23
Scheme 13. Direct Cyclometalation.....	24
Scheme 14. Various Metalation Techniques	26
Scheme 15. Preparation of ^{iPr} PNP-Rh-Cl 29 and ^{Cy} PNP-Rh-Cl 30.....	27
Scheme 16. Attempted Syntheses of PNP-Rh-H Complexes.....	32
Scheme 17. Preparation of ^{tBu} PNP-Rh-OTf 31, ^{iPr} PNP-Rh-OTf 32, and ^{Cy} PNP-Rh- OTf 33.....	33
Scheme 18. Preparation of [^R PNP-Rh(H) ₂][OTf].....	37
Scheme 19. Preparation of ^R PNP-Rh-H Complexes	41
Scheme 20. Synthesis of ^{tBu} PCP-Pd-OOH 41	44

Scheme 21. Attempted Syntheses of PNP Rh Hydroperoxides.....	45
Scheme 22. Preparation of ^{iPr} PNP 44, ^{Cy} PNP 45, and ^{Ph} PNP 46	56
Scheme 23. Preparation of ^{iPr} PNP-M-Cl and ^{Cy} PNP-M-Cl.....	60
Scheme 24. Preparation of ^{iPr} PNP-M-H and ^{Cy} PNP-M-H.....	64
Scheme 25. Preparation of ^{Ph} PNP ^{iPr} 56 and ^{Ph} PNP ^{Cy} 57.....	68
Scheme 26. Preparation of ^{Ph} PNP ^{iPr} -M-Cl and ^{Ph} PNP ^{Cy} -M-Cl	71
Scheme 27. Preparation of ^{Ph} PNP ^{iPr} -M-H and ^{Ph} PNP ^{Cy} -M-H.....	81
Scheme 28. Preparation of ^R PNP-Ni-H	86
Scheme 29. Preparation of Racemic Chiral PNP Ligands.....	94
Scheme 30. Preparation of Racemic PNP-based Metal Halides	102

List of Abbreviations

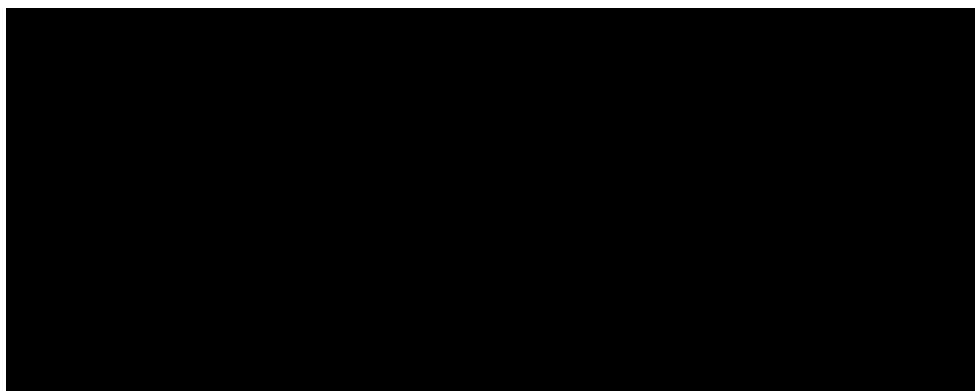
Ar	aryl
bs	broad singlet (NMR)
COD	cyclooctadiene
COE	cyclooctene
cy	cyclohexyl, -C ₆ H ₁₁
d	doublet (NMR)
dba	dibenzylideneacetone
dd	doublet of doublets (NMR)
diphoe	Ph ₂ PCH=CHPPh ₂
ee	enantiomeric excess
en	ethylenediamine
EO	ethylene oxide
et	ethyl, -CH ₂ CH ₃
IMes	mesityl/carbene ligand
IPA	<i>iso</i> -propyl alcohol
iPr	isopropyl, -CH(CH ₃) ₂
M	metal
m	multiplet (NMR)
Me	methyl, -CH ₃
MTBE	methyl <i>tert</i> -butyl ether
NMR	nuclear magnetic resonance
<i>o</i>	<i>ortho</i>
OTf	triflate anion, CF ₃ SO ₃ ⁻
<i>p</i>	<i>para</i>
PEG	polyethylene glycol
Ph	phenyl, -C ₆ H ₅
PO	propylene oxide
ppm	parts per million
R	organic substrate
RT	room temperature
s	singlet (NMR)
t	triplet (NMR)
tBu	<i>tert</i> -butyl, -C(CH ₃) ₃
td	triplet of doublets (NMR)
THF	tetrahydrofuran
TON	turnover numbers
Tp	trispyrazolylborate
vt	virtual triplet (NMR)

Chapter 1

1.1 Potential Catalytic Route for Partial Oxidation of Organic Substrates

A catalyst increases the rate of a reaction without itself being consumed. Catalytic processes have existed since 1836, when Jons Jakob Berzelius coined the phrase “catalysed processes” to describe this phenomena.¹ Today, catalysis generates billions of dollars worth of value-enhanced products worldwide.² While the field of catalysis is broad, one particular area of interest in catalysis and of high interest to the population is the generation of large-scale chemical products. Catalytic oxidation, via molecular oxygen, is one method used to generate a number of high-volume products such as nitric acid, sulfuric acid, terephthalic acid, acrylonitrile, and epoxides. The last class of chemicals is of particular interest to the fundamental work discussed in this dissertation. Epoxides are three-membered heterocyclic ethers that are highly strained, which makes them very reactive (due to ring opening) when compared to typical acyclic ethers. The two most important epoxides produced commercially are ethylene oxide (EO) and propylene oxide (PO). In 2009, 19 and 6 million tonnes of EO and PO were produced commercially worldwide.^{3, 4} The major uses for EO are in the synthesis of ethylene glycol (over 70% of EO is used for this) and in the syntheses of ethylene glycol ethers (brake fluid, detergents, and lacquers), ethanolamines (detergents), and ethoxylates (surfactants, emulsifiers, and dispersants). On a lesser scale, ethylene glycol is also used in the syntheses of polyesters and polyethylene terephthalate (plastics), liquid coolants, and solvents.

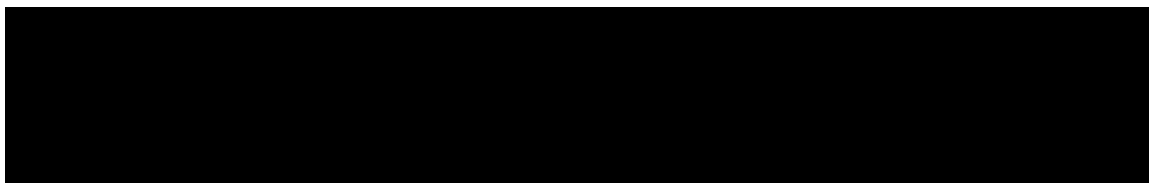
The major outlets (60-70%) for PO are in the synthesis of polyether polyols (polyurethane plastics) and in the synthesis of propylene glycol (solvents, moisturizers, and coolants), polypropylene glycol (polyurethanes), propylene glycol ethers (solvents), and propylene carbonate (solvents and adhesives). The synthesis of a majority of organic epoxides manufactured on an industrial scale involve multi-step processes that require oxidants other than molecular oxygen, with the notable exceptions of ethylene oxide (EO) and butadiene mono- and di-epoxides (BME, BDE).⁵ As shown in Scheme 1, EO and BME/BDE can be manufactured directly by using heterogeneous Ag-based catalysts prepared on low surface area α -Al₂O₃ supports.⁶ Improvements over the years to the heterogeneous system have led to selectivities to EO of approximately 90%.⁷⁻¹³



Scheme 1. Direct Epoxidations Using Heterogeneous Catalysts

However, this is not the case when attempting to directly epoxidize, with molecular oxygen and the identical heterogeneous Ag-based catalysts, propylene or higher olefins that possess allylic hydrogens. As shown in Scheme 2, oxidation occurs at the reactive allylic positions and leads to total combustion to CO₂ and water.^{14, 15} Despite the tremendous number of investigations by

academic and industrial laboratories into improving the production of PO, the need for a more efficient method remains.

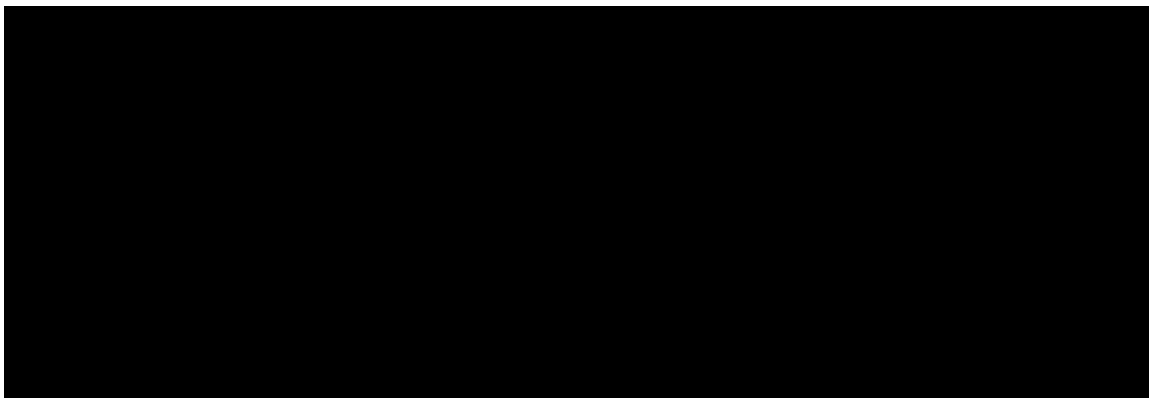


Scheme 2. Attempted Direct Oxidation of PO

Propylene oxide is currently produced commercially by one of two major routes (Scheme 3); however, novel routes to prepare PO without the production of co-products or use of environmentally-unfriendly chlorine are constantly being sought. The Cl-containing route employs chlorine to convert propylene to chloropropanol, which is then dehydrochlorinated to produce PO.¹⁶ This route is being used less and less due to environmental issues associated with chlorine, as well as high operating costs. A co-product route is much more common and involves the oxidation of selected organic compounds into organic peroxides, the active species that actually does the epoxidation of propylene.¹⁶ The two most common organic species used are isobutane and ethylbenzene, and these are transformed into their respective peroxides. After epoxidation occurs via oxygen transfer, either *tert*-butyl alcohol or hydroxyethylbenzene are generated as co-products. Markets must then be developed for these co-products in order to have an economical process. The major outlet for *tert*-butyl alcohol is in the production of methyl *tert*-butyl ether (MTBE), and in the case of hydroxyethylbenzene it can be dehydrated to form styrene and eventually lead to polystyrene. MTBE is prepared from *tert*-butyl alcohol and methanol and is a

gasoline additive. However, with the declining need for MTBE due to environmental issues, the need for *tert*-butyl alcohol also decreases.

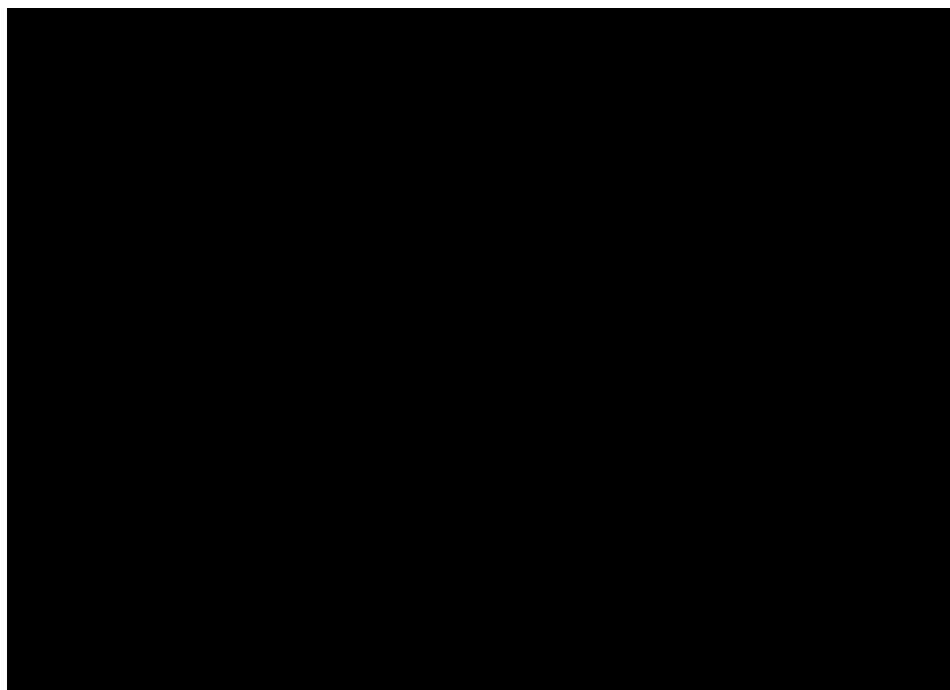
More recently, two novel routes have been developed to try to manufacture PO more efficiently. The first route is somewhat similar to the oxidation routes mentioned earlier. In this case, a cumene hydroperoxide is generated from cumene and also does the epoxidation of propylene.¹⁷ After losing the oxygen atom, cumyl alcohol is generated and is dehydrated to α -methyl styrene. This product can then be hydrogenated back to cumene, which is overall more efficient than the other oxidation routes as cumene is regenerated and a co-product business does not have to be developed. The second route employs a powerful and traditional oxidant (H_2O_2) to epoxidize propylene with water the lone co-product¹⁶. Only two commercial plants currently exist and are located in Belgium (Solvay/Dow-BASF) and in Korea (EvonikHeadwaters/SK Chemicals). However, the manufacture, transportation, and storage of hydrogen peroxide are relatively expensive and several safety issues also exist. Due to these issues of safety, co-products, and environmental-unfriendly, a more efficient method for production of PO is highly desired.



Scheme 3. Commercial Production Routes to Propylene Oxide

The proposed catalytic route shown below (Scheme 4) provides the basis for the research examined in this dissertation. The first step involves the generation of a new catalyst (L-M-H), followed by insertion of molecular oxygen into the M-H bond to produce a metal hydroperoxide (L-M-OOH). The next step details the transfer of an oxygen atom to an organic substrate to form an oxidized species and a metal hydroxide (L-M-OH). From this point, the metal hydride can then be regenerated in two potentially viable pathways. The first route involves the addition of CO to the L-M-OH resulting in a metal carboxylate or hydroxycarbonyl intermediate followed by decarboxylation of CO₂ to regenerate the starting metal hydride. Both of these reactions have precedent in a limited number of late transition metal complexes.¹⁸⁻²⁰ However, one drawback is associated with this particular reaction. While studies show that regeneration of the metal hydride is possible, the reinsertion of CO₂ into the M-H bond produces a stable formyl complex, which greatly hinders the success of the catalytic cycle as the metal formyl cannot eliminate CO₂.²¹ However, a second pathway has been proposed. The second route involves the oxidative addition of H₂ to the

metal hydroxide to generate an intermediate, followed by reductive elimination of water to regenerate the starting metal hydride. Once again, literature precedent exists for this alternative pathway including work from our research group using phosphorus-containing pincer palladium complexes.²²⁻²⁵ Mechanistically, it has been shown that the loss of water could also proceed via σ -bond metathesis rather than oxidative addition and reductive elimination.²⁶



Scheme 4. Proposed Catalytic Cycle for the Partial Oxidation of Organic Substrates

Several examples of epoxidation of olefins by metal hydroperoxides and peroxy complexes exist in the literature.²⁷ The majority of the work focuses on early transition metals, while reports of late transition metal epoxidation reactions remain scarce. The work detailed in this dissertation investigates the synthesis

and characterization of late transition metal complexes to act as possible catalysts in this proposed catalytic system.

1.2 Pincer Ligands

Initial investigations into a metal/ligand system ideal for this catalytic cycle have centered on metal pincer ligand complexes. Metal complexes containing pincer ligands have been known since the 1970's.²⁸⁻³¹ Generally, the pincer ligand consists of an anionic or neutral aryl ring with di*ortho*-substituted heteroatoms. All three donor atoms bind to the metal center in a meridional manner. This binding mode to the metal center generally determines the abbreviation for each pincer ligand, such as PCP, PNP, and SCS, denoting the atoms that serve as points of attachment to the metal.

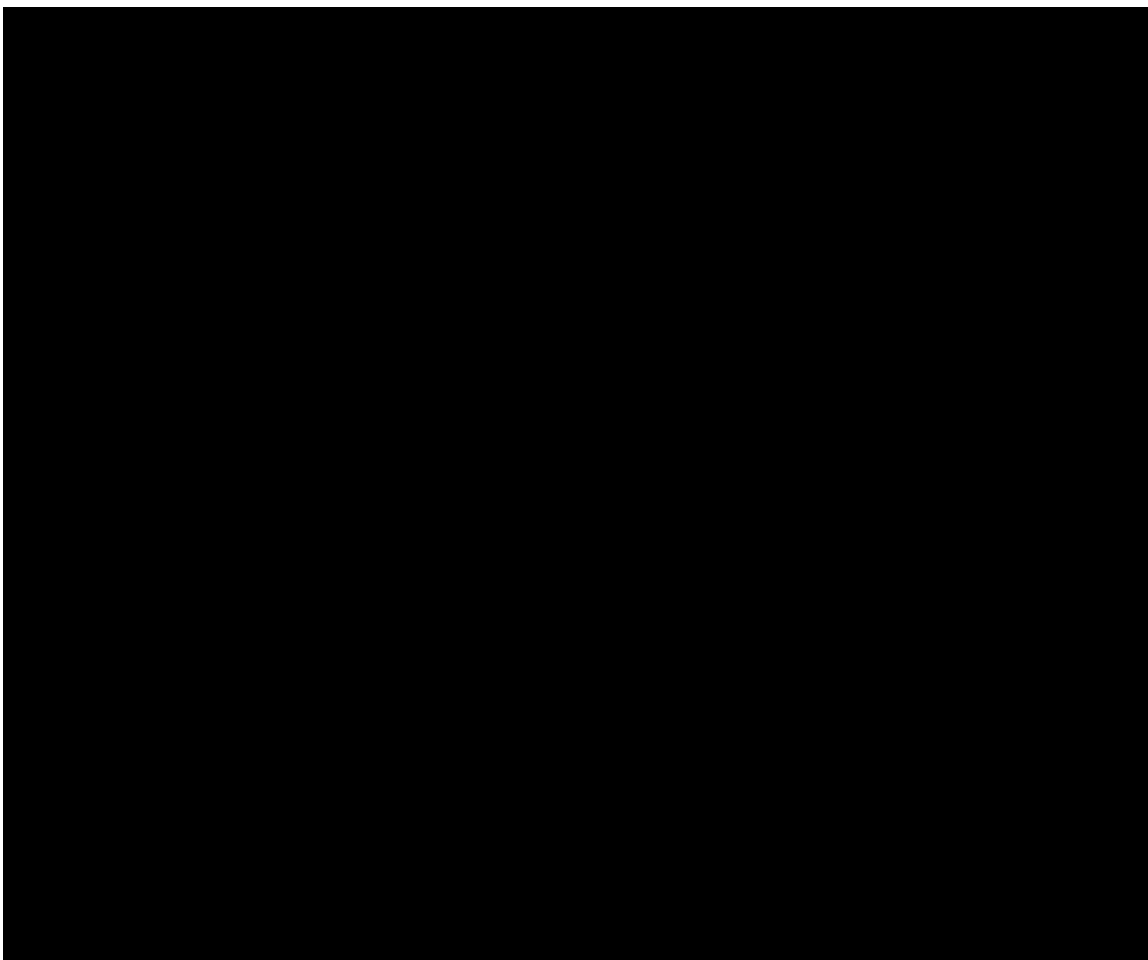


Figure 1. Examples of Pincer Ligands

As shown in Figure 1, a wide variety of pincer ligands exist with a number of anionic and neutral ligands being possible. The variety of pincer ligand types coupled with the possible differences in metal oxidation states gives a large number of possible precursors to investigate. Another advantage of investigating these pincer ligands is that a sizeable amount of pincer literature exists with various preparation and synthetic modifications highlighted. The most common types of pincers are anionic ligands with the negative charge residing on the central carbon or nitrogen; however, if the central N atom is part of an aromatic

ring the ligand is neutral. In this dissertation work attention is directed at both anionic and neutral PNP-based ligand systems.

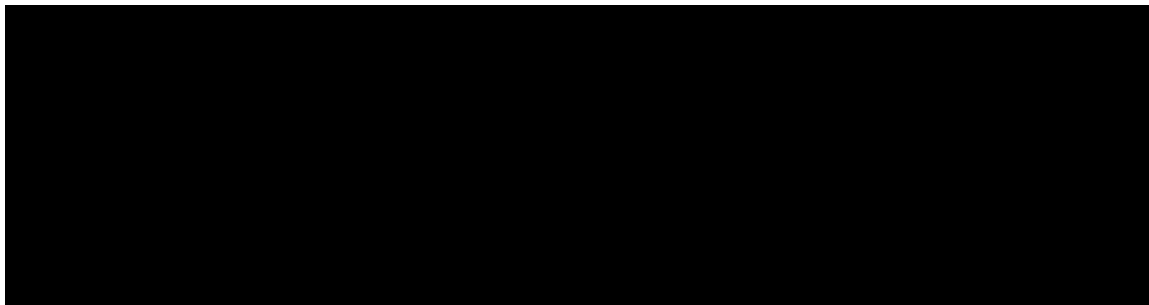


Figure 2: Modification Options of Pincer Ligands

As shown in Figure 2, the sterics of the pincer system can be altered by changing the R groups attached to the donor atom (X), which can then allow or deny access to the metal center. The electronics of the system can be modified by changing the donor atoms or by varying the substituents on donor atoms (electron withdrawing/donating), the Z on the aryl ring and the Y at the *para* position of the ring.

1.3 Applications of Pincer Ligands

Pincer ligands have proven to be very useful in catalysis and synthetic organometallic chemistry. As mention above, the synthetic variations possible in pincer chemistry can lead to the formation of a great variety of metal complexes. Important for our purposes in this project are both the thermal and moisture stabilities of pincer-metal complexes. Pincer complexes are more thermally-stable than their non-chelating counterparts due to the extra stability provided by the chelate effect, particularly in square planar late transition metal complexes.³²

The three meridional points of attachment by the pincer afford relatively thermally-robust species. As well, these species are more stable towards water or other protic species than their non-chelated analogues. This feature is extremely important as the proposed regeneration step will include the formation of water. Stability towards water is thus a requirement for the proposed catalytic system. By way of illustration, the reactivity and use of various pincer-containing metal complexes in a number of important processes will be presented in this section. In many cases, the use of the pincer-complex allowed the desired chemistry to occur when the non-pincer versions did not give desired products of reactivity.

1.3.1 Heck Reaction

The Heck reaction involves the catalyzed cross-coupling between aryl halides or vinyl halides and activated alkenes. This transformation is usually accomplished in the presence of an organopalladium (Pd^0 or Pd^{II}) catalyst and a strong base resulting in a substituted alkene. The Heck reaction is a very useful carbon-carbon-bond forming process in synthetic chemistry and its application has been widely used in other areas.³³⁻³⁷ As an aside, the Heck reaction was recently noted as a key component in the 2010 Nobel Prize in Chemistry announcement, indicating its fundamental importance.³⁸



Scheme 5. Heck Reaction

One drawback associated with this reaction is the instability of the intermediates formed during the reaction. In most cases, the intermediate is sensitive to oxygen and can also be thermally unstable. Another drawback with these catalysts, as with other coupling catalysts, is their inability to activate aryl chlorides, thus requiring utilization of other expensive halides.³⁹ From an industrial standpoint, these shortcomings have greatly hindered its appeal and have led to explorations of more efficient catalysts.

Milstein first investigated the use of PCP-based Pd complexes (**1**, **2**, and **3**) in the Heck reaction in the coupling of aryl halides with various alkenes.⁴⁰ These new catalysts exhibited high catalytic activity at temperatures as high as 140 °C and further showed no signs of decomposition after 300 hours of operation. The PCP-Pd catalyst achieved excellent turnover numbers for iodobenzene (TON = 500,000 hr⁻¹) and bromobenzene (TON = 132,9000 hr⁻¹).⁴⁰ However, as with other analogues, this catalyst was unable to couple aryl chlorides.

With the success of employing complexes with non-chelating phosphite ligands for the coupling of aryl chlorides, investigations of utilizing phosphinito-type PCP pincer ligands were initiated.⁴¹ These Pd-PCP phosphinito complexes demonstrated efficient coupling of aryl halides comparable in performance to Milstein's catalyst, and also demonstrated the ability to activate chlorobenzene.⁴²⁻

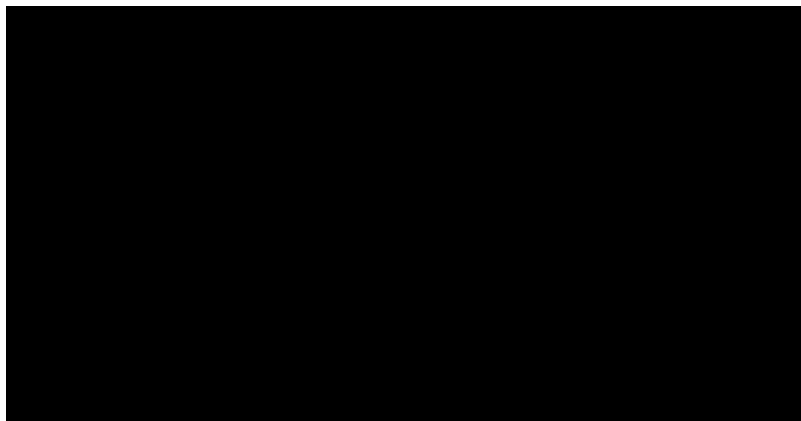


Figure 3. Heck Coupling Catalysts

Other phosphine-free pincer complexes were also investigated to gauge their potential catalytic activity in the Heck coupling reaction. One particular catalyst that was examined was a Pd-based SCS complex, **4** (Figure 4). This complex **4** showed the ability to couple various aryl iodides with alkenes with average yields but low TONs when compared to Pd-PCP complexes.⁴⁵ One interesting aspect of these complexes is the ability to tether the catalyst to a polyethylene glycol (PEG) support. This catalyst **5** is highly stable and can be isolated after each reaction and reused with little or no loss in performance for at least three cycles.⁴⁵

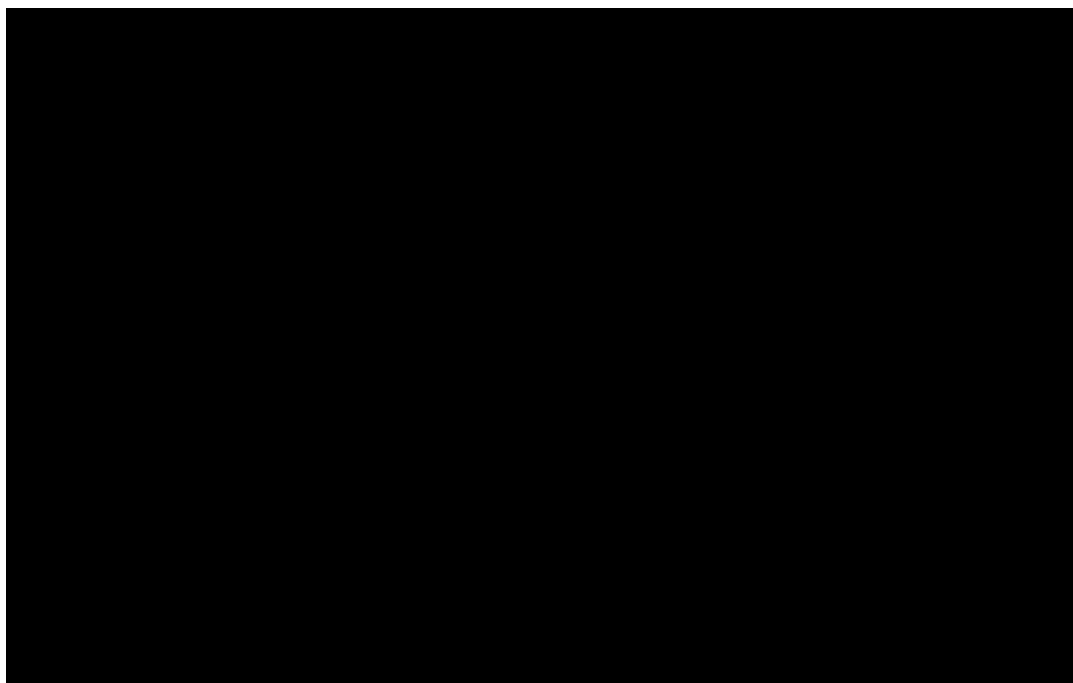


Figure 4. Pd-SCS Heck Catalysts

Another type of pincer-based ligand system that has shown the ability to catalyze the Heck reaction is the PNP-based Pd pincer family of complexes. These complexes play a part in chemistry described in Chapter 3. The PNP-based Pd complexes have high thermal stabilities along with the ability to catalyze the Heck reaction with the coupling of bromo- and iodoarenes with ethyl acrylate and styrene.⁴⁶

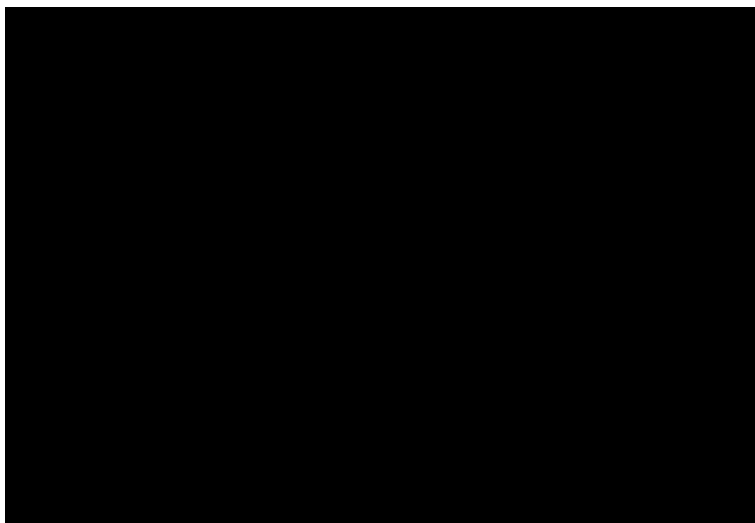


Figure 5. PNP-based Heck Catalysts

Both reactions show comparable results as their Pd PCP-based counterparts, with TONs ranging from a few hundred to as high as 45,000,000 hr⁻¹.^{46, 47} However, these pincer-based catalysts show little or no catalytic activity for the coupling of aryl chlorides.

1.3.2 Suzuki-Miyaura Coupling

The Suzuki-Miyaura coupling is the reaction between an aryl or vinyl boronic acid with an aryl or vinyl halide. This reaction is also generally catalyzed by an organopalladium catalyst and is used to produce polyolefins, styrenes, and substituted biphenyls.⁴⁸⁻⁵⁰ Since the reaction mechanism is similar to the Heck reaction, most of the catalysts used in that system can also be used in this system.⁵¹

Scheme 6. Suzuki-Miyaura Coupling

Several drawbacks are associated with using these palladium catalysts in this coupling reaction. As was seen in the Heck reaction, these catalysts also suffer from thermal stability issues and are air- and moisture- sensitive. Another drawback is the requirement of high catalyst concentrations in order for the reaction to proceed. The other shortcomings deal with the cost and difficulties related with removal of these palladium catalysts from the product. These obstacles have severely hindered its potential industrial utility.⁵¹

With the success of employing PCP-based pincer complexes by Milstein and Shibasaki in the Heck reactions, related species were also used in investigations for potential activity in the Suzuki coupling. In 2000, Bedford was successful in using phosphinito Pd PCP-based pincer complexes **6** and **7** in the coupling of aryl halides with phenyl boronic acid. These catalysts gave very high turnover numbers.⁵² These pincer complexes are relatively easy to synthesize and show no decomposition when exposed to air and moisture.

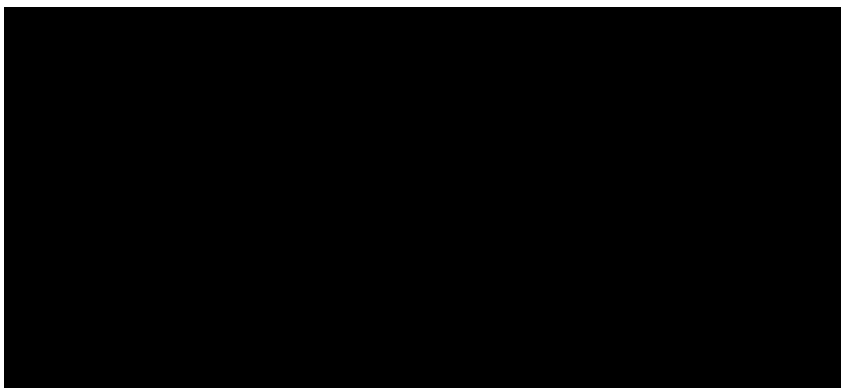
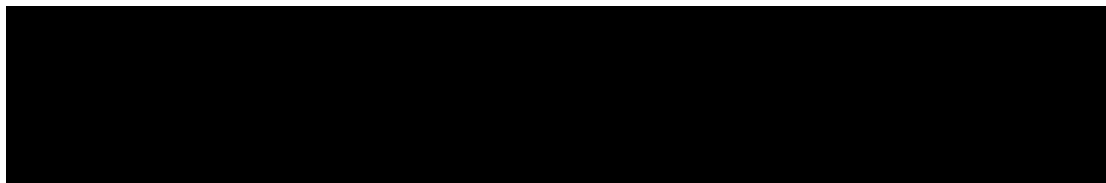


Figure 6. Suzuki-Miyaura Catalysts

As with the Heck reaction, other pincer complexes are being investigated to gauge their Suzuki coupling potential. In 2000, Monteiro demonstrated that a Pd(II) SCS-based complex **8** is capable of coupling *p*-bromotoluene with phenyl boronic acid with moderate turnover.⁵³

1.3.3 Hydrogen Transfer Catalyst

Another potential catalytic application for these pincer complexes is as a hydrogen transfer catalyst. Recently, van Koten has shown that ruthenium pincer complexes are capable of catalyzing transfer hydrogenation of several ketones to their respective alcohols.⁵⁴ As shown in Scheme 7, the reductions of diacyl or diaryl ketones are done in the presence of the pincer catalyst along with *iso*-propyl alcohol (IPA) and KOH as the reductant.



Scheme 7: Hydrogen Transfer Reaction⁵⁴

van Koten has shown that these ruthenium pincer complexes **9**, **10**, and **11** are effective hydrogenation catalysts with excellent conversions and high turnover numbers. An example is the hydrogenation of cyclohexanone which yielded a 98% conversion with a TON of 27,000 hr⁻¹.⁵⁴

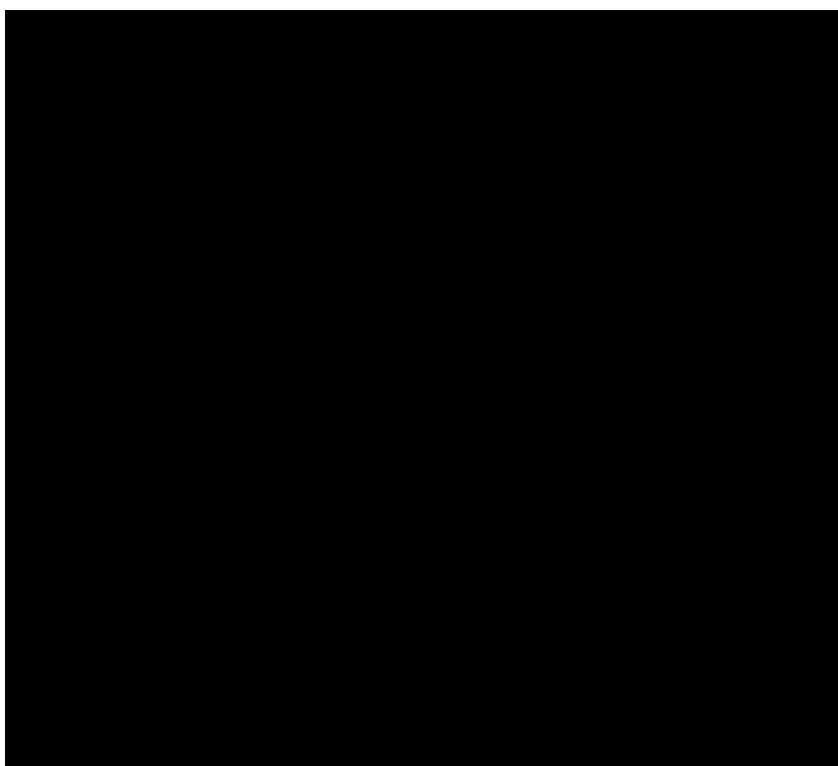
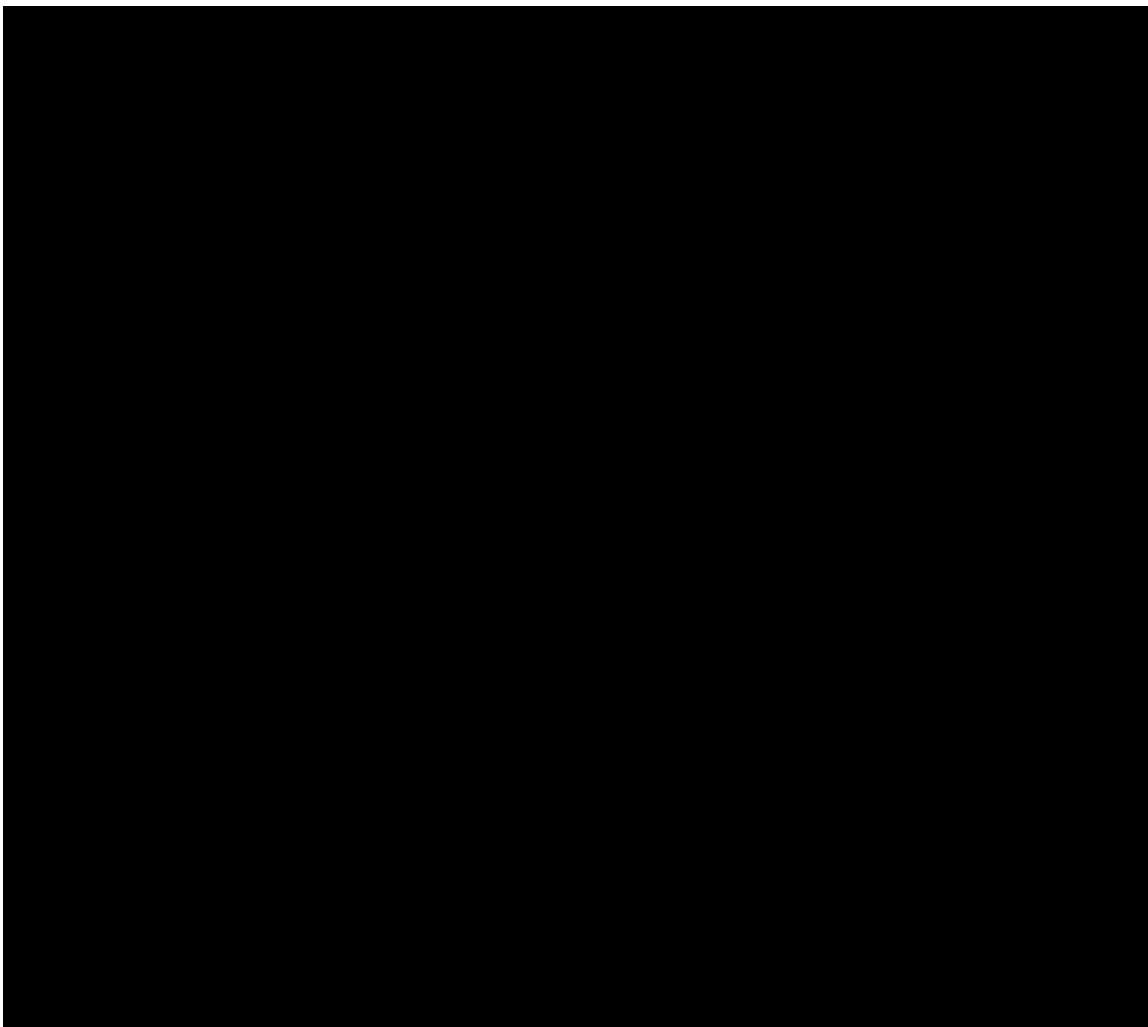


Figure 7. Hydrogen Transfer Catalysts

With the PCP-based complexes showing significant conversion rate improvements over their NCN counterparts, further research into using chiral ruthenium pincer complexes for stereoselective reduction has been investigated. Once again, van Koten has shown that chiral ruthenium complexes **12** and **13** have the ability to catalyze the reduction of the diaryl and dialky ketones but resulted only in meager enantioselectivity excesses.^{55, 56}

1.3.4 Alkane Dehydrogenation

The first attempt at alkane dehydrogenation with transition metal catalysts was initiated by Crabtree in 1979 and over the years was followed by other efforts to improve the reactivity. These groups employed iridium and rhodium catalysts such as $[H_2Ir(PR_3)_2]$ but all catalysts suffered from poor turnovers and catalyst decomposition.^{57, 58} With the initial success of iridium and rhodium catalysts in alkane dehydrogenation, several groups explored pincer ligands due to their high thermal stabilities.⁵⁹⁻⁶¹ In 1998, Jensen explored the use of a dihydride rhodium pincer complex, $^{tBu}PCP-Rh-H_2$, in the dehydrogenation of cyclooctane with *tert*-butylethylene (tbe) as the sacrificial hydrogen acceptor. The reaction was initiated at 200 °C and resulted in only 1.8 turnovers.⁶² Further expansion into this system resulted in an iridium derivative, $^{tBu}PCP-Ir-H_2$, which showed improved catalytic activity. Under similar conditions, the dehydrogenation of cyclooctane resulted in 720 turnovers at 200 °C with excellent thermal stability.⁶³⁻⁶⁵



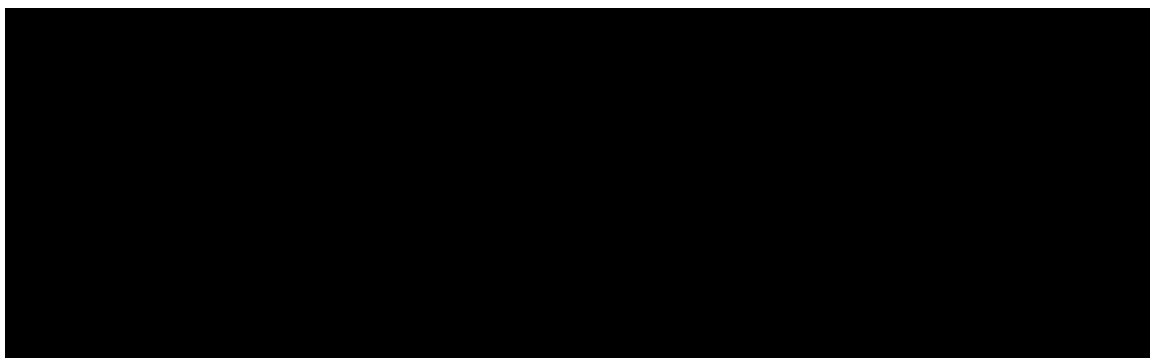
Scheme 8. Alkane Dehydrogenation Catalyst⁶⁶

As shown in Scheme 8, the dihydrido iridium pincer complex, ^tBuPCP-Ir-H₂ **14**, has been investigated in various dehydrogenation reactions.^{59, 63, 64, 67} In order to generate the active catalytic species, a sacrificial hydrogen acceptor was used to reduce the iridium intermediate **15** but further studies have indicated that similar reduction was obtained when only heat was used to liberate H₂.^{68, 69} Recent modifications to this system, such as changing the substituents on the

phosphorus atoms and using an acridine-based iridium pincer complex, have shown slight improvements in the system.^{70, 71}

1.3.5 Asymmetric Allylic Alkylation Catalysts

With the generation of hundreds of chiral phosphines for potential asymmetric catalysts, only a few are practical enough for commercial applications.^{72, 73} With the never-ending search for more efficient stereospecific catalysts, a chiral pincer ligand has been studied as a potential catalyst for asymmetric allylic alkylations.



Scheme 9. Asymmetric Allylic Alkylation Catalyst⁷⁴

As shown in Scheme 9, Longmire has investigated the use of a chiral ligand **16** into the allylic alkylations of 1,3-diphenyl-2-propenyl acetate with dimethyl malonate. This reaction eventually resulted in a 94% yield and a 79% enantiomeric excess (ee) of the (R)-enantiomer.⁷⁴ While these results do not compete with the commercially-produced ligands, the ease of synthesis and promising results merit further investigations into asymmetric syntheses.

Chapter 2

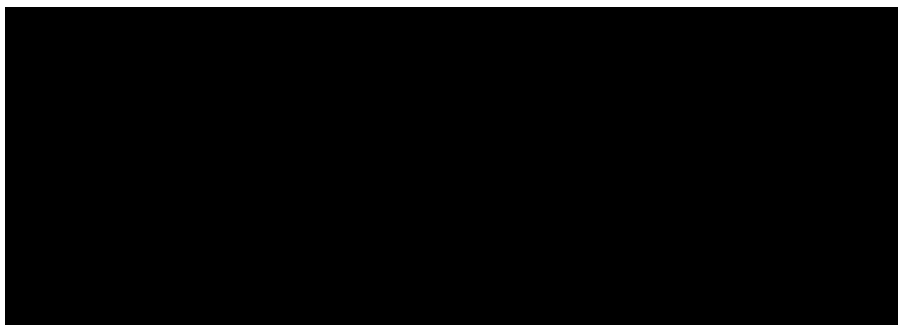
2.1 Attempted Synthesis of PNP-Rh-H with Commonly-Used Hydrides

Palladium-based pincer metal complexes were first reported in 1976 in a seminal paper by Moulton and Shaw²⁸ and since that time numerous complexes have been developed for various applications.⁷⁵ The need to expand the types of pincer ligands for the proposed catalytic route (Scheme 4) led to the development of complexes that utilize PNP-type ligands. In the PCP Pd-pincer complexes mentioned above, the overall charge on the complex remains neutral with two negative charges coming from the ligand and the halide, balanced by the two positive charges from the Pd(II) ion. In the case of the PNP-type complexes, charge neutrality was achieved by employing Group 9 metals. The work covered in this chapter includes the development of neutral PNP-type complexes for the possible epoxidation of olefins.

As shown in Scheme 4, the potential active catalyst is a pincer-based metal hydride. The general scheme developed for the synthesis of the pincer metal hydride begins with the synthesis of the free ligand followed by generation of a metal halide, which is eventually converted into a metal hydride. Since the majority of the work detailed in this dissertation centers on PNP-type ligands, the focus here will be placed on their preparation.

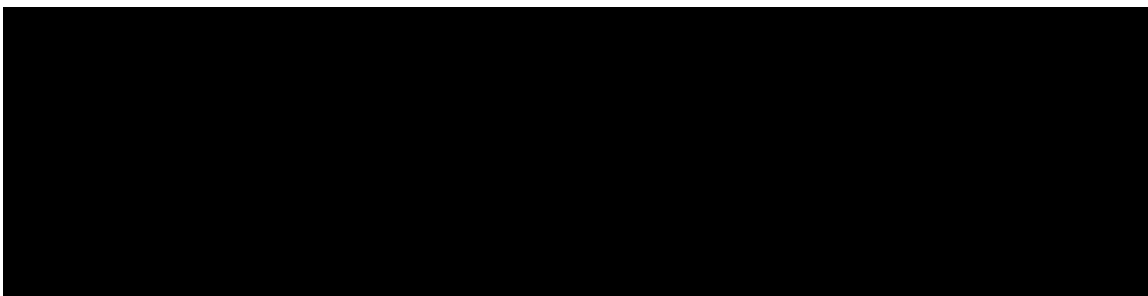
The syntheses of PNP-based free ligands have previously been accomplished by routes depending on the R groups of the target system. For derivatives containing alkyl substituents, the phosphorus atom lone pairs are nucleophilic enough to allow displacement as shown in Scheme 10. Two

equivalents of a secondary dialkylphosphine are refluxed with 2,6-bis(chloromethyl)pyridine **17** for a period of time to generate a diphosponium salt, which is then deprotonated with a base to generate ligand **18**. As reported by Milstein et al, compound ^tBuPNP **19** was generated in this manner as a white solid in a 79% yield.⁷⁶



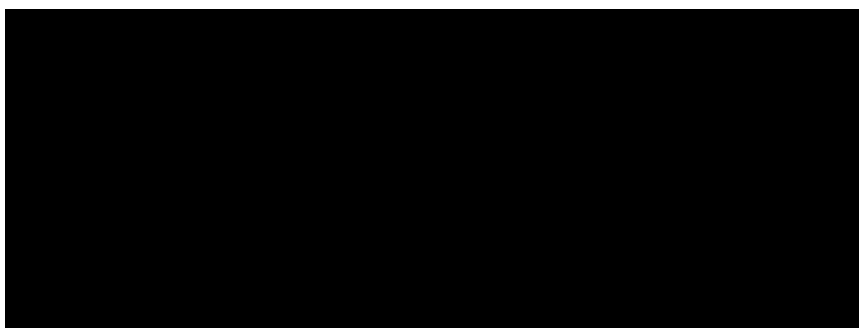
Scheme 10. Preparation of PNP-based Ligands

Another route for synthesizing these pincer ligands involves the generation of a metal phosphide solution prior to addition to **17**. As shown in Scheme 11, this is the preferred route for the preparation of phosphine ligands with diaryl substituents, as the lone pairs on the phosphorus atom in these cases are less nucleophilic in nature. Due to the reduced nucleophilicity, the generation of these types of ligands will not proceed via Scheme 10. The diarylphosphide, however, reacts with **17** to produce ligand **18**. Ligands ^{Cy}PNP **21** and ^{Ph}PNP **22** were generated in similar fashions using this procedure.^{77, 78}



Scheme 11. Preparation of PNP-based Ligands

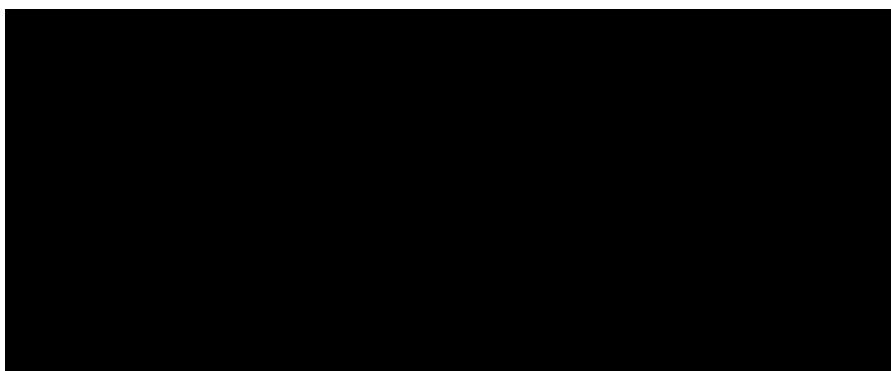
While the two routes just mentioned are the standards in generating PNP and PCP ligands, another route also exists. In the case in which dialkylphosphines or metal phosphides are not available or viable, a PNP-based ligand can still be generated. As shown in Scheme 12, the roles of nucleophile and electrophile have been reversed. Two equivalents of *n*-BuLi are added to a solution of 2,6-lutidine **20**, which is then combined with two equivalents of the proper chlorophosphine. Compound ⁱPrPNP **23** has been previously prepared in this manner.⁷⁹



Scheme 12. Preparation of PNP-based Ligands

Several routes have been described for the metalation of PNP pincer ligands.⁶⁶ In the case of PCP-based complexes, the most common approach employs direct cyclometalation (Scheme 13). This method has been successfully

employed since 1976 with the direct cyclometalation of several Group 9 and 10 metals with PCP-based ligands.²⁸⁻³¹



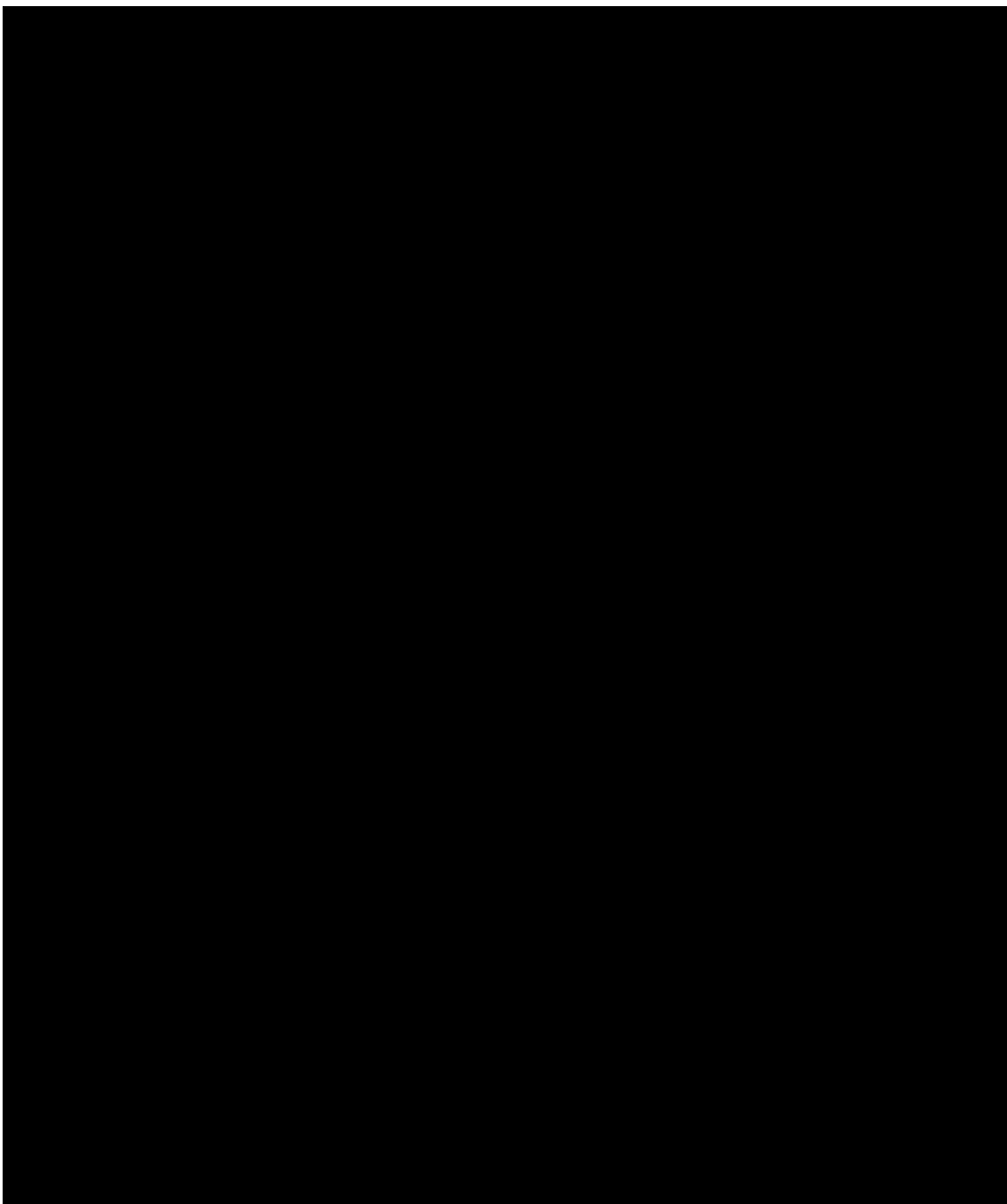
Scheme 13. Direct Cyclometalation

A wide range of metal precursors, such as $[\text{PdCl}_2(\text{COD})]$, $[\text{PtCl}_2(\text{COD})]$, $[\text{PdCl}_2(\text{CH}_3\text{CN})]$, and $[\text{RhCl}(\text{COE})_2]_2$, have been employed in these reactions. These precursors contain the desired metal, halogen, and labile ligands that both enhance solubility of the complex as a whole and can be easily displaced.⁶⁶

A few more techniques, if needed, are available for metalation of these pincer ligands. As shown below, another method involves the oxidative addition of pincer ligands to low-valent metals. With the success and ease of the direct cyclometalation method, oxidative addition is uncommon when generating PCP-based metal complexes. This method is used exclusively for generating NCN-based metal complexes by substituting a more labile C-X bond ($X = \text{Cl}, \text{Br}$) for the stronger aryl C-H bond.⁸⁰ Common precursors used in this reaction include $[\text{Ni}(\text{COD})_2]$, $[\text{Ni}(\text{PPh}_3)_4]$, $[\text{Pd}_2(\text{dba})_3]$, and $[\text{Pt}(4\text{-tol})_2(\text{SEt}_2)]_2$.⁸⁰⁻⁸² While this reaction scheme is not utilized in generating the PNP-based metal complexes with neutral ligands described in the dissertation, it is utilized in Chapter 3 in generating metal

hydrides with anionic PNP-based ligands. More discussion on this attractive direct generation of PNP-based Ni hydrides is given in Chapter 3.

Another method that avoids activation of C-X or N-H bonds involves transmetalation of the pincer ligands. Generally, lithiation of a typical PCP ligand does not lithiate at the desired location on the aryl ring, but rather occurs at the benzylic position of the arms. Even with the use of an aryl halide precursor to initiate lithium/halogen exchange, the generated species is unstable and isomerizes to the benzyl/lithium complex.⁶⁶ However, this method can be quite effective in certain instances, such as the generation of NCN metal complexes, when other metalation routes are very slow and difficult.

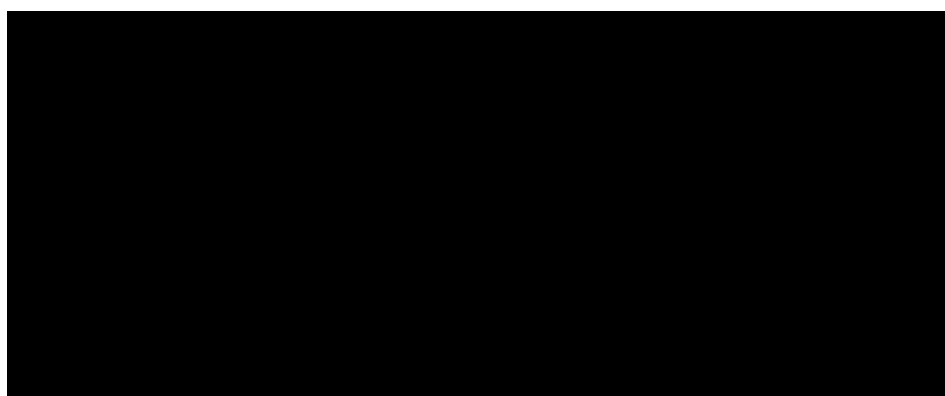


Scheme 14. Various Metalation Techniques⁶⁶

Transcyclometalation reaction is another technique in generating pincer-cyclometalated metal complexes. As shown in Scheme 14, technique (3)

involves the substitution of one cyclometalated ligand with another, a process that is facilitated by the stronger bond strengths of the metal-heteroatoms in the desired product.⁶⁶ This can be demonstrated in the substitution of NCN-based Pt and Ru complexes with PCP-based ligands, as the hard amine ligands are replaced by softer phosphine ligands.^{55, 83} This type of reaction was not employed in the dissertation studies. Fortunately, the direct cyclometalation reaction was very effective in generating PNP-based metal halides.

A small number of PNP-containing Rh halides have been reported in the literature and they serve as an excellent starting point. Milstein first synthesized the complex, ^tBuPNP-Rh-Cl **28**, in 2002.⁷⁶ The compound was synthesized by the addition of the pincer ligand to a stirred benzene solution of [Rh(COE)₂Cl]₂ at room temperature. This resulted in a 35% isolated yield of **28**. Similar methodology was used in the current study for the syntheses of both ⁱPrPNP-Rh-Cl **29** and ^{Cy}PNP-Rh-Cl **30**. However, here the reaction mixture was heated and this led to (Scheme 15) increased yields, 83% and 91% respectively.



Scheme 15. Preparation of ⁱPrPNP-Rh-Cl **29 and ^{Cy}PNP-Rh-Cl **30****

The $^{31}\text{P}\{^1\text{H}\}$ NMR spectrum of **29** reveals a doublet at 47.3 ppm with a $J_{\text{PRh}} = 144.7$ Hz, indicating symmetry due to the equivalency of the phosphorus atoms. The validity of this assumption is confirmed by ^1H NMR spectroscopy, which shows identical chemical shifts for the methylene protons, a virtual triplet due to coupling to the P and Rh atoms. The molecular structure of **29** was confirmed by X-ray diffraction analysis. A single crystal suitable for X-ray study (Figure 8) was grown from slow evaporation of a benzene solution at room temperature. The solid-state structure exhibits a square planar geometry adopted by the Rh metal center, consistent with its $^t\text{BuPNP-Rh(I)-Cl}$ counterpart.⁸⁴ A list of selected bond lengths and angles are shown in Table 1.

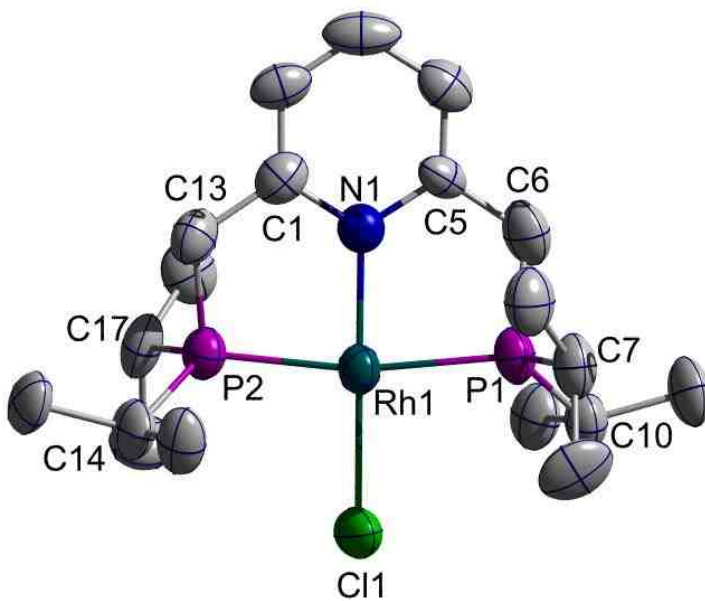


Figure 8. Thermal Ellipsoid Plot of 29 Shown at 50% Probability Level with Hydrogens Omitted for Clarity

Table 1. Selected Bond Lengths and Angles for Compound 29

Bond Lengths (Å)

Atom 1	Atom 2	Distance
Rh1	Cl1	2.347(2)
Rh1	P1	2.238(1)
Rh1	P2	2.238(1)
Rh1	N1	2.026(1)
P1	C6	1.811(1)
P1	C7	1.812(2)
P1	C10	1.841(2)
P2	C13	1.816(1)
P2	C14	1.833(2)
P2	C17	1.846(2)

Bond Angles (°)

Atom 1	Atom 2	Atom 3	Angle
Rh1	N1	Cl1	179.65
Rh1	N1	P1	84.18
Rh1	N1	P2	84.93
Rh1	Cl1	P1	95.56
Rh1	Cl1	P2	95.33
Rh1	P1	P2	169.10
Rh1	P1	C6	99.65
Rh1	P1	C7	120.00
Rh1	P2	C19	99.35
Rh1	P2	C20	120.30

In a similar manner, compound **30** was isolated as a red solid in 91% yield. The $^{31}\text{P}\{^1\text{H}\}$ NMR spectrum of **30** exhibits a doublet at 38.9 ppm with a $J_{\text{PRh}} = 144.2$ Hz. X-ray diffraction analysis was used to confirm the molecular structure of **30**. A single crystal suitable for X-ray study (Figure 9) was grown by slow evaporation of a benzene solution at room temperature. The X-ray crystal structure exhibits a square planar geometry around the Rh metal center, which is

quite similar overall to compound **29** and **28**. A list of selected bond lengths and bond angles of **30** are shown in Table 2.

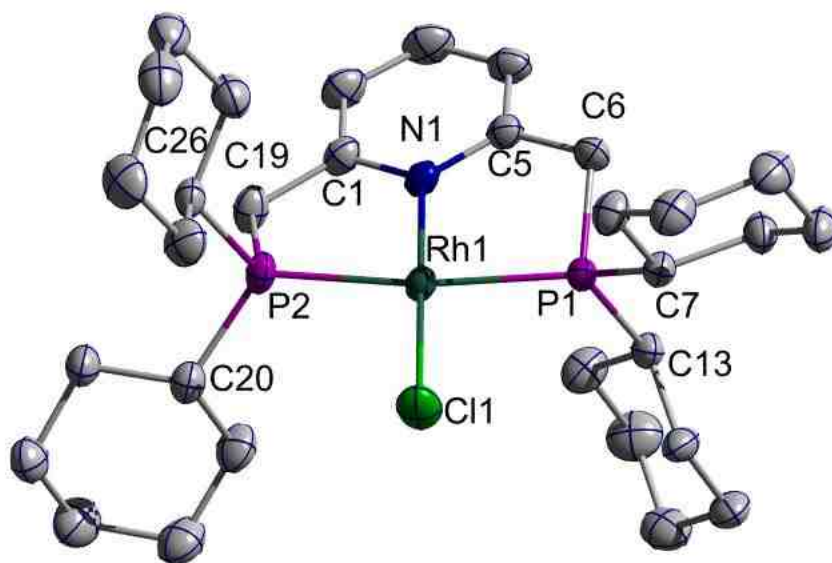


Figure 9. Thermal Ellipsoid Plot of 30 Shown at 50% Probability Level with Hydrogens Omitted for Clarity

Table 2. Selected Bond Lengths and Angles for Compound 30

Bond Lengths (Å)

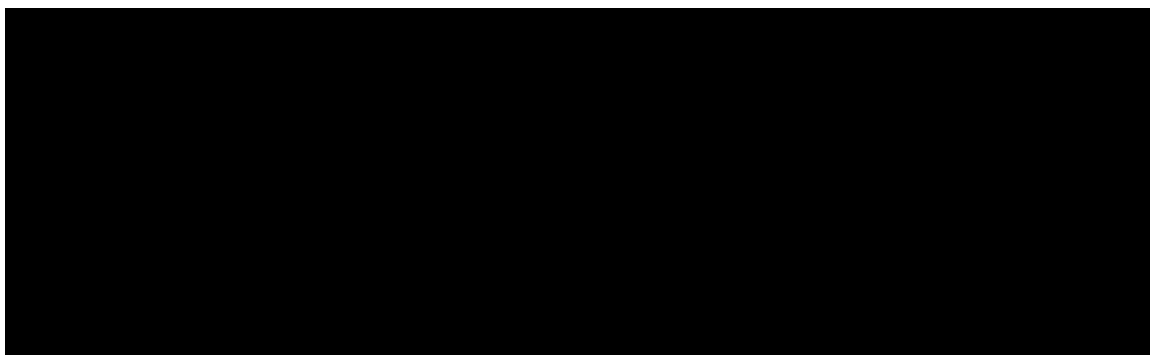
Atom 1	Atom 2	Distance
Rh1	Cl1	2.346(6)
Rh1	P1	2.259(5)
Rh1	P2	2.246(6)
Rh1	N1	2.032(2)
P1	C6	1.844(2)
P1	C7	1.841(2)
P1	C13	1.847(2)
P2	C19	1.841(2)
P2	C20	1.855(2)
P2	C26	1.845(2)

Bond Angles (°)

Atom 1	Atom 2	Atom 3	Angle
Rh1	N1	Cl1	179.04(5)
Rh1	N1	P1	84.38(5)
Rh1	N1	P2	84.24(5)
Rh1	Cl1	P1	95.61(2)
Rh1	Cl1	P2	95.75(2)
Rh1	P1	P2	168.53(2)
Rh1	P1	C6	99.02(7)
Rh1	P1	C7	122.27(6)
Rh1	P2	C19	100.63(7)
Rh1	P2	C20	120.04(7)

After the successful generation of new ^RPNP-Rh-Cl complexes with R = ⁱPr and Cy, the next step involved the synthesis of the respective hydrides. In 1976, Moulton and Shaw synthesized a PCP pincer-based palladium hydride ^tBuPCP-Pd-H from its corresponding Pd-Cl complex using NaBH₄ as the hydride source.²⁸ More recently, LiAlH₄ was used to generate the same palladium hydride ^tBuPCP-Pd-H.⁸⁵ With the initial success of the conversion to the metal

hydrides for this PCP system, a similar route was also employed for the conversion of **28**, **29**, and **30**. The hydride sources employed were LiAlH_4 , NaBH_4 , a K-Selectride[®] solution (1.0 M $\text{KHB}(\text{sec-butyl})_3$ in THF), and Super Hydride[®] solution (1.0 M LiHBEt_3 in THF). However, none of these proved successful in converting the PNP-Rh-Cl complexes to their corresponding hydrides.



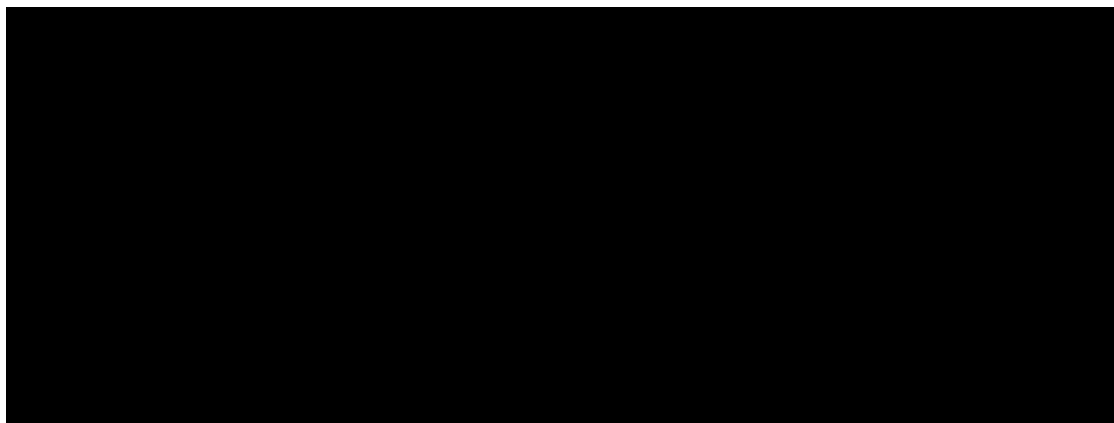
Scheme 16. Attempted Syntheses of PNP-Rh-H Complexes

In all cases, no reaction took place as the metal halide remained intact or resulted in the formation of an unknown species that contained no hydride signal in the ^1H NMR. However, in one particular case, a signal was observed in the ^1H NMR around -3 ppm after employing NaBH_4 as the hydride source.

Unfortunately, this chemical shift corresponded to a borohydride anion (BH_4^-) coordinated to the metal center. Borohydride anions are known to coordinate to various metals across the periodic table.⁸⁶ Unfortunately, difficulties with the direct reduction route using hydride sources are also consistent with previous work involving other Group 10 PCP complexes.⁸⁷

2.2 Alternative Route to PNP-Rh-H Complexes

The unsuccessful conversion of the Rh halides to hydrides using conventional hydride sources led to examinations of alternative routes to the hydrides. One route involved a PNP-containing Rh triflate complex prepared by Goldberg, ^tBuPNP-Rh-OTf **31**, in 2008.⁸⁸ As shown in Scheme 17, the neutral compound was prepared by stirring Ag(OTf) and [ClRh(COE)₂]₂ together for several minutes followed by removal of the AgCl via filtration and immediate addition of the PNP ligand to the filtrate. The reaction generated the product in 98% yield. The ³¹P{¹H} NMR spectrum of **31** exhibits a doublet at 61.7 ppm due to coupling to the Rh, $J_{\text{PRh}} = 145.0$ Hz. In the present study the new compounds ⁱPrPNP-Rh-OTf **32** and ^{Cy}PNP-Rh-OTf **33** were prepared in high yields by using the same method.



Scheme 17. Preparation of ^tBuPNP-Rh-OTf **31, ⁱPrPNP-Rh-OTf **32**, and ^{Cy}PNP-Rh-OTf **33****

Compound **32** was generated as a red/orange solid in a 97% yield. The ³¹P{¹H} NMR spectrum of **32** exhibits a doublet at 45.9 ppm with a $J_{\text{PRh}} = 130.9$

Hz, indicating symmetry within the complex due to the two equivalent phosphorus atoms. The ^1H NMR spectrum verifies this by showing identical chemical shifts for the methylene protons (virtual triplet) due to coupling to the P and Rh atoms, as compared to a doublet in the free ligand.

Compound **33** was also produced in high yield (95%) as an orange solid. The $^{31}\text{P}\{^1\text{H}\}$ NMR spectrum of **33** displays a doublet at 36.9 ppm with a $J_{\text{PRh}} = 129.2$ Hz. As shown in Figure 10, a single crystal X-ray structure of **31** indicates that the triflate is loosely bound to the Rh with a bond distance of 2.132 Å. However, in solution the triflate anion is readily displaced as it converts to $^t\text{BuPNP-Rh-N}_2\text{OTf}$ when allowed to react with N_2 over several days.⁸⁸ This demonstrates that **31** is in equilibrium with the dinitrogen complex as it readily converts back to **31** as heat or vacuum is applied.⁸⁸ A list of selected bond lengths and angles for **31** are shown in Table 3.

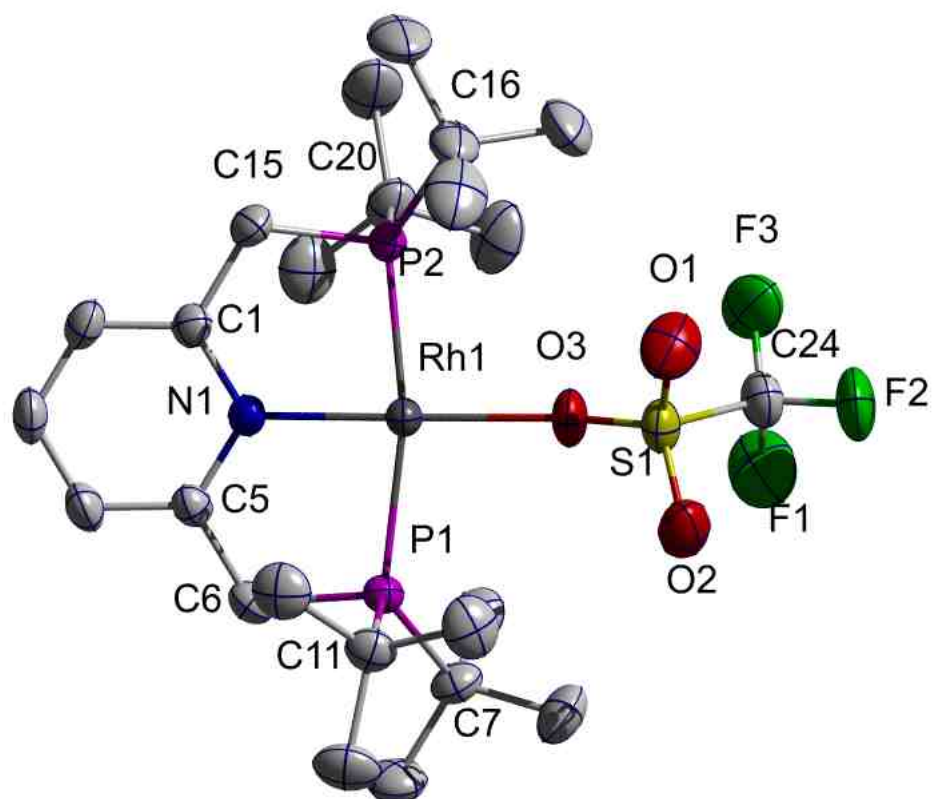


Figure 10. Thermal Ellipsoid Plot of 31 Shown at 50% Probability Level with Hydrogens Omitted for Clarity

Table 3. Selected Bond Lengths and Angles for Compound 31

Bond Lengths (Å)

Atom 1	Atom 2	Distance
Rh1	N1	2.022(2)
Rh1	P1	2.2946(8)
Rh1	P2	2.2817(9)
Rh1	O3	2.132(2)
P1	C6	1.830(3)
P1	C7	1.881(3)
P2	C15	1.836(3)
P2	C16	1.878(3)
S1	O3	1.456(2)
S1	O2	1.426(3)
S1	O1	1.419(2)
S1	C24	1.814(4)

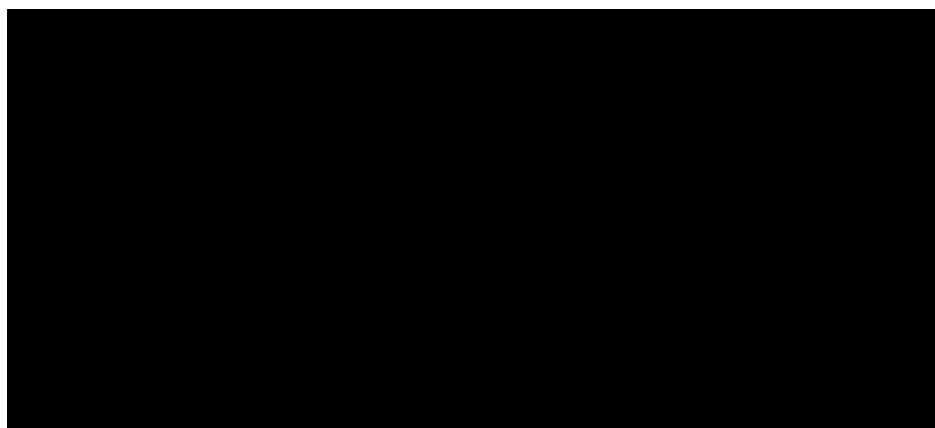
Bond Angles (°)

Atom 1	Atom 2	Atom 3	Angle
Rh1	N1	O3	176.26(8)
P2	Rh1	P1	167.38(3)
P2	Rh1	N1	83.69(6)
P1	Rh1	N1	84.20(6)
P2	Rh1	O3	95.34(6)
P1	Rh1	O3	96.51(6)
Rh1	O3	S1	142.4(1)
O3	S1	C24	99.7(1)
O2	S1	C24	103.3(2)
O1	S1	C24	105.0(2)

The next step in the synthesis of the PNP-based Rh hydrides involves the generation of a $[\text{R}^{\text{PNP-Rh}}\text{III}(\text{H})_2][\text{OTf}]$ complex. As shown in Scheme 18, this is accomplished via oxidative addition of H_2 to the $\text{R}^{\text{PNP-Rh}}\text{I-OTf}$ complex.

Experimentally, this is accomplished by addition of $\text{R}^{\text{PNP-Rh}}\text{I-OTf}$ into a medium wall J. Young NMR tube with benzene- d_6 as the solvent for NMR monitoring.

When the NMR tube was exposed to 1 atm of H₂ clear pale yellow solutions were obtained.



Scheme 18. Preparation of [RPNP-Rh(H)₂][OTf]

In the example of [t^{Bu}PNP-Rh^{III}(H)₂][OTf] **34**, the addition of H₂ took six days, resulting in a pale yellow solution. The reaction was primarily monitored by ³¹P{¹H} NMR, in which the doublet at 61.7 ppm, $J_{\text{PRh}} = 145.0$ Hz, of **34** slowly disappears and is replaced with a doublet at 81.5 ppm with a $J_{\text{PRh}} = 118.2$ Hz, which is indicative of a Rh(III) species. In the ¹H NMR spectrum of **34**, the virtual triplet of the methylene protons still remains, which confirms that the pincer-metal moiety still exists. As well, a broad signal appears at -13.9 ppm with an integrated ratio of 2H, consistent with oxidative addition of the H₂ to the metal center. In 2006, Goldberg developed a similar structure, [t^{Bu}PNPIr^{III}(H)₂][PF₆], indirectly as a side product and later in a deliberate synthesis as an orange solid in a 78% yield.⁸⁸

X-ray diffraction analysis was used to confirm the molecular structure of **34**. A single crystal suitable for X-ray study (Figure 11) was grown from a

concentrated benzene solution at room temperature. The X-ray crystal structure of **34** exhibits a square planar geometry around the metal center, which is quite similar to its Rh(I) counterpart. The X-ray crystal structure reveals that the triflate anion has been displaced, which was expected as mentioned above and is consistent with the NMR data. A list of selected bond lengths and bond angles of **34** are shown in Table 4. Even with the quality of the crystal and the data set (R-factor (5.3%)), the hydride ligands could not be located and refined.

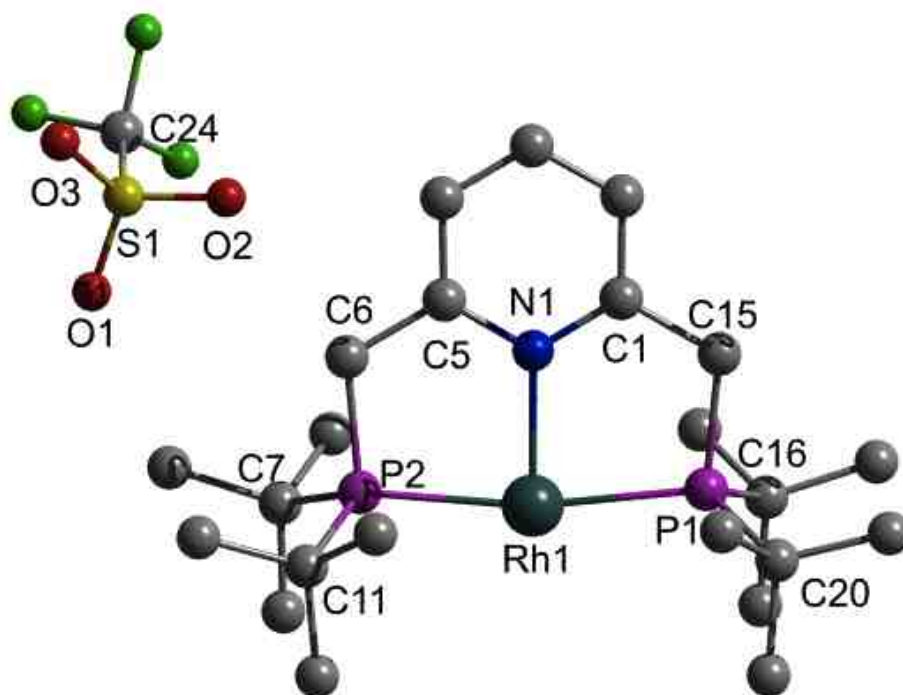


Figure 11. Ball and Stick Plot of 34 Shown at 50% Probability Level with Hydrogens Omitted for Clarity

Table 4. Selected Bond Lengths and Angles for Compound 34

Bond Lengths (Å)

Atom 1	Atom 2	Distance
Rh1	N1	2.083(3)
Rh1	P1	2.263(2)
Rh1	P2	2.266(2)
P2	C6	1.817(8)
P2	C7	1.886(7)
P1	C15	1.821(5)
P1	C16	1.873(7)
S1	O3	1.374(5)
S1	O2	1.365(7)
S1	O1	1.375(9)
S1	C24	1.634(9)

Bond Angles (°)

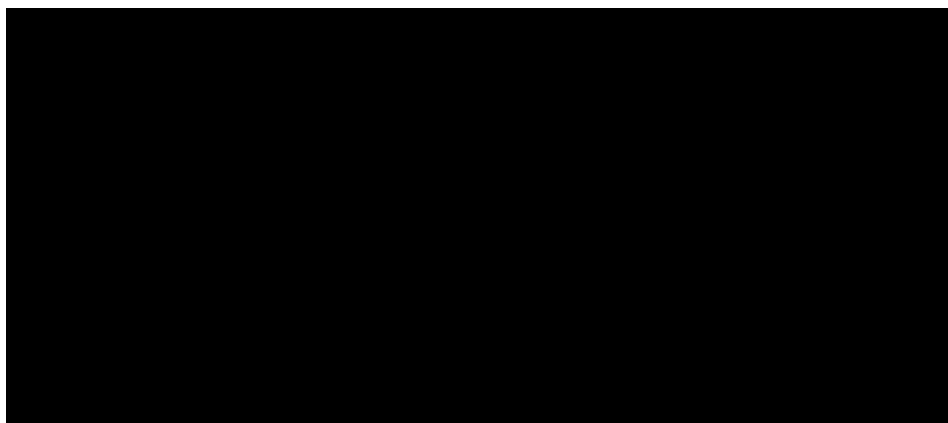
Atom 1	Atom 2	Atom 3	Angle
P2	Rh1	P1	169.13(5)
P2	Rh1	N1	84.3(1)
P1	Rh1	N1	85.0(1)
O3	S1	C24	104.5(5)
O2	S1	C24	104.0(4)
O1	S1	C24	101.9(6)

Complexes [ⁱPrPNP-Rh^{III}(H)₂][OTf] **35** and [^{Cy}PNP-Rh^{III}(H)₂][OTf] **36** were prepared using the same procedure. In both of these cases, the addition of H₂ only took overnight for completion, as compared to six days for the *tert*-butyl system. This is most likely due to the increased steric repulsion provided by the *tert*-butyl groups on the phosphorus atoms. The ³¹P{¹H} NMR spectrum of **35** exhibits a doublet at 66.1 ppm with a $J_{\text{PRh}} = 113.9$ Hz, indicating symmetry of the phosphorus atoms and the complex as a whole. The ¹H NMR spectrum of **35** still exhibits a virtual triplet for the methylene protons at 3.68 ppm and a chemical

shift for the hydride ligands appears as a broad signal at -18.95 ppm that integrates to 2H.

Compound **36** was also generated overnight after the addition of 1 atm of H₂ to the J. Young NMR tube. The ³¹P{¹H} NMR spectrum of **36** displays a doublet at 56.9 ppm with a $J_{\text{PRh}} = 113.7$ Hz, indicating symmetry among the phosphorus atoms and the complex. The ¹H NMR spectrum of **36** still exhibits a virtual triplet for the methylene protons at 3.73 ppm. The chemical shift for the hydride ligands appears at -18.80 ppm that integrates to 2H.

As shown in Scheme 19, the final step in the syntheses of the new Rh hydrides involves the addition of a strong base, K^tBuO, to the [^RPNP-Rh^{III}(H)₂][OTf] complexes. As mentioned before, the syntheses of the [^RPNP-Rh^{III}(H)₂][OTf] complexes utilized NMR monitoring to confirm complete conversion to the Rh(III) species from their Rh(I) precursors. It is assumed that with the disappearance of the Rh(I) species in the ³¹P{¹H} NMR spectrum that complete conversion has occurred. With this in mind, after 100% conversion the reaction workup details include emptying the contents of the J. Young NMR tube into a round bottom flask and rinsing the NMR tube with excess benzene. This is followed by the addition of one equivalent of K^tBuO and stirring at RT for one hour. The workup eventually resulted in a red solid.



Scheme 19. Preparation of ^RPNP-Rh-H Complexes

The ³¹P{¹H} NMR spectrum of ^tBuPNP-Rh-H **37** exhibits a doublet at 83.1 ppm with a $J_{\text{PRh}} = 166.6$ Hz indicating the presence of a Rh(I) species and equivalency among the phosphorus atoms. The ¹H NMR spectrum of **37** exhibits a virtual triplet at 2.93 ppm for the methylene protons. The resonance for the hydride ligand should have shown a doublet of triplets but instead displayed a distorted quartet at -12.8 ppm, indicating overlap between the two chemical shifts. The two distinct coupling constants for the hydride ligand were determined by selective ¹H{³¹P} NMR experiments, which resulted in the doublet generated by coupling to the rhodium ($J_{\text{HRh}} = 19.0$ Hz). From this, the coupling constant associated with the phosphorus atoms and hydrogen atom can then be determined, $J_{\text{HP}} = 20.0$ Hz.

Compounds ⁱPrPNP-Rh-H **38** and ^{Cy}PNP-Rh-H **39** were prepared using the same procedure in moderate yields, 73% and 63% respectively. The ³¹P{¹H} NMR spectrum of **38** exhibited a doublet at 61.7 ppm with $J_{\text{PRh}} = 163.5$ Hz, indicating symmetry within the molecule. The ¹H NMR spectrum of **38** still

displays the virtual triplet at 2.82 ppm for the methylene protons, indicating that the PNP-metal moiety still exists. The hydride ligand also appears upfield at -13.1 ppm with $J_{HRh} = 17.9$ Hz and $J_{HP} = 22.2$ Hz. The $^{31}\text{P}\{^1\text{H}\}$ NMR spectrum of **39** also exhibited a doublet at 52.2 ppm with $J_{PRh} = 162.1$ Hz, which is also indicative of a Rh(I) species. The ^1H NMR spectrum of **39** also displays the virtual triplet at 2.94 ppm and a doublet of triplets for the hydride ligand at -13.1 ppm with $J_{HRh} = 18.3$ Hz and $J_{HP} = 22.9$ Hz.

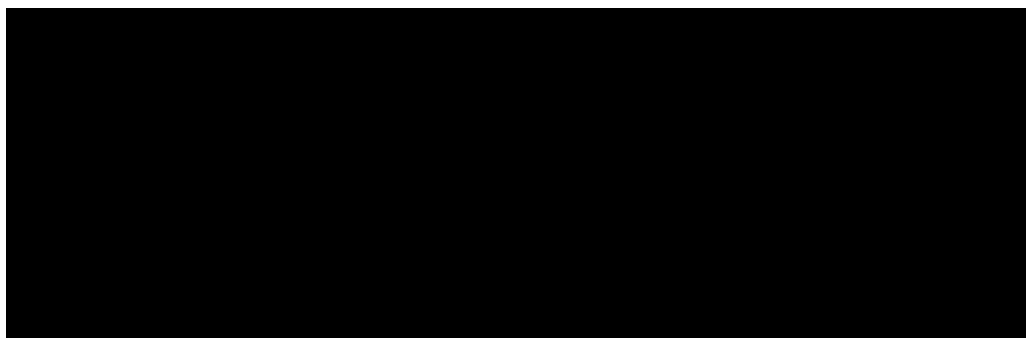
2.3 Reactions with O₂

The next step involved the generation of a metal hydroperoxide. Metal hydroperoxides have been reported for several systems and the majority have been generated with H₂O₂ as the oxidant.⁸⁹ However, several metal hydroperoxides have been generated through the insertion of O₂ into a metal hydride bond. Two cobalt complexes, $\text{Tp}^{\text{tBu,Me}}\text{Co-OOH}$ (Tp = trispyrazolylborate) and $\text{K}_3[(\text{CN})_5\text{Co-OOH}]$, have been generated from the insertion of O₂ into their respective metal hydrides.^{90, 91} However, these species were never isolated but only identified through vibrational spectroscopy. Several rhodium-based hydroperoxides, such as $[\text{Rh}(\text{NH}_3)_4(\text{OH})(\text{OOH})]^+$, $[\text{Rh}(\text{NH}_3)_4(\text{H}_2\text{O})(\text{OOH})]^{2+}$, $[\text{Rh}(\text{en})_2(\text{OH})(\text{OOH})]^+$, and $[\text{Rh}(\text{OOH})(\text{CN})_4(\text{H}_2\text{O})]^{2-}$, and an iridium hydroperoxide, $\text{Ir}(\text{OOH})\text{Cl}_2(\text{C}_8\text{H}_{12})$, were all prepared in a similar manner.⁹²⁻⁹⁶

Two platinum-based hydroperoxides, $\text{Pt}(\text{OOH})(\text{diphoe})\text{CF}_3$ and $\text{Tp}^{\text{Me}}_2\text{PtMe}_2\text{OOH}$, have been generated with the addition of O₂ to their respective hydrides; however, these complexes proceeded via a radical mechanism.^{97, 98} UV radiation was required to enhance the reaction and the radical nature of the

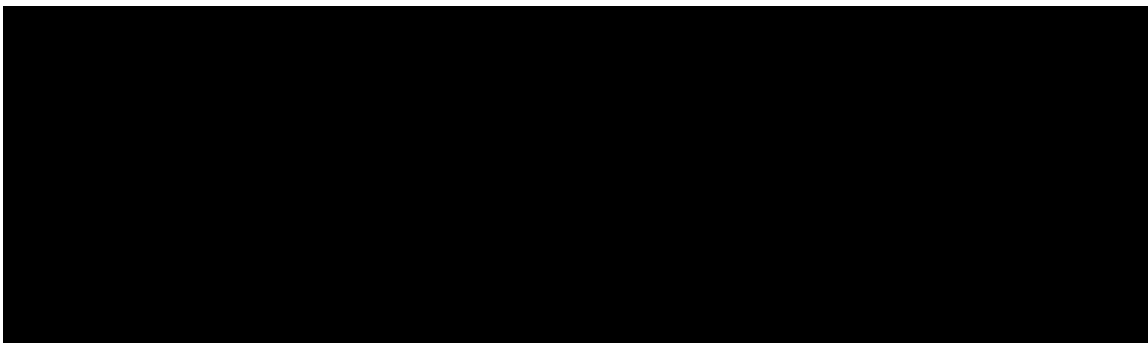
reaction was further verified as radical inhibitors and initiators exhibited considerable effects on the rates of reaction.^{97, 98}

More recently, several palladium-based hydroperoxides have been generated using molecular oxygen as the oxidant. One complex in particular is essential to the discussion detailed in this dissertation. In 2006, Goldberg and Kemp isolated and characterized a PCP-pincer based palladium hydroperoxide complex generated by insertion of O₂ into its metal hydride precursor. As shown in Scheme 20, the metal hydride was exposed to molecular oxygen and cleanly produced the pincer-based metal hydroperoxide, ^tBuPCP-Pd-OOH **41**.⁸⁵ The ^tBuPCP-Pd-OOH complex **41** was characterized by ¹H NMR and ³¹P NMR spectroscopies, as well as single crystal X-ray crystallography. The reaction was further investigated and showed no signs of proceeding via a radical mechanism as the added inhibitors and initiators had no effect on the rates.⁸⁵ As well, the rates were identical if the insertion reactions were performed in the dark or in the light. In the same year, Stahl also generated a Pd-based hydroperoxide, *trans*-[Pd(OOH)(O₂CR)(IMes)₂], (IMes = mesityl/carbene ligand), with O₂ and also concluded that the reaction proceeded via a non-radical pathway.⁹⁹



Scheme 20. Synthesis of ^tBuPCP-Pd-OOH **41**

With the proven successful generation and isolation of various metal hydroperoxides via insertion of molecular oxygen into their metal hydride bonds, this strategy was used exclusively in the investigation of the new Rh PNP-based hydrides. The protocol used for the oxygen insertion reactions followed the approach used for the synthesis of **41**, which involved placing a small amount of metal hydride into a medium-walled J. Young NMR tube and dissolving it into an appropriate amount of deuterated solvent. The NMR tube was then attached onto a specifically-designed apparatus which was connected to a Schlenk line. The apparatus allowed for manipulation of the NMR tube under air-sensitive conditions. The NMR tube was then freeze-thawed three times using liquid nitrogen in order to remove any residual oxygen from the solution. The system was then pressurized with 5 atm of O₂ and monitored by ³¹P and ¹H NMR spectroscopy.



Scheme 21. Attempted Syntheses of PNP Rh Hydroperoxides

For example, a small amount of **37** was placed into a J. Young NMR tube and a small volume of benzene d_6 was added, resulting in a red solution. Upon addition of 5 atm of O_2 to the system, the red solution turned green. The solution was then monitored for several minutes with no further observable change in color. The $^{31}P\{^1H\}$ NMR spectrum of the greenish solution showed the disappearance of the doublet at 83.2 ppm for **37** and the appearance of two signals at 62.5 and 56.8 ppm. The disappearance of the doublet indicates that the phosphine donor atoms are no longer bound to the Rh metal center due to the absence of any Rh coupling. The 1H NMR spectrum showed the disappearance of the doublet of triplets for the hydride peak at -12.84 ppm. With the presence of the two unknown signals and the absence of a signal for the free ligand **19** at 37.5 ppm in the $^{31}P\{^1H\}$ NMR spectrum, it is apparent that the rhodium complex has undergone decomposition with the formation of an oxidized Rh(III) species and/or possibly an unknown phosphine-containing species. Changes in the pressure of O_2 introduced into the system - lowering to 1 atm and atmospheric pressure bubbling - also showed comparable results. Similar results

occurred when either **38** or **39** was reacted with varying pressures of O₂. In both cases, we observed the disappearance of the doublet in the ³¹P{¹H} NMR spectrum and the hydride peak in the ¹H NMR spectrum.

2.4 Concluding Remarks

The discussion in Chapter 2 describes the investigation of preparing new ^RPNP-Rh-H complexes and examination of their reaction with molecular oxygen. The general route established for the synthesis of the pincer hydride complexes first involves the metalation of free ligands with a rhodium precursor that resulted in the PNP-Rh-Cl complexes. Literature precedent exists for the preparation of ^tBuPNP-Rh-Cl **28**, via direct cyclometalation, in moderate yields.⁷⁶ New ⁱPrPNP-Rh-Cl **29** and ^{Cy}PNP-Rh-Cl **30** complexes were prepared in a similar manner with high yields. The proposed catalytic cycle calls for the conversion of the ^RPNP-Rh-Cl complexes into metal hydrides via a hydride source. Common hydride sources were employed in screening reactions under varying conditions. However, we were unable to prepare the metal hydrides with this direct route, causing us to seek alternative methods.

With assistance from our collaborators in the Goldberg group, an alternative method for the synthesis of the new Rh hydrides was achieved. This multi-step process first involved the formation of a ^RPNP-Rh-OTf complex from the reaction of a rhodium dimer with silver triflate, followed by addition of the free ligand. This literature preparation resulted in the synthesis of ^tBuPNP-Rh-OTf **31** in high yields. The following new complexes, ⁱPrPNP-Rh-OTf **32** and ^{Cy}PNP-Rh-OTf **33**, were prepared in the same manner, both with excellent yields. These

complexes were then reacted with H₂, which oxidatively added to the metal center resulting in [R^RPNP-Rh(H)₂][OTf], (R = ^tBu **34**, ⁱPr **35**, and Cy **36**). The reaction was accomplished in a medium-walled J. Young NMR tube and the conversion was monitored by ³¹P{¹H} and ¹H NMR spectroscopy. These compounds were then used immediately in the next step, which involved using a base to deprotonate the complex to give the new rhodium hydrides, ^RPNP-Rh-H, (R = ^tBu **37**, ⁱPr **38**, and Cy **39**).

Upon generation of the metal-hydride complex, the next step involved insertion of molecular oxygen into the metal hydride bond. The metal hydrides were reacted with O₂ directly at several pressures; however, none showed direct insertion of O₂. The reactions were monitored by ³¹P{¹H} and ¹H NMR spectroscopy and revealed that the Rh(I) hydrides decompose and generate an oxidized Rh(III) species and/or an unknown phosphine-containing species.

2.5 Experimental

2.5.1 General Experimental

All procedures and manipulations were carried out under argon using an MBRAUN UL-03-143 glove box or by standard Schlenk techniques. All solvents used were of high purity (anhydrous) or were dried by using standard methods. All reagents were purchased from Acros, Aldrich, Alfa Aesar, or Strem and were used as received. [Rh(COE)₂Cl]₂,¹⁰⁰ ^tBu¹⁰⁰PNP-Rh-Cl **28**,⁷⁶ ^tBu⁷⁶PNP-Rh-OTf **31**,⁸⁸ 2,6-bis(di-*tert*-butylphosphinomethyl)pyridine (^tBuPNP) **19**,⁷⁶ 2,6-bis(di-*iso*-propylphosphinomethyl)pyridine (ⁱPrPNP) (**23**),⁷⁹ 2,6-bis(dicyclohexylphosphinomethyl)pyridine (^{Cy}PNP) (**21**),⁷⁷ 2,6-

bis(diphenylphosphinomethyl)pyridine (^{Ph}PNP) (**22**),⁷⁸ were prepared according to literature procedures.

NMR spectra were obtained at room temperature on a Bruker AMX 250 MHz spectrometer or on a Bruker AC 250 MHz spectrometer with a Tecmag MacSpect upgrade. All chemical shifts are reported in (δ) ppm with ¹H and ¹³C spectra referenced to tetramethylsilane or to their respective residual solvent peaks. ³¹P NMR spectra were referenced externally using 85% H₃PO₄ at δ 0 ppm. Elemental analyses were performed by Columbia Analytical Services of Tucson, AZ.

2.5.2 Crystallographic Determination

Data for X-ray crystallographic determination were collected and solved with the assistance of Dr. Eileen Duesler at the University of New Mexico and Dr. Diane Dickie of the Kemp research group. Crystallographic figures shown in this dissertation were generated using Diamond 3.1d.¹⁰¹

Crystallographic data were collected on a Bruker X8 APEX CCD-based X-ray diffractometer using monochromated Mo-K α radiation ($\lambda = 0.71073 \text{ \AA}$). The single crystals were coated in oil (Paratone-NTM) and mounted on nylon cryoloops (Hampton Research). Bruker APEX2 was used to collect and process the data.¹⁰² The structures were solved by either the direct or Patterson method with XSHL and were refined by full matrix least-squares method on F² with SHELXTL.¹⁰³ All non-hydrogens were refined anisotropically and hydrogen atoms were fixed at calculated geometric positions. PLATON squeeze was used to treat

disordered solvent molecules. All crystallographic data are located in the Appendix.

2.5.3 Synthesis of Rhodium Compounds

ⁱPrPNP-Rh-Cl 29

[Rh(COE)₂Cl]₂ (1.97 g, 2.70 mmol) was placed into a round bottom flask along with 20 mL of benzene. ⁱPrPNP (1.86 g, 5.49 mmol) was dissolved in 5 mL benzene. The ⁱPrPNP/benzene solution was added dropwise to the stirring Rh solution. The reaction mixture was refluxed for 4 hrs. The volatiles were removed under reduced pressure, resulting in a dark red solid. The red solid was washed with pentane and dried under vacuum to give **29** (2.19 g, 83%). ¹H NMR (C₆D₆, 250.13 MHz): δ 7.04 (t, 1H, *J*_{HP} = 7.50, Ar), 6.43 (d, 2H, *J*_{HP} = 7.50, Ar), 2.50 (vt, 4H, CH₂), 2.09 (m, 4H, CHMe₂), 1.52 (dd, 12H, CHMe₂), 1.08 (dd, 12H, CHMe₂). ³¹P{¹H} NMR (C₆D₆, 101.26 MHz): δ 47.3 (d, *J*_{PRh} = 144.8). Observable ¹³C{¹H} NMR (C₆D₆, 250.13 MHz): δ 163.9 (vt, *J*_{CP} = 6.4, Ar), 129.4 (s, Ar), 120.1 (s, Ar), 35.8 (vt, *J*_{CP} = 5.8, CH₂), 24.2 (vt, *J*_{CP} = 9.4, CHMe₂), 19.3 (s, CHMe₂), 18.0 (s, CHMe₂).

^{Cy}PNP-Rh-Cl 30

[Rh(COE)₂Cl]₂ (0.060 g, 0.084 mmol) was placed into a round bottom flask along with 15 mL of benzene. ^{Cy}PNP (0.084 g, 0.167 mmol) was dissolved in 5 mL benzene. The ^{Cy}PNP/benzene solution was added dropwise to the stirring Rh solution. The reaction mixture was refluxed for 2 hrs. The volatiles were removed under reduced pressure, resulting in a dark red solid. The red solid was washed

with pentane and dried under vacuum to give **30** (0.097 g, 91%). ^1H NMR (C_6D_6 , 250.13 MHz): δ 6.99 (t, 1H, $J_{\text{HP}} = 8.00$, Ar), 6.42 (d, 2H, $J_{\text{HP}} = 7.75$, Ar), 2.59 (vt, 4H, $J_{\text{HP}} = 3.25$, CH_2), 2.10 – 1.01 (m, 44H, Cy). $^{31}\text{P}\{^1\text{H}\}$ NMR (C_6D_6 , 101.26 MHz): δ 38.9 (d, $J_{\text{PRh}} = 144.2$).

[^tBuPNP-Rh(H)₂][OTf] **34**

31 (0.017 g, 0.026 mol) was placed into a J.Young NMR tube along with 0.4 mL of benzene- d_6 , resulting in red/orange solution. The system was pressurized with 1 atm of H_2 and monitored for six days via NMR spectroscopy. The reaction resulted in a clear pale yellow solution containing **34**. ^1H NMR (C_6D_6 , 250.13 MHz): δ 7.71 (d, 2H, $J_{\text{HP}} = 7.75$, Ar), 7.52 (t, 1H, $J_{\text{HP}} = 7.75$ Ar), 3.82 (vt, 4H, CH_2), 1.08 (vt, 36H, $J_{\text{HP}} = 6.75$, $\text{C}(\text{CH}_3)_3$), -13.92 (bs, 2H, H_2). $^{31}\text{P}\{^1\text{H}\}$ NMR (C_6D_6 , 101.26 MHz): δ 81.5 (d, $J_{\text{PRh}} = 118.2$).

^tBuPNP-Rh-H **37**

The contents of the J. Young NMR tube containing **34** (0.026 mmol) were transferred into a 50 mL round bottom flask. The NMR tube was washed with 0.4 mL of benzene and transferred to the round bottom flask. K^tBuO (0.003 g, 0.026 mmol) was placed into the flask along with 5 mL of benzene. The reaction mixture was stirred for 1 hr, filtered through a bed of Celite, and evaporated to dryness under reduced pressure resulting in a red solid. The red solid was dried under vacuum to give **37** (0.01 g, 77%). ^1H NMR (C_6D_6 , 250.13 MHz): δ 7.09 (t, 1H, $J_{\text{HP}} = 7.69$, Ar), 6.58 (d, 2H, $J_{\text{HP}} = 7.69$, Ar), 2.93 (vt, 4H, CH_2), 1.39 (vt, 36H,

$J_{HP} = 5.98$, $C(CH_3)_3$, -12.84 (dt, 1H, $J_{HRh} = 19.01$ and $J_{HP} = 20.01$, Rh-H). $^{31}P\{^1H\}$ NMR (C_6D_6 , 101.26 MHz): δ 83.2 (d, $J_{PRh} = 165.6$).

iPr PNP-Rh-OTf 32

$[Rh(COE)_2Cl]_2$ (0.106 g, 0.148 mmol) was placed into a round bottom flask along with $Ag(OTf)$ (0.070 g, 0.295 mmol) and 20 mL of THF. The reaction mixture was stirred for 15 minutes, filtered through Celite, and iPr PNP (0.100 g, 0.295 mmol) was immediately added to the filtrate. The solution was stirred for 30 minutes and evaporated to dryness under reduced pressure resulting in a red/orange solid. The red/orange solid was washed with pentane and dried under vacuum to give **32** (0.17 g, 97%). 1H NMR (C_6D_6 , 250.13 MHz): δ 7.85 (d, 2H, $J_{HP} = 7.50$, Ar), 7.55 (t, 1H, $J_{HP} = 7.75$, Ar), 3.49 (vt, 4H, CH_2), 1.81 (m, 4H, $CHMe_2$), 1.43 (dd, 12H, $CHMe_2$), 0.94 (dd, 12H, $CHMe_2$). $^{31}P\{^1H\}$ NMR (C_6D_6 , 101.26 MHz): δ 45.9 (d, $J_{PRh} = 130.9$).

$[iPr$ PNP-Rh(H) $_2$][OTf] 35

32 (0.015 g, 0.025 mmol) was placed into a J. Young NMR tube along with 0.4 mL of benzene- d_6 resulting in a red solution. The system was pressurized with 1 atm of H_2 and monitored for 24 hrs via NMR spectroscopy. The reaction resulted in a clear pale yellow solution containing **35**. 1H NMR (C_6D_6 , 250.13 MHz): δ 6.97 (t, 1H, $J_{HP} = 7.50$, Ar), 6.63 (d, 2H, $J_{HP} = 6.75$, Ar), 3.59 (vt, 4H, CH_2), 2.17 (m, 4H, $CHMe_2$), 1.46 (dd, 12H, $CHMe_2$), 1.03 (dd, 12H, $CHMe_2$), -18.95 (bs, 2H, H_2). $^{31}P\{^1H\}$ NMR (C_6D_6 , 101.26 MHz): δ 66.1 (d, $J_{PRh} = 113.9$).

ⁱPrPNP-Rh-H **38**

The contents of the J. Young NMR tube containing **35** (0.025 mmol) were transferred into a 50 mL round bottom flask. The NMR tube was washed with 0.4 mL of benzene and transferred to the round bottom flask. K^tBuO (0.003 g, 0.025 mmol) was placed into the flask along with 5 mL of benzene. The reaction mixture was stirred for 3 hrs, filtered through a bed of Celite, and evaporated to dryness under reduced pressure, resulting in a red solid. The red solid was dried under vacuum to give **38** (0.08 g, 73%). ¹H NMR (C₆D₆, 250.13 MHz): δ 7.07 (t, 1H, *J*_{HP} = 6.84, Ar), 6.58 (d, 2H, *J*_{HP} = 7.69, Ar), 2.82 (vt, 4H, *J*_{HP} = 3.42, CH₂), 1.93 (m, 4H, CHMe₂), 1.34 (dd, 12H, CHMe₂), 1.09 (dd, 12H, CHMe₂), -13.12 (dt, 1H, *J*_{HRh} = 17.94 and *J*_{HP} = 22.22, Rh-H). ³¹P{¹H} NMR (C₆D₆, 101.26 MHz): δ 61.7 (d, *J*_{PRh} = 163.5).

^{Cy}PNP-Rh-OTf **33**

[Rh(COE)₂Cl]₂ (0.302 g, 0.421 mmol) was placed into a round bottom flask along with Ag(OTf) (0.220 g, 0.842 mmol), and 30 mL of THF. The reaction mixture was stirred for 15 minutes, filtered through Celite, and ^{Cy}PNP (0.420 g, 0.842 mmol) was immediately added to the filtrate. The solution was stirred for 30 minutes and evaporated to dryness under reduced pressure, resulting in an orange solid. The orange solid was washed with pentane and dried under vacuum to give **33** (0.61 g, 95%). ¹H NMR (C₆D₆, 250.13 MHz): δ 7.98 (d, 2H, *J*_{HP}

= 7.75, Ar), 7.58 (t, 1H, $J_{HP} = 7.75$, Ar), 3.68 (vt, 4H, CH₂), 2.42 – 0.85 (m, 44H, Cy). ³¹P{¹H} NMR (C₆D₆, 101.26 MHz): δ 36.9 (d, $J_{PRh} = 129.2$).

[^{Cy}PNP-Rh(H)₂][OTf] **36**

33 (0.020 g, 0.027 mmol) was placed into a J. Young NMR tube along with 0.4 mL of benzene-*d*₆, resulting in a red solution. The system was pressurized with 1 atm of H₂ and monitored for 24 hrs via NMR spectroscopy. The reaction resulted in a clear pale yellow solution containing **36**. ¹H NMR (C₆D₆, 250.13 MHz): δ 7.06 (t, 1H, $J_{HP} = 7.25$, Ar), 6.74 (d, 2H, $J_{HP} = 7.50$, Ar), 3.73 (vt, 4H, CH₂), 2.40 – 1.01 (m, 44H, Cy), -18.80 (bs, 2H, RhH₂). ³¹P{¹H} NMR (C₆D₆, 101.26 MHz): δ 56.9 (d, $J_{PRh} = 113.7$).

^{Cy}PNP-Rh-H **39**

The contents of the J. Young NMR tube containing **36** (0.027 mmol) were transferred into a 50 mL round bottom flask. The NMR tube was washed with 0.4 mL of benzene and transferred to the round bottom flask. K^tBuO (0.003 g, 0.025 mmol) was placed into the flask along with 5 mL of benzene. The reaction mixture was stirred for 3 hrs, filtered through a bed of Celite, and evaporated to dryness under reduced pressure resulting in a red solid. The red solid was dried under vacuum to give **39** (0.01 g, 63%). ¹H NMR (C₆D₆, 250.13 MHz): δ 7.10 (t, 1H, $J_{HP} = 7.32$, Ar), 6.65 (d, 2H, $J_{HP} = 7.32$, Ar), 2.94 (vt, 4H, CH₂), 2.40 – 1.03 (m, 44H, Cy), -13.12 (dt, 1H, $J_{HRh} = 18.31$ and $J_{HP} = 22.89$, Rh-H). ³¹P{¹H} NMR (C₆D₆, 101.26 MHz): δ 52.2 (d, $J_{PRh} = 162.1$).

Chapter 3

3.1 Syntheses of Symmetric PNP Free Ligands and Complexes

With the success of generating rhodium hydrides with neutral PNP-based ligands, the next approach was to incorporate anionic PNP ligands into metal complexes for optimization of the proposed catalytic cycle. The number of anionic PNP ligands was limited to Fryzuk's silyl-based ligands (**A**) until the reports of PNP ligands with aliphatic linkers (**B**), and more recently *o*-arylene units between the N and P positions (**C**). Fryzuk's pioneering work in developing a chelating amido phosphine ligand (**A**) with a $-\text{SiCH}_2\text{CH}_2-$ backbone was shown by the formation of complexes throughout the periodic table.¹⁰⁴⁻¹¹¹

In 2003, Kaska¹¹² and Liang¹¹³, independently developed the same diphenyldiarylamido phosphine ($^{\text{Ph}}\text{PNP}$) ligand (type **C**) through different synthetic approaches, both with the intent of creating a more robust and rigid chelating amidophosphine ligand with *o*-arylene components. The idea behind the new ligand design was to remedy several drawbacks associated with ligand **A**. One major issue associated with ligand **A** is the high oxophilicity of the silyl backbone, which unfortunately often led to undesired results.¹¹⁴⁻¹¹⁶ Another issue arises from the flexibility of the backbone, when under certain circumstances can lead to phosphine dissociation from the metal.¹¹⁷ Eventually, derivatives containing various substituents on the phosphorus donor atoms of **C** were prepared in order to study their steric and electronic properties.

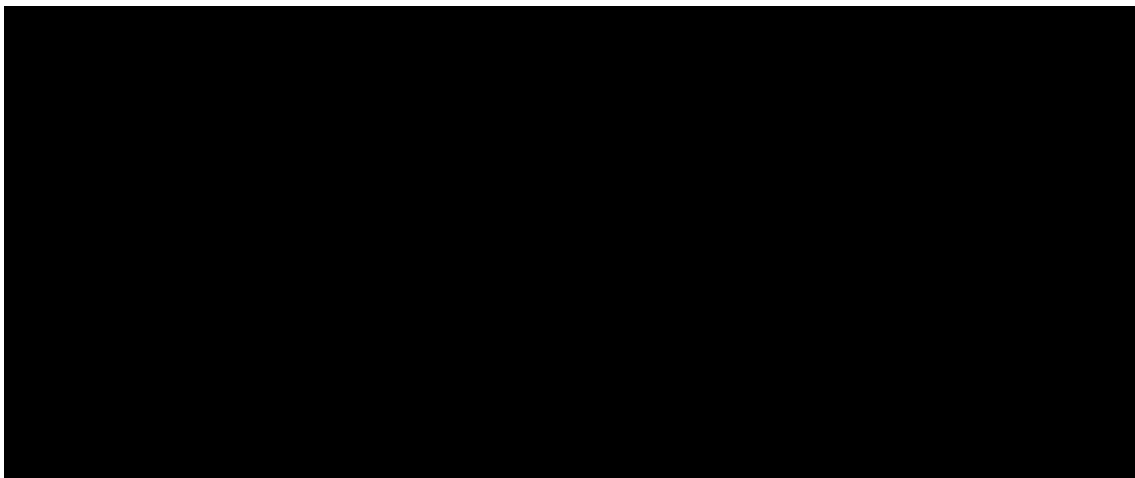
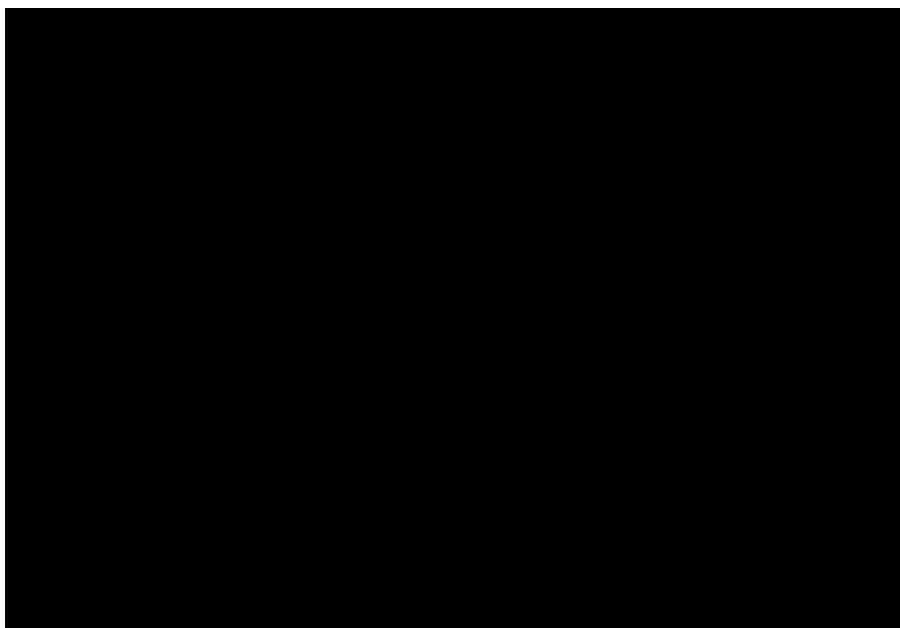


Figure 12. Examples of PNP-based Ligands

In 2004, Ozerov developed a tolyl-based amidophosphine ligand (**D**) with similar intentions of overcoming the shortcomings associated with **A**. As shown in Scheme 22, the general route for the production of this type of PNP ligand first involves the synthesis of bis(2-bromo-4-methylphenyl)amine **43** from the bromination of di-*p*-tolylamine.¹¹⁸ Lithium-bromine exchange was then employed followed by selective phosphination and hydrolysis to afford compound **44** as a pale white solid in 56% yield.⁴⁶



Scheme 22. Preparation of ^{iPr}PNP **44, ^{Cy}PNP **45**, and ^{Ph}PNP **46****

Compound **45** was generated in a similar manner as an off-white solid in 39% yield. The ³¹P{¹H} NMR spectrum of **45** exhibits a broad singlet at – 20.7 ppm, indicating symmetry within the ligand. The ¹H NMR spectrum of **45** displays a triplet at 8.26 ppm with a $J_{HP} = 8.25$ Hz for the N-*H* proton. The solid-state structure of **45** was determined by X-ray diffraction (Figure 13). A single crystal suitable for X-ray diffraction analysis was grown from a concentrated solution of **45** in diethyl ether at - 30 °C. A list of selected bond lengths and bond angles of **45** are shown in Table 5. The crystal structure of **45** exhibits the characteristic deviation from planarity of the ligand backbone, which is also found in other structurally-characterized PNP-based free ligands and is result of the repulsion between the *ortho* hydrogens on the aromatic rings

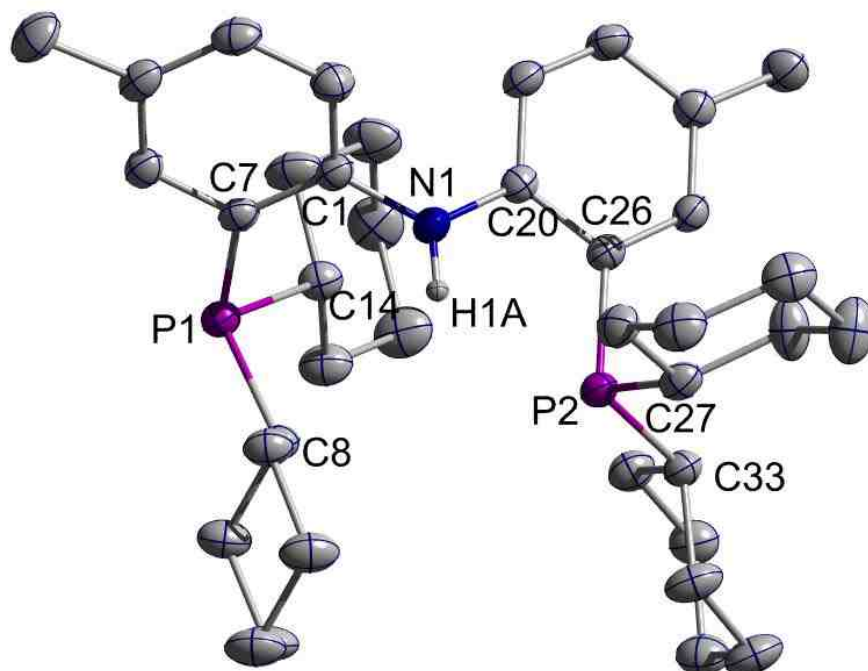


Figure 13. Thermal Ellipsoid Plot of 45 Shown at 50% Probability Level with Hydrogens Omitted for Clarity

Table 5. Selected Bond Lengths and Angles for Compound 45

Bond Lengths (Å)

Atom1	Atom2	Distance
P1	C7	1.839(2)
P1	C8	1.865(2)
P1	C14	1.861(2)
P2	C26	1.842(2)
P2	C27	1.860(2)
P2	C33	1.852(2)
N1	C1	1.408(3)
N1	C20	1.398(3)
N1	H1A	0.880(2)

Bond Angles (°)

Atom 1	Atom 2	Atom 3	Angle
C7	P1	C8	105.71(9)
C7	P1	C14	102.32(9)
C8	P1	C14	102.51(9)
P1	C7	C1	128.2(1)
C1	N1	H1A	116.8(2)
C20	N1	H1A	116.8(2)
C1	N1	C20	126.3(2)
C26	P2	C27	102.04(9)
C26	P2	C33	104.64(9)
C27	P2	C33	103.65(9)
P2	C26	C20	117.7(1)

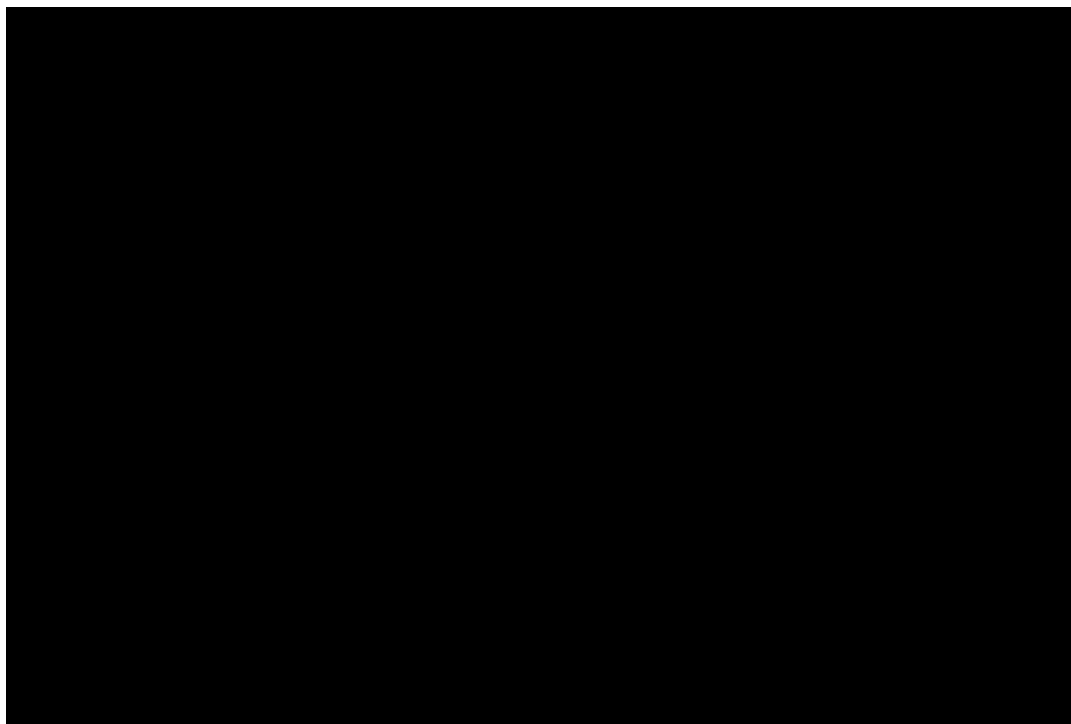
At an earlier stage in this project, compound **46** was synthesized in a similar manner as **44** in moderate yield (67%). The $^{31}\text{P}\{^1\text{H}\}$ NMR spectrum of **46** is also consistent with an average C_{2v} symmetry in solution, showing a single resonance at -18.8 ppm. The ^1H NMR spectrum of **46** displays a triplet at 7.07 ppm with $J_{\text{HP}} = 6.1$ Hz for the N-*H* proton. In 2008, after we had independently prepared **46**, Kiplinger reported the synthesis of **46** in a similar manner with the same NMR results.¹¹⁹

Also mentioned in the 2004 paper by Ozerov was the development of a palladium PNP halide complex, $^{\text{iPr}}\text{PNP-Pd-Cl}$ **47**, from the diarylamine-based PNP ligand **44**.⁴⁶ Complex **47** was synthesized from ligand **44** and the metal precursor (COD) PdCl_2 . The COD is easily displaced, followed by coordination of the phosphines to the metal center to generate a solution of $^{\text{iPr}}\text{PNPH-Pd-Cl}_2$.⁴⁶ The addition of a base, NEt_3 , allows for the conversion to **47**. The loss of HCl in the absence of added base has been seen in other reactions between palladium precursors and PCP ligands.^{28, 42, 75, 120-122} In the case of PCP-M-Cl complexes, it

is believed that the HCl generated protonates the donor atoms of other free ligands and prohibits coordination to other metals. The addition of NEt₃ increases the yields in these metalation reactions.¹²³⁻¹²⁵

The behavior exhibited from the dichloropalladium complex also occurs in the other forms of PNP type ligands mentioned earlier. Reactions of ligand **A** with other metal precursors (M = Ni, Pd, Pt) generate similar complexes, ((Ph₂PCH₂SiMe₂)₂NH)MCl₂, without the immediate loss of HCl.¹²⁶ Complexes formed from ligand **B** and other palladium precursors also show similar behavior such as [(Ph₂PNH-PPh₂)PdCl]Cl.^{127, 128}

As shown in Scheme 23, the generation of the metal halides reported here utilize reactions similar to those reported by Ozerov. Both the PNP ligand and metal precursor were placed into a round-bottom flask with one equivalent of triethylamine and 20 mL of THF. The reaction mixture was then refluxed for one hour at 80 °C. In the case of the platinum complexes, the reaction required two hours of reflux time at 90 °C. The workup resulted in high yields of red/purple solids for the palladium PNP halides and yellow/orange solids for the platinum PNP halides.



Scheme 23. Preparation of ^{iPr}PNP-M-Cl and ^{Cy}PNP-M-Cl

Compound **48** (^{Cy}PNP-Pd-Cl) was isolated as a red solid in 82% yield. The ³¹P{¹H} NMR data of **48** are consistent with an average C_{2v} symmetry in solution with the resonance showing a singlet at 40.6 ppm. The metalation is confirmed by the disappearance of the N-*H* proton chemical resonance at 8.26 ppm. X-ray diffraction analysis was also used to confirm the molecular structure of **48**. A single crystal suitable for X-ray study (Figure 14) was grown from the slow evaporation of a benzene solution at room temperature. A list of selected bond lengths and bond angles of **48** are shown in Table 6. The X-ray crystal structure exhibits a distorted square planar geometry around the palladium metal center with a P-Pd-P angle of 165.83(3)°, similar to that seen in **47** (163.54(2)°). The deviation from an ideal square planar geometry can be attributed to the

constraint imposed by the chelating PNP ligand, which is also seen in other known PNP metal halides.^{46,129} One other significant observation from the crystal structure is the deviation from planarity of the chelate backbone, also found in other structurally-characterized palladium PNP halides.¹²⁹ This deviation can be attributed to the preferred staggered conformation of the phosphine substituents and the repulsion between the *ortho* hydrogens on the aromatic rings.¹²⁹

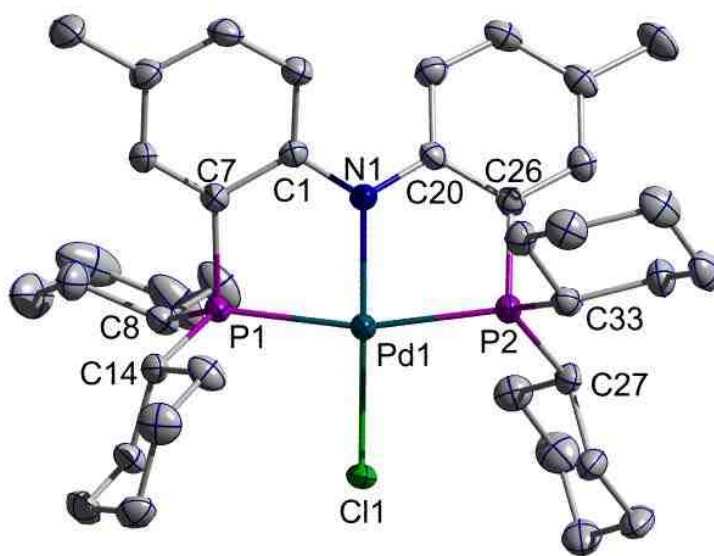


Figure 14. Thermal Ellipsoid Plot of 48 Shown at 50% Probability Level with Hydrogens Omitted for Clarity

Table 6. Selected Bond Lengths and Angles for Compound 48

Bond Lengths (Å)

Atom 1	Atom 2	Distance
Pd1	Cl1	2.331(8)
Pd1	P1	2.289(7)
Pd1	P2	2.284(7)
Pd1	N1	2.024(3)
P1	C7	1.809(3)
P1	C8	1.838(3)
P1	C14	1.841(3)
P2	C26	1.810(3)
P2	C27	1.836(3)
P2	C33	1.838(3)

Bond Angles (°)

Atom1	Atom 2	Atom3	Angle
P2	Pd1	P1	165.83(3)
N1	Pd1	Cl1	178.86(7)
Cl1	Pd1	P1	96.33(3)
Cl1	Pd1	P2	97.78(3)
N1	Pd1	P1	83.14(7)
N1	Pd1	P2	82.73(7)
Pd1	P1	C7	98.58(9)
Pd1	P1	C8	115.3(1)
Pd1	P2	C26	98.8(1)
Pd1	P2	C33	116.8(1)
C1	N1	Pd1	117.8(2)
C20	N1	Pd1	118.7(2)

Compound **49** (^{Ph}PNP-Pd-Cl) was prepared via two different methods. The first method followed the procedure used to generate the previous palladium PNP halides. A purple solid was generated in varying yields. The reaction did not go to completion after one hour of reflux at 80°C and required additional reflux

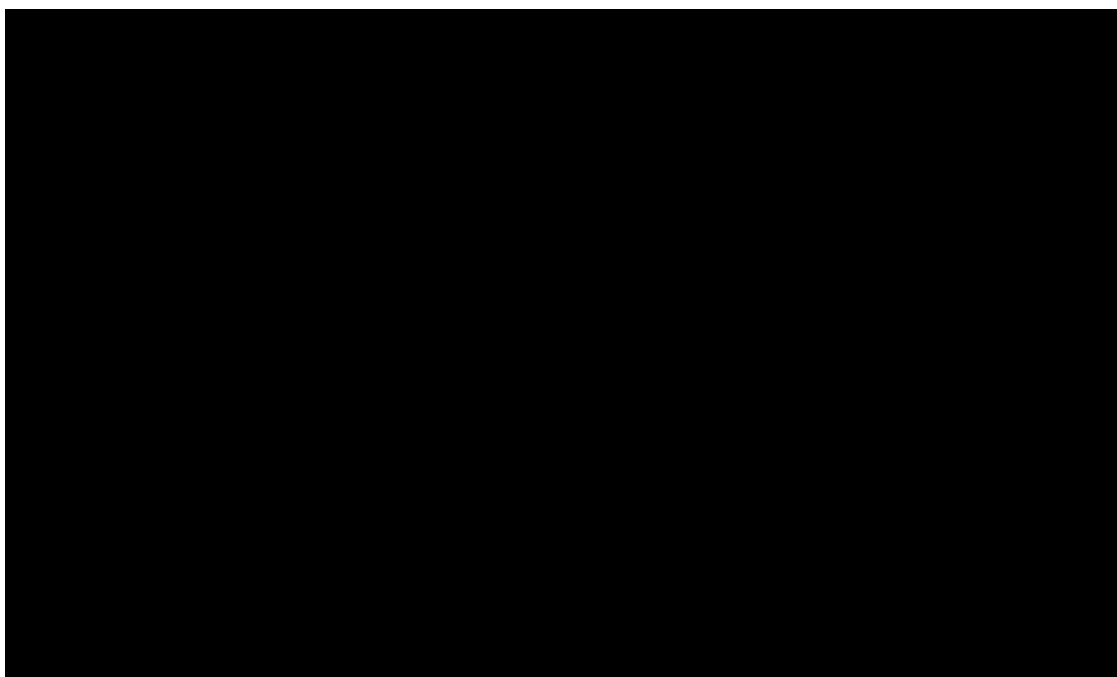
time. This can be attributed to the smaller donating ability of the phosphorus donor atoms that bear aryl substituents. The yields of the desired product ranged from 40% to 81%. The $^{31}\text{P}\{^1\text{H}\}$ NMR spectrum of **49** displayed a singlet at 29.8 ppm which is also indicative of an average C_{2v} symmetry in solution and an approximate square planar geometry around the metal center.

An alternative method for the preparation of compound **49** resulted in complete conversion and higher yields. A transmetalation route was used for the synthesis of **49** that was related to Liang's procedure also used for the synthesis of a diaryldiphenylphosphino palladium chloride complex.⁴⁷ A lithium amide complex, $(^{\text{Ph}}\text{PNP})\text{Li}(\text{THF})_2$, was first prepared from *n*-BuLi and $^{\text{Ph}}\text{PNP}$ **46** and was isolated as a yellow solid. This yellow solid was then allowed to react with $\text{Cl}_2\text{Pd}(\text{PhCN})_2$ at -35 °C to afford **49** as a dark red solid in 92% yield after workup. The $^{31}\text{P}\{^1\text{H}\}$ NMR data was identical with that seen in the first method used to prepare **49**.

Compound **51** ($^{\text{Cy}}\text{PNP-Pt-Cl}$) was prepared in a similar manner as **50** as a yellow solid in 78% yield. The $^{31}\text{P}\{^1\text{H}\}$ NMR spectrum of **51** exhibits a resonance at 33.8 ppm with $J_{\text{PPt}} = 2666.6$ Hz, indicating an approximate square planar geometry (C_{2v} symmetry) about the platinum center. The J_{PPt} values are characteristic of square planar Pt^{II} complexes with *trans*-spanning phosphines.³²

As mentioned in Chapter 2, the general scheme for the synthesis of the potential catalyst in the proposed cycle calls for the conversion of a metal halide to a metal hydride via a hydride source. Mentioned in the seminal 1976 journal article by Moulton and Shaw was the conversion of a PCP-Pd-Cl species to PCP-

Pd-H complex using a hydride source.²⁸ In that case, the hydride source was sodium borohydride (NaBH₄) and the product was produced in a 95% yield.²⁸ That procedure was also used by Ozerov to convert **47** to ^{iPr}PNP-Pd-H **52**.⁴⁶ As shown in Scheme 24, the generalized synthetic plan calls for the addition of a hydride source to the metal halide to generate the metal hydride. In the synthesis of **52**, NaBH₄ was added to the metal halide and heated at 80 °C in THF for 10 hours in a closed system. After the workup, a brown solid was isolated in a 65% yield.⁴⁶



Scheme 24. Preparation of ^{iPr}PNP-M-H and ^{Cy}PNP-M-H

Several other potential hydride sources were screened for this reaction. In the synthesis of ^{Cy}PNP-Pd-H **53**, a Super Hydride solution (1.0 M LiHBEt₃ in THF) was added via syringe to a cooled - 35 °C solution of **48** in THF and allowed to stir at RT for 3.5 hrs. After the workup, a brown solid was isolated in

74% yield. The $^{31}\text{P}\{^1\text{H}\}$ NMR spectrum of **53** reveals a singlet at 50.4 ppm indicating an average C_{2v} symmetry in solution and an approximate square planar geometry around the metal center. The ^1H NMR spectrum of **53** exhibits a triplet at -10.22 ppm with $J_{\text{HP}} = 7.0$ Hz, indicating the presence of Pd-H moiety. The molecular structure of **53** was determined by X-ray diffraction analysis (Figure 15). A single crystal suitable for X-ray diffraction was grown from a concentrated solution of **53** in pentane at -30 °C. A list of selected bond lengths and bond angles of **53** are shown in Table 7. When attempting to solve the crystal structure of **53**, the hydride ligand could not accurately be located and refined, but its presence is known with certainty as shown by the ^1H NMR data. The single crystal X-ray results indicate an approximate square planar geometry around the palladium center with a P-Pd-P angle of 166.87° , as compared to $165.83(3)^\circ$ for **48**. This widening of the bond angle corresponds to the presence of a slightly less sterically-bulky ligand as $\text{H} < \text{Cl}$ in size. The Pd-N bond distance of **53** (2.096 Å) is slightly elongated from that of **48** ($2.024(3)$ Å), which can be attributed to the *trans*-influence of the hydride ligand. All other noted bond distances show no remarkable differences from other related compounds.

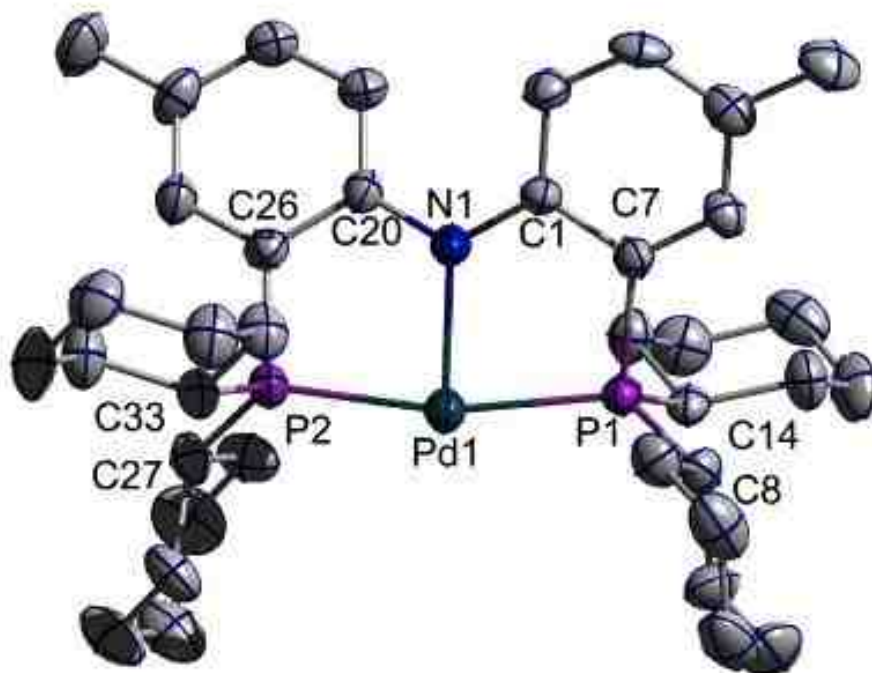


Figure 15. Thermal Ellipsoid Plot of 53 Shown at 50% Probability Level with Hydrogens Omitted for Clarity

Table 7. Selected Bond Lengths and Angles for Compound 53

Bond Lengths (Å)

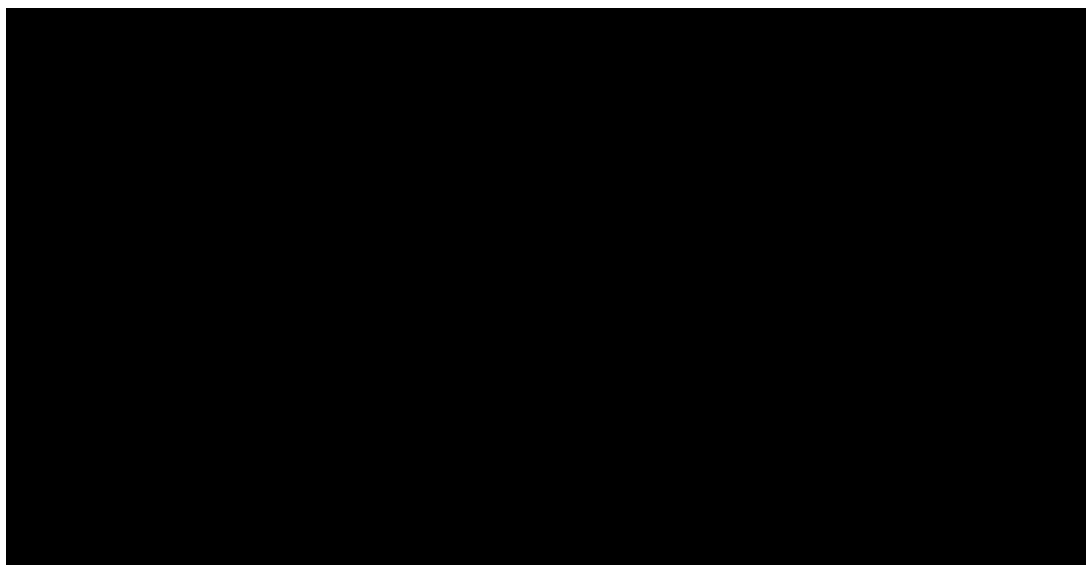
Atom 1	Atom 2	Distance
Pd1	P1	2.252
Pd1	P2	2.259
Pd1	N1	2.096
P1	C7	1.818
P1	C8	1.835
P1	C14	1.839
P2	C26	1.808
P2	C27	1.828
P2	C33	1.832

Bond Angles (°)

Atom1	Atom 2	Atom3	Angle
P2	Pd1	P1	166.87
N1	Pd1	P1	83.03
N1	Pd1	P2	83.86
Pd1	P1	C7	99.95
Pd1	P1	C14	115.01
Pd1	P2	C26	99.29
Pd1	P2	C33	115.44
C1	N1	Pd1	117.95
C20	N1	Pd1	118.09

3.2 Syntheses of Unsymmetric PNP Free Ligands and Complexes

One unique and attractive feature of these pincer ligands is their potential for steric and electronic modification. Aside from investigating symmetric ligands and metal complexes described in previous sections, there is also interest in examining unsymmetric ligands and complexes. Unsymmetric PNP ligands contain a different pair of R groups ($^R\text{PNP}^{R'}$) on each phosphorus atom. The unsymmetric ligands, $^{\text{Ph}}\text{PNP}^{\text{iPr}}$ **56** and $^{\text{Ph}}\text{PNP}^{\text{Cy}}$ **57** were prepared following the literature procedure (Scheme 25) developed by Liang.¹³⁰ The key step in the reaction sequence is the addition of the dialkylchlorophosphine (R_2PCl) before the diphenylchlorophosphine (Ph_2PCl) due to the higher electrophilic character of the diphenylchlorophosphine.¹³⁰ The reverse addition leads to a mixture of products, such as $^{\text{Ph}}\text{PNP}$ and $^{\text{Ph}}\text{PNP}^{\text{R}}$. The workup of the reaction mixtures led to an orange brown oil, which was then dissolved in diethyl ether, layered with pentane (3:1), and cooled to $-35\text{ }^\circ\text{C}$. This resulted in relatively low yields of a pale yellow solid.



Scheme 25. Preparation of ^{Ph}PNP^{iPr} **56 and ^{Ph}PNP^{Cy} **57****

Compound **56** has been successfully prepared in 39% yield and fully characterized by ¹H, ¹³C, and ³¹P NMR spectroscopy, elemental analysis, and X-ray crystallography. The ³¹P{¹H} NMR spectrum of compound **56** exhibits two distinct chemical shifts - a broad singlet at -14.5 ppm (PⁱPr₂) and a doublet at -16.5 ppm (PPh₂) with a $J_{PP} = 8.1$ Hz, indicating inequivalency among the phosphorus atoms. The ¹H NMR spectrum of **56** displays a doublet of doublets at 7.66 ppm with a $J_{HP} = 10.5$ Hz and $J_{HP} = 3.2$ Hz for the N-*H* proton. The solid-state structure of **56** was determined by X-ray diffraction (Figure 16). A single crystal suitable for X-ray diffraction analysis was grown from a concentrated solution of **56** in diethyl ether at -30 °C. A list of selected bond lengths and bond angles of **56** are shown in Table 8.

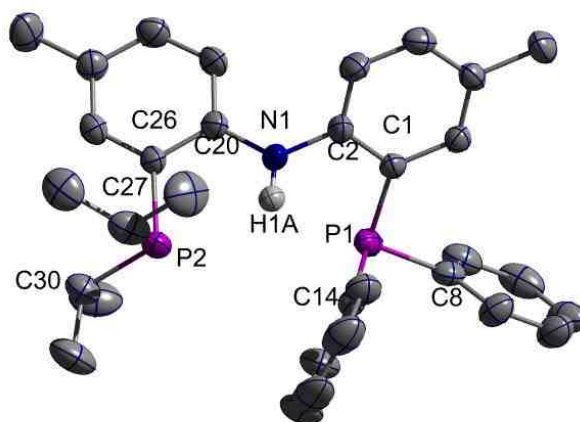


Figure 16. Thermal Ellipsoid Plot of 56 Shown at 50% Probability Level with Hydrogens Omitted for Clarity

Table 8. Selected Bond Lengths and Angles for Compound 56

Bond Lengths (Å)

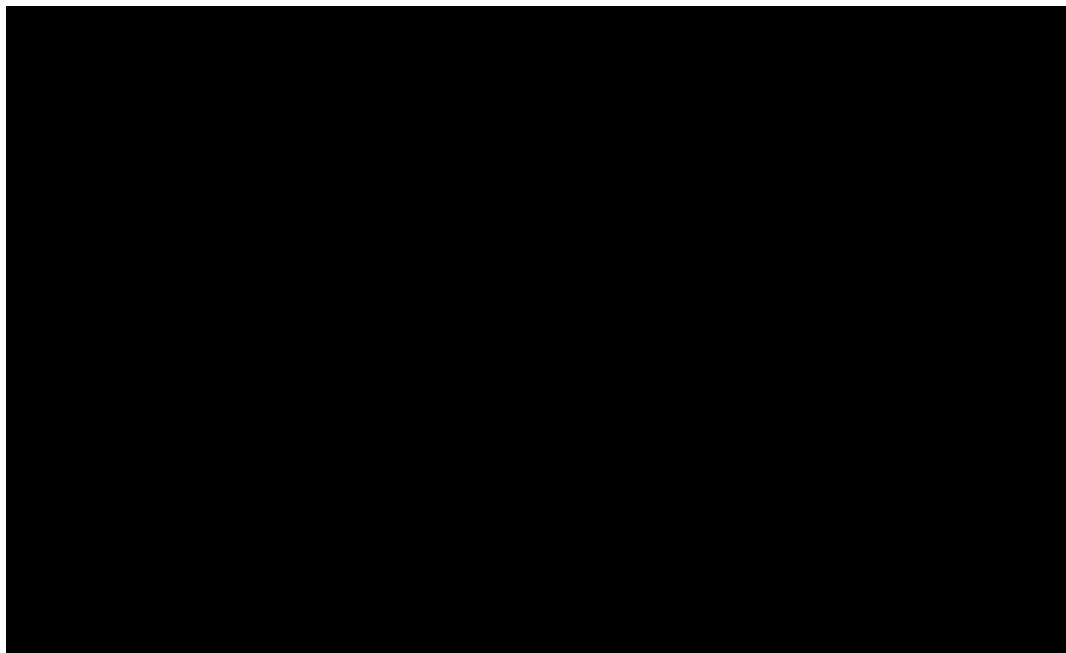
Atom 1	Atom 2	Distance
P1	C1	1.833(3)
P1	C8	1.825(3)
P1	C14	1.840(3)
P2	C26	1.840(2)
P2	C27	1.854(3)
P2	C30	1.847(3)
N1	C2	1.412(3)
N1	C20	1.397(3)
N1	H1A	0.869(2)

Bond Angles (°)

Atom1	Atom 2	Atom3	Angle
C1	P1	C8	103.25(11)
C1	P1	C14	102.41(13)
C26	P2	C27	102.40(1)
C26	P2	C30	103.52(1)
C20	N1	H1A	116.6(3)
C2	N1	H1A	116.6(3)
C2	N1	C20	126.8(2)

Compound **57** was produced in low yield (33%) and characterized by ^1H , ^{13}C , and ^{31}P NMR spectroscopy, elemental analysis, and X-ray crystallography. The $^{31}\text{P}\{^1\text{H}\}$ NMR spectrum of compound **57** exhibits two distinct chemical shifts as did **56** - a doublet at -16.3 ppm (PPh_2) with a $J_{\text{PP}} = 7.6$ Hz and a broad singlet at -23.8 ppm (PCy_2), indicating inequivalency among the phosphorus atoms. The ^1H NMR spectrum of **57** displays a doublet of doublets at 7.10 ppm with a $J_{\text{HP}} = 10.1$ Hz and $J_{\text{HP}} = 3.2$ Hz for the N-H proton. The $^{31}\text{C}\{^1\text{H}\}$ NMR spectra of **56** and **57** exhibited fewer resonances in the aromatic region than what was expected, most likely due to overlap of several signals.

The procedure used for the generation of the symmetric PNP metal halides was also implemented in the syntheses of metal halide complexes containing the unsymmetric PNP ligands. As shown in Scheme 26, the metal precursor and the PNP ligand were placed into a round bottom flask with one equivalent of NEt_3 and THF. The reaction mixture was then heated at the appropriate temperature and duration, resulting in the metal complexes in high yields.



Scheme 26. Preparation of $^{\text{Ph}}\text{PNP}^{\text{iPr}}\text{-M-Cl}$ and $^{\text{Ph}}\text{PNP}^{\text{Cy}}\text{-M-Cl}$

The synthesis of $^{\text{Ph}}\text{PNP}^{\text{iPr}}\text{-Pd-Cl}$ **58** required one hour of reflux time at 80°C , resulting in a 96% yield of a red solid. The $^{31}\text{P}\{^1\text{H}\}$ NMR spectrum of **58** reveals two signals corresponding to the two distinct phosphorus environments within the molecule. A doublet exists at 54.0 ppm with a $J_{\text{PP}} = 437.2$ Hz, corresponding to the phosphorus with the *iso*-propyl substituents. Another doublet exists further upfield at 25.7 ppm with a $J_{\text{PP}} = 437.2$ Hz, which corresponds to the other phosphorus environment (PPh_2). The large J_{PP} values for the two signals are characteristic of phosphines in the *trans* orientation, which suggests that the binding mode is similar to other PNP metal halides (square planar geometry).³² The solid-state structure of **58** was determined using X-ray diffraction analysis. A single crystal suitable for X-ray diffraction analysis was

grown from the slow evaporation of a benzene solution at room temperature. A list of selected bond lengths and angles of **58** are located in Table 9.

As shown in Figure 17, the geometry of **58** is confirmed to be approximately square planar around the metal center. The P-Pd-P angle is 163.72° , which is similar to the symmetric metal complexes **47** ($163.54(2)^\circ$) and **48** ($165.83(3)^\circ$). All other bond lengths and angles show no remarkable differences from previously-characterized related complexes

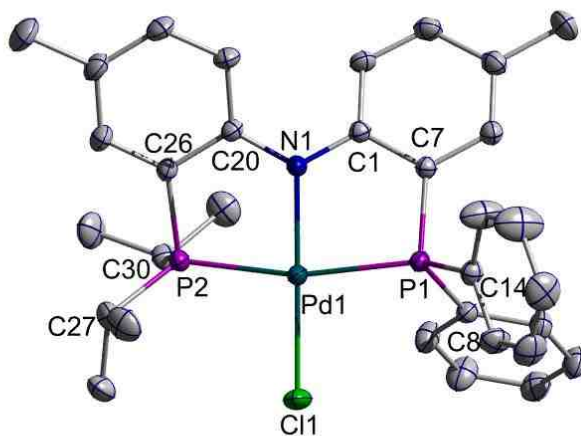


Figure 17. Thermal Ellipsoid Plot of 58 Shown at 50% Probability Level with Hydrogens Omitted for Clarity

Table 9. Selected Bond Lengths and Angles for Compound 58

Bond Lengths (Å)

Atom 1	Atom 2	Distance
Pd1	Cl1	2.314(4)
Pd1	P1	2.300(4)
Pd1	P2	2.277(4)
Pd1	N1	2.028(1)
P1	C7	1.803(1)
P1	C8	1.823(2)
P1	C14	1.813(1)
P2	C26	1.800(2)
P2	C27	1.838(2)
P2	C30	1.844(2)

Bond Angles (°)

Atom1	Atom 2	Atom3	Angle
P2	Pd1	P1	163.72(1)
N1	Pd1	Cl1	179.12(4)
Cl1	Pd1	P1	96.10(2)
Cl1	Pd1	P2	97.61(2)
N1	Pd1	P1	84.14(4)
N1	Pd1	P2	82.28(4)
Pd1	P1	C7	98.77(5)
Pd1	P1	C8	111.76(5)
Pd1	P2	C26	99.19(5)
Pd1	P2	C27	122.24(6)
C20	N1	Pd1	118.42(9)
C1	N1	Pd1	117.91(9)

Additionally, the platinum analogue of **58** was generated in 78% yield as a yellow solid, ^{Ph}PNP^{iPr}-Pt-Cl **60**. The ³¹P{¹H} NMR spectrum of **60** reveals two sets of doublet of triplets for the two inequivalent phosphorus environments. The first environment has two triplets at 45.7 ppm ($J_{PPt} = 2754.5$ Hz and $J_{PP} = 401.6$

Hz) and 41.7 ppm ($J_{\text{PPt}} = 2754.2$ Hz and $J_{\text{PP}} = 401.6$ Hz) for the phosphorus with the isopropyl substituents. The second set occurs at 26.7 ppm ($J_{\text{PPt}} = 2673.9$ Hz and $J_{\text{PP}} = 401.9$ Hz) and 22.7 ppm ($J_{\text{PPt}} = 2673.9$ Hz and $J_{\text{PP}} = 401.9$ Hz) for the diphenylphosphino environment. In both cases, the J_{PPt} coupling constants are consistent with other similar structures, and the large J_{PP} values are characteristic of phosphines binding in the *trans* orientation, in a square planar motif. The proposed molecular structure of **60** was confirmed by X-ray diffraction analysis (Figure 18). A single crystal suitable for X-ray diffraction analysis was grown from the slow evaporation of a benzene solution at room temperature. A list of selected bond lengths and angles for **60** are shown in Table 10. The crystal structure confirmed a distorted square planar geometry around the metal center. As before, all other bond distances and angles showed no remarkable differences from related compounds.

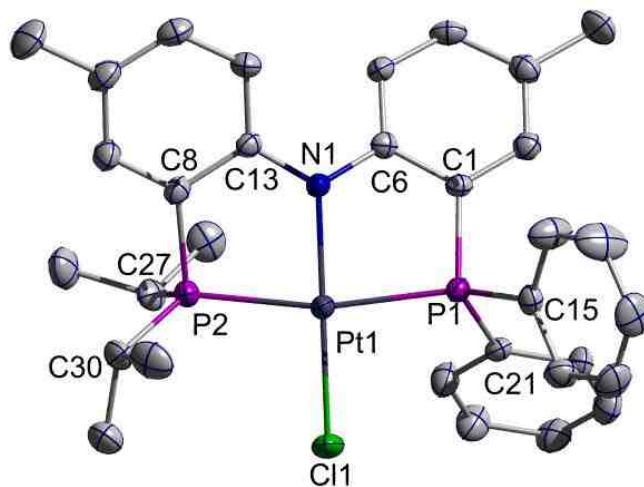


Figure 18. Thermal Ellipsoid Plot of 60 Shown at 50% Probability Level with Hydrogens Omitted for Clarity

Table 10. Selected Bond Lengths and Angles for Compound 60

Bond Lengths (Å)

Atom 1	Atom 2	Distance
Pt1	Cl1	2.321(1)
Pt1	P1	2.282(9)
Pt1	P2	2.273(1)
Pt1	N1	2.028(3)
P1	C1	1.804(3)
P1	C15	1.817(4)
P1	C21	1.831(3)
P2	C8	1.804(4)
P2	C27	1.842(4)
P2	C30	1.834(4)

Bond Angles (°)

Atom1	Atom 2	Atom3	Angle
P2	Pt1	P1	164.02(3)
N1	Pt1	Cl1	179.26(9)
Cl1	Pt1	P1	95.62(3)
Cl1	Pt1	P2	97.96(4)
N1	Pt1	P1	84.45(9)
N1	Pt1	P2	82.09(9)
Pt1	P1	C1	99.20(1)
Pt1	P1	C21	112.20(1)
Pt1	P2	C8	99.30(1)
Pt1	P2	C30	122.10(1)
C6	N1	Pt1	118.80(2)
C13	N1	Pt1	118.30(2)

The syntheses of $\text{CyPNP}^{\text{Ph}}\text{-Pd-Cl}$ **59** and $\text{CyPNP}^{\text{Ph}}\text{-Pt-Cl}$ **61** were accomplished using similar routes established earlier, although in moderate yields. The $^{31}\text{P}\{^1\text{H}\}$ NMR spectrum of **59** exhibits a doublet of doublets at 46.5 ppm ($J_{\text{PP}} = 437.5$ Hz, PCy_2) and at 25.7 ppm ($J_{\text{PP}} = 437.4$ Hz, PPh_2), which is consistent with the spectrum of **58**. The $^{31}\text{P}\{^1\text{H}\}$ NMR scan of **61** reveals two sets of doublet of triplets for two inequivalent phosphorus environments. The first environment displays two triplets at 38.4 ppm ($J_{\text{PPt}} = 2758.7$ Hz and $J_{\text{PP}} = 402.2$ Hz) and 34.5 ppm ($J_{\text{PPt}} = 2758.2$ Hz and $J_{\text{PP}} = 402.2$ Hz) for the phosphorus with the cyclohexyl substituents. The second set of triplets occurs at 26.6 ppm ($J_{\text{PPt}} = 2670.9$ Hz and $J_{\text{PP}} = 402.8$ Hz) and 22.6 ppm ($J_{\text{PPt}} = 2670.90$ Hz and $J_{\text{PP}} = 402.83$ Hz) for the diphenylphosphine environment. In both cases of metal complexes, the coupling constant values are consistent with earlier complexes and suggest a square planar geometry. The solid-state structure of **59** was

determined by X-ray diffraction analysis (Figure 19). A single crystal suitable for X-ray diffraction was grown from the slow evaporation of a benzene solution at room temperature. A list of selected bond lengths and angles for **59** are shown in Table 11.

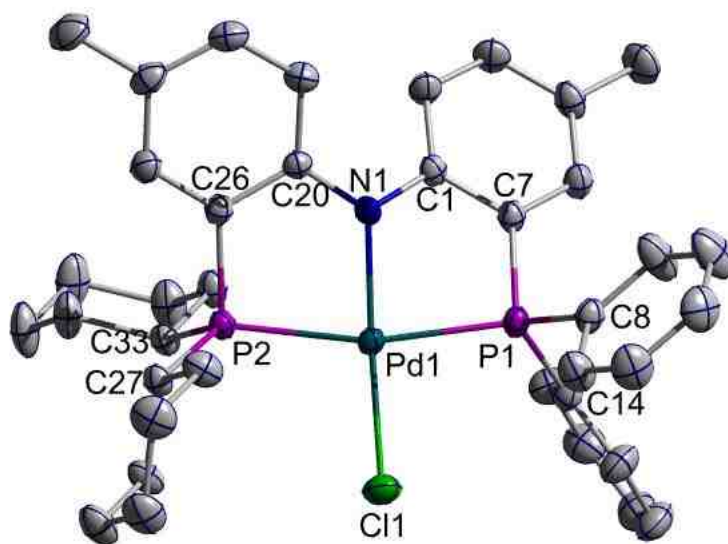


Figure 19. Thermal Ellipsoid Plot of 59 Shown at 50% Probability Level with Hydrogens Omitted for Clarity

Table 11. Selected Bond Lengths and Angles for Compound 59

Bond Lengths (Å)

Atom 1	Atom 2	Distance
Pd1	Cl1	2.317(5)
Pd1	P1	2.284(4)
Pd1	P2	2.304(4)
Pd1	N1	2.023(1)
P1	C7	1.798(2)
P1	C8	1.812(2)
P1	C14	1.814(2)
P2	C26	1.808(2)
P2	C27	1.834(2)
P2	C33	1.845(2)

Bond Angles (°)

Atom1	Atom 2	Atom3	Angle
P2	Pd1	P1	164.23(2)
N1	Pd1	Cl1	176.23(4)
Cl1	Pd1	P1	95.24(2)
Cl1	Pd1	P2	99.68(2)
N1	Pd1	P1	82.72(4)
N1	Pd1	P2	82.65(4)
Pd1	P1	C7	99.32(6)
Pd1	P1	C8	117.62(6)
Pd1	P2	C26	98.61(5)
Pd1	P2	C27	121.46(6)
C20	N1	Pd1	118.1(1)
C1	N1	Pd1	118.9(1)

The molecular structure of **61** was determined by X-ray diffraction analysis (Figure 20). A single crystal suitable for X-ray diffraction was grown from the slow evaporation of a benzene solution at room temperature. A list of selected bond lengths and angles for **61** are shown in Table 12. In both pincer metal

complexes, **59** and **61**, the crystal structure confirms a square planar geometry around the metal center. The overall structures were similar to previous structures and deserve no special comments.

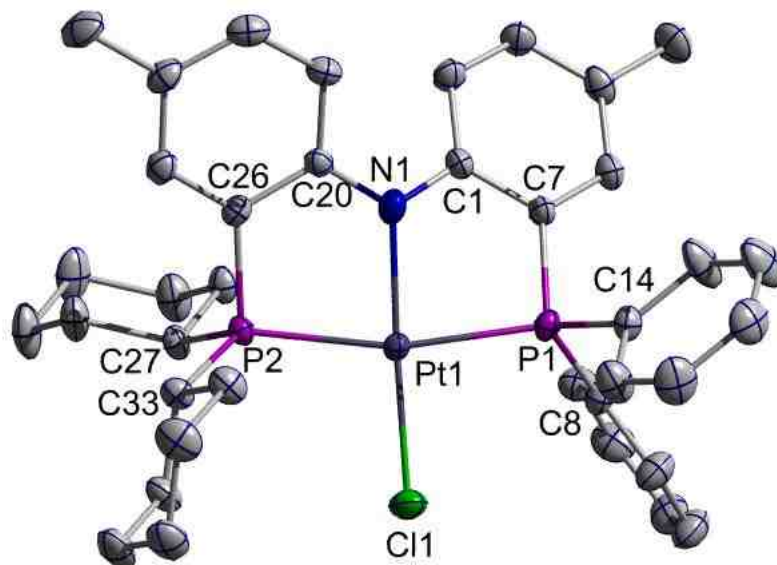


Figure 20. Thermal Ellipsoid Plot of 61 Shown at 50% Probability Level with Hydrogens Omitted for Clarity

Table 12. Selected Bond Lengths and Angles for Compound 61

Bond Lengths (Å)

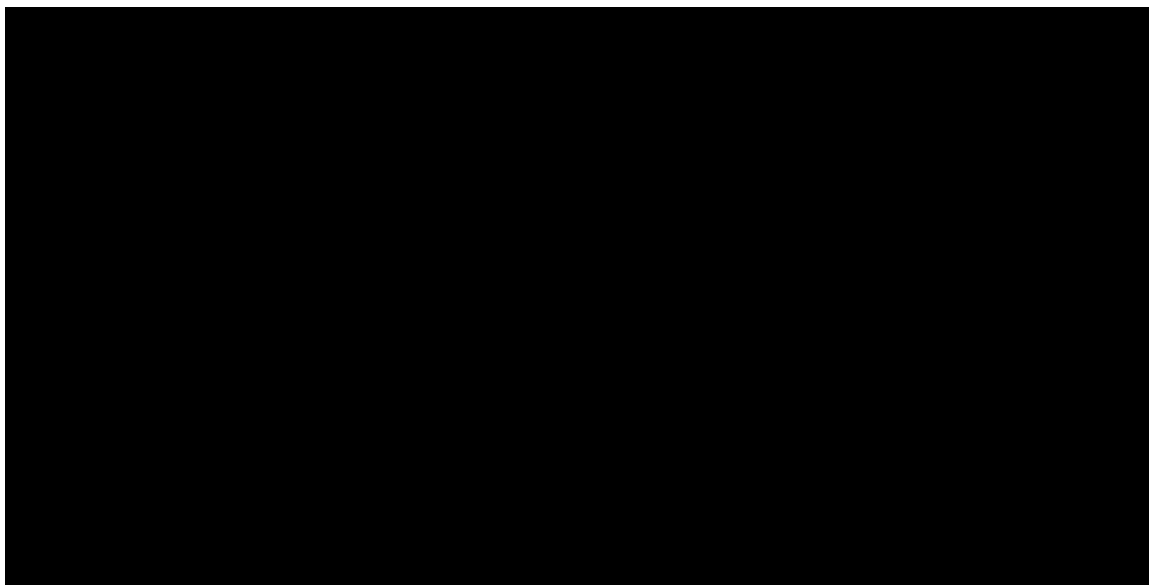
Atom 1	Atom 2	Distance
Pt1	Cl1	2.322(1)
Pt1	P1	2.274(1)
Pt1	P2	2.291(1)
Pt1	N1	2.047(5)
P1	C7	1.802(4)
P1	C8	1.812(7)
P1	C14	1.812(4)
P2	C26	1.807(5)
P2	C27	1.848(4)
P2	C33	1.825(4)

Bond Angles (°)

Atom1	Atom 2	Atom3	Angle
P2	Pt1	P1	164.79(4)
N1	Pt1	Cl1	176.10(1)
Cl1	Pt1	P1	95.26(5)
Cl1	Pt1	P2	99.22(5)
N1	Pt1	P1	83.00(1)
N1	Pt1	P2	82.80(1)
Pt1	P1	C7	99.60(2)
Pt1	P1	C14	117.70(2)
Pt1	P2	C26	99.30(2)
Pt1	P2	C33	121.70(2)
C1	N1	Pt1	117.80(3)
C20	N1	Pt1	117.40(3)

The generation of the unsymmetric metal hydrides followed the protocol used for the generation of the symmetric hydrides. A Super Hydride solution proved to be the most effective hydride source. The syntheses of $^{\text{Ph}}\text{PNP}^{\text{iPr}}\text{-Pd-H}$

62 and $^{\text{Ph}}\text{PNP}^{\text{iPr}}\text{-Pt-H}$ **64** complexes were accomplished in 84% and 85% yields, respectively.



Scheme 27. Preparation of $^{\text{Ph}}\text{PNP}^{\text{iPr}}\text{-M-H}$ and $^{\text{Ph}}\text{PNP}^{\text{Cy}}\text{-M-H}$

The $^{31}\text{P}\{^1\text{H}\}$ NMR spectrum of **62** exhibits a characteristic downfield shift from **58** with a set of doublets present. The first doublet appeared at 63.6 ppm ($J_{\text{PP}} = 354.2$ Hz, $\text{P}^{\text{iPr}}\text{Pr}_2$) and the second doublet at 31.4 ppm ($J_{\text{PP}} = 354.3$, PPh_2). The ^1H NMR spectrum of **62** displays a virtual triplet for the hydride ligand at -9.97 ppm. The $^{31}\text{P}\{^1\text{H}\}$ NMR scan of **64** also displays a set of doublet of triplets downfield from **60**. The first set of doublet of triplets occurs at 61.6 ppm ($J_{\text{PPt}} = 2860.4$ Hz and $J_{\text{PP}} = 361.5$ Hz, $\text{P}^{\text{iPr}}\text{Pr}_2$) and 58.0 ppm ($J_{\text{PPt}} = 2860.3$ Hz and $J_{\text{PP}} = 361.5$ Hz, $\text{P}^{\text{iPr}}\text{Pr}_2$). The second set of doublet of triplets occurs at 36.3 ppm ($J_{\text{PPt}} = 2824.0$ Hz and $J_{\text{PP}} = 361.4$ Hz, PPh_2) and 32.8 ppm ($J_{\text{PPt}} = 2823.9$ Hz and $J_{\text{PP}} = 361.4$ Hz, PPh_2). The ^1H NMR spectrum of **64** exhibits a triplet of virtual triplets at -11.60 ppm. In both metal complexes, the $^{31}\text{P}\{^1\text{H}\}$ and ^1H NMR data indicate that

both complexes still possess the square planar geometry and unequivocally show the presence of the hydride ligand. Unfortunately, a suitable crystal for X-ray diffraction analysis could not be grown for either complex in order to conclusively show the structure and confirm the presence of the hydride ligand by X-ray analysis.

The synthesis of ^{Ph}PNP^{Cy}-Pd-H **63** followed a similar procedure with the isolation of a brown solid in 87% yield. The ³¹P{¹H} NMR of **63** exhibits a doublet of doublets at 54.4 ppm ($J_{PP} = 354.5$ Hz, PCy₂) and 31.6 ppm ($J_{PP} = 354.5$ Hz, PPh₂) which showed the characteristic downfield shift from **59**. The ¹H NMR spectrum of **63** displays a virtual triplet for the hydride ligand at -9.92 ppm. The molecular structure of **63** was determined by X-ray diffraction analysis (Figure 21). A single crystal suitable for X-ray diffraction was grown from a concentrated solution of **63** in diethyl ether at -30 °C. A list of selected bond lengths and angles for **63** are shown in Table 13. When attempting to solve the crystal structure of **63**, the hydride ligand could not accurately be located and refined, but its presence is known with certainty as shown by the ¹H NMR data. The single crystal x-ray data displays an approximate square planar geometry around the palladium center with a P-Pd-P angle of 164.98° as compared to 164.23(2)° of **59**. This minor widening of the bond angle corresponds to the presence of a slightly less sterically-crowded ligand. The Pd-N bond distance of **63** (2.065(1) Å) is slightly elongated from that of **59** (2.023(1) Å), which is due to the *trans*-influence of the hydride ligand. All other noted bond distances and angles are similar to earlier complexes that have been structurally-characterized.

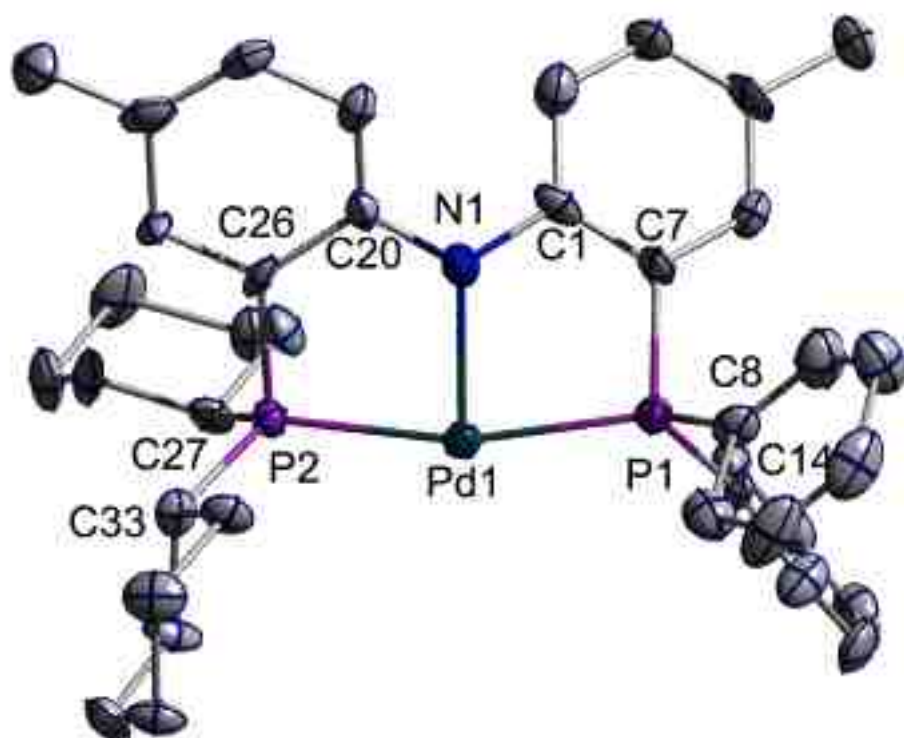


Figure 21. Thermal Ellipsoid Plot of 63 Shown at 50% Probability Level with Hydrogens Omitted for Clarity

Table 13. Selected Bond Lengths and Angles for Compound 63

Bond Lengths (Å)

Atom 1	Atom 2	Distance
Pd1	P1	2.263(1)
Pd1	P2	2.267(1)
Pd1	N1	2.065(1)
P1	C7	1.786(1)
P1	C8	1.818(1)
P1	C14	1.851(1)
P2	C26	1.797(1)
P2	C27	1.828(1)
P2	C33	1.853(1)

Bond Angles (°)

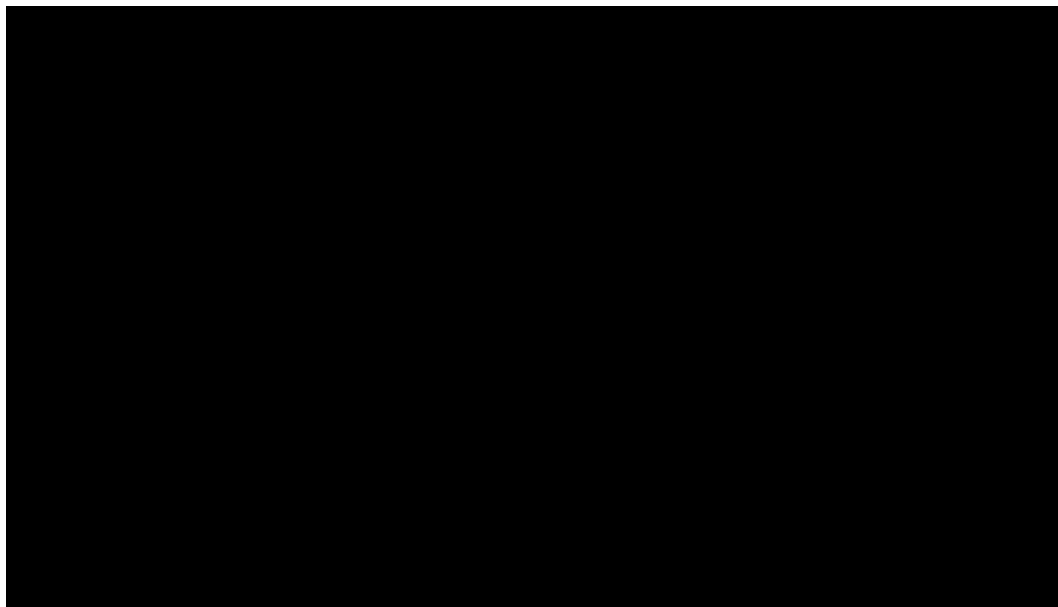
Atom1	Atom 2	Atom3	Angle
P2	Pd1	P1	164.98
N1	Pd1	P1	82.96
N1	Pd1	P2	83.10
Pd1	P1	C7	98.95
Pd1	P1	C14	118.18
Pd1	P2	C26	98.61
Pd1	P2	C33	114.54
C1	N1	Pd1	116.75
C20	N1	Pd1	119.85

3.3 Oxidative Addition Reactions

Another route for the syntheses of the desired PNP metal hydrides exists through oxidative addition. As in the case of PNP ligands, the oxidative method is quite attractive due to the lability of the N-H bond. Ozerov has shown that oxidative addition of a tolyl-based amidophosphine ligand (**D**) is possible with several M^0 precursors.¹²⁹ In the original paper describing the synthesis of **D**,

Ozerov details the synthesis of **63** via two different routes. This first route illustrates the process from free ligand to metal hydride via a hydride source. The second route demonstrates that generation of the metal hydride is feasible through oxidative addition. In this case, a zerovalent metal precursor $[\text{Pd}_2(\text{dba})_3]$ is used. Harsh conditions (24 hours at 120 °C) are required to obtain a 90% conversion to the product and isolation of the pure product is unattainable due to difficulty in separating the desired metal hydride from the by-products.⁴⁶ In a followup paper, Ozerov illustrates that his ligand **D** is able to undergo oxidative addition with several zerovalent Group 10 metal precursors.¹²⁹ Several zerovalent metal precursors, such as $\text{Ni}(\text{COD})_2$, $\text{Ni}(\text{PPh}_3)_4$, $\text{Pd}(\text{PPh}_3)_4$, $\text{Pd}(\text{P}^t\text{Bu}_3)_2$, $\text{Pt}(\text{PPh}_3)_4$, and $\text{Pt}(\text{P}^t\text{Bu}_3)_2$, were treated with ligand **D** and monitored by NMR spectroscopy. Most reactions required harsh conditions and resulted in only marginal conversions. One palladium precursor, $\text{Pd}(\text{P}^t\text{Bu}_3)_2$, was able to undergo 100% conversion at 100 °C for 3.5 hr. However, isolation of the product was not attempted in any of these cases. In the present study oxidative addition syntheses of **52** and **53** produced marginal results.

Ozerov also showed that syntheses of PNP nickel hydrides via oxidative addition was possible. In particular, reaction of **D** with $\text{Ni}(\text{COD})_2$ gave a 95% conversion under mild conditions.¹²⁹ In 2006, Liang repeated formation of nickel hydrides from ligand **C** through oxidative addition.^{130, 131} Liang¹³¹ and Ozerov¹²⁹ also showed that nickel hydrides could be generated through the conventional route established earlier. As shown below in Scheme 28, we decided it was more efficient to produce our PNP nickel hydrides in a facile, one-step process.



Scheme 28. Preparation of R PNP-Ni-H

The synthesis of Cy PNP-Ni-H **67** was accomplished using both methods described earlier. The first method required the generation of Cy PNP-Ni-Cl **66** from the reaction of **45** and $NiCl_2$, which resulted in a green solid in 82% yield. The $^{31}P\{^1H\}$ NMR data of **66** reveals a singlet at 26.9 ppm that indicated an average C_{2V} symmetry in solution. A Super Hydride solution was then used to convert **66** to **67**, which was isolated as a brown solid in 96% yield. The $^{31}P\{^1H\}$ NMR data of **67** shows a singlet at 46.8 ppm, indicating a square planar geometry among for the metal center. The 1H NMR data of **67** displays a triplet at -18.4 ppm with $J_{HP} = 63.3$ Hz, indicating the presence of the Ni-*H* ligand. The second method involved the oxidative addition of **45** with $Ni(COD)_2$, a route that resulted in 70% yield of a brown solid. The $^{31}P\{^1H\}$ and 1H NMR spectra are identical with those obtained via the first method. The solid-state structure of **67** was confirmed by X-ray diffraction analysis. A single crystal suitable for X-ray

diffraction (Figure 22) was grown from a concentrated solution of **67** in diethyl ether at - 30 °C. A list of selected bond lengths and angles for **67** are shown in Table 14.

The crystal structure of **67** confirms the distorted square planar geometry around the metal center. The P-Ni-P bond angle of **67** is 173.80°, which is somewhat closer to linearity when compared to other diarylamido PNP-Ni-Cl species, ^{Ph}PNP-Ni-Cl (171.22(4)°) and ^{iPr}PNP-Ni-Cl (168.81(2)°). Unfortunately, after several attempts, we could not grow a suitable crystal of **66** for analysis and comparison. The “closer to linear” P-Ni-P angle may indicate the presence of the hydride ligand, as the smaller hydride ligand replaces the bigger chloride ligand, but this cannot be confirmed without comparing it to a crystal structure of **66**. As has been seen previously, the hydride ligand could not accurately be located and refined but its presence is known and confirmed due to ¹H NMR data.

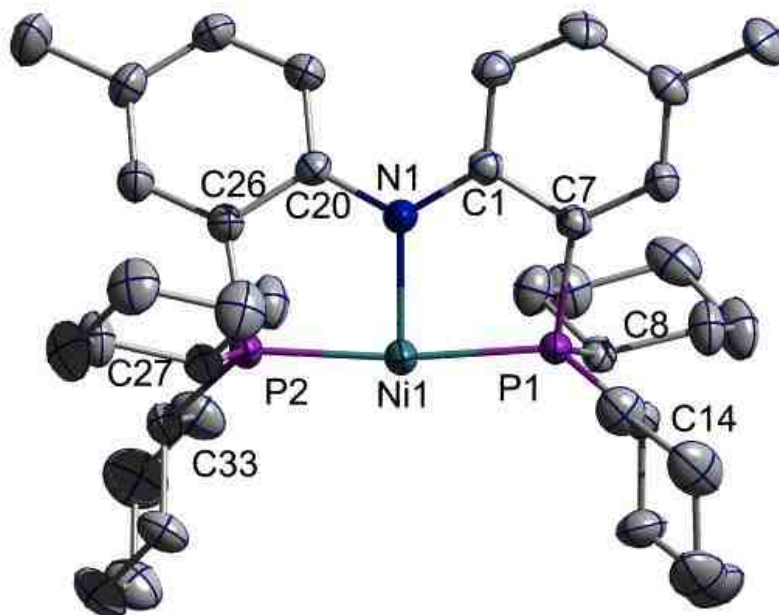


Figure 22. Thermal Ellipsoid Plot of 67 Shown at 50% Probability Level with Hydrogens Omitted for Clarity

Table 14. Selected Bond Lengths and Angles for Compound 67

Bond Lengths (Å)

Atom 1	Atom 2	Distance
Ni1	P1	2.134(1)
Ni1	P2	2.136(1)
Ni1	N1	1.925(1)
P1	C7	1.808(1)
P1	C8	1.849(1)
P1	C14	1.829(1)
P2	C26	1.816(1)
P2	C27	1.842(1)
P2	C33	1.834(1)

Bond Angles (°)

Atom1	Atom 2	Atom3	Angle
P2	Ni1	P1	173.80
N1	Ni1	P1	86.54
N1	Ni1	P2	87.26
Ni1	P1	C7	99.16
Ni1	P1	C8	115.26
Ni1	P2	C26	99.56
Ni1	P2	C27	114.65
C1	N1	Ni1	118.74
C20	N1	Ni1	118.51

The syntheses of the unsymmetric metal hydrides, $^{\text{Ph}}\text{PNP}^{\text{iPr}}\text{-Ni-H}$ **68** and $^{\text{Ph}}\text{PNP}^{\text{Cy}}\text{-Ni-H}$ **69**, were done via the oxidative addition route. The $^{31}\text{P}\{^1\text{H}\}$ NMR spectrum of **68** reveals a doublet of doublets, corresponding to the two different phosphorus environments. The first doublet appeared at 60.2 ppm with a $J_{\text{PP}} = 244.2$ Hz (P^{iPr}_2) and the second doublet appeared at 32.6 ppm with a $J_{\text{PP}} = 244.1$ Hz (P^{Ph}_2). The large J_{PP} values indicate that the phosphine donor atoms are coordinated to the metal in a *trans*-orientation. The ^1H NMR spectrum of **68** exhibits a doublet of doublets for the Ni-*H* at -18.17 ppm with $J_{\text{HP}} = 68.0$ Hz (P^{iPr}_2) and $J_{\text{HP}} = 68.0$ Hz (P^{Ph}_2). The molecular structure of **68** was determined by X-ray diffraction analysis (Figure 23). A single crystal suitable for X-ray diffraction was grown from a concentrated solution **68** in diethyl ether at -30°C . A list of selected bond lengths and angles for **68** are shown in Table 15.

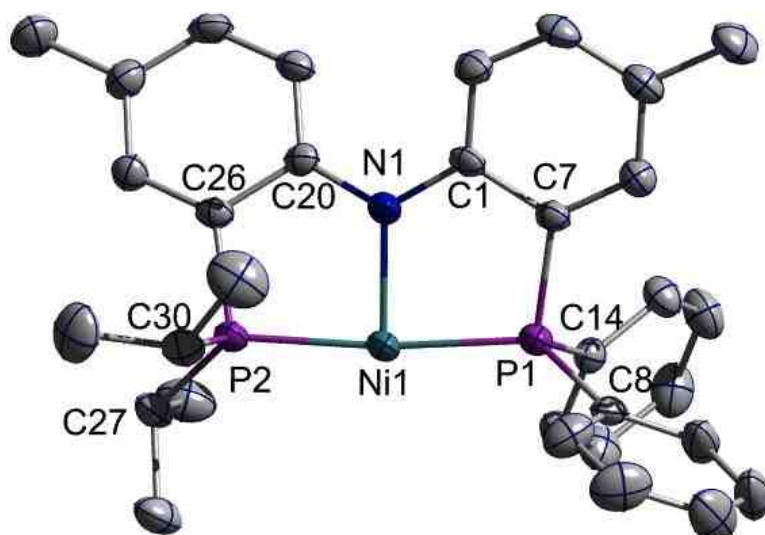


Figure 23. Thermal Ellipsoid Plot of 68 Shown at 50% Probability Level with Hydrogens Omitted for Clarity

Table 15. Selected Bond Lengths and Angles for Compound 68

Bond Lengths (Å)

Atom 1	Atom 2	Distance
Ni1	P1	2.134(1)
Ni1	P2	2.135(1)
Ni1	N1	1.921(3)
P1	C7	1.812(4)
P1	C8	1.816(4)
P1	C14	1.815(4)
P2	C26	1.809(3)
P2	C27	1.839(4)
P2	C30	1.847(4)

Bond Angles (°)

Atom1	Atom 2	Atom3	Angle
P2	Ni1	P1	173.78(5)
N1	Ni1	P1	87.1(1)
N1	Ni1	P2	86.9(1)
Ni1	P1	C7	99.4(1)
Ni1	P1	C14	116.3(1)
Ni1	P2	C26	99.7(1)
Ni1	P2	C30	114.6(1)
C1	N1	Ni1	118.4(3)
C20	N1	Ni1	118.6(3)

The crystal structure of **68** confirms the square planar geometry around the metal center. The P-Ni-P bond angle is 173.78°, which is also consistent with **67**. The hydride ligand could not accurately be located and refined but its presence is known due to ¹H NMR data. Interestingly, in previous work done by Boro, the hydrides in a series of ^RPCP-Ni-H complexes could be located in the X-ray pattern and refined to give accurate Ni-H bond lengths.⁸⁷

The ³¹P{¹H} NMR spectrum of **69** reveals a doublet of doublets corresponding to the two significantly-different phosphorus environments. The first doublet appeared at 49.6 ppm with a $J_{PP} = 244.9$ Hz (PCy₂) and the second doublet appeared at 31.8 ppm with a $J_{PP} = 244.2$ Hz (PPh₂). Once again, the large J_{PP} values indicate that the two phosphine donor atoms are coordinated to the metal in a *trans*-orientation. The ¹H NMR spectrum of **69** contains a doublet of doublets for the Ni-H at -18.15 ppm with $J_{HP} = 68.0$ Hz (PCy₂) and $J_{HP} = 68.0$ Hz (PPh₂). Unfortunately, even after multiple attempts to grow crystals, a suitable sample for X-ray diffraction analysis could not be obtained.

3.4 Racemic Chiral PNP ligands and complexes

As mentioned earlier, a very attractive feature of these pincer ligands is the numerous modifications possible. Along with the syntheses of symmetric and unsymmetric ligands, three types of PNP-based racemic chiral ligands were generated. With the majority of research focusing on symmetric pincer ligands, several chiral derivatives of these ligands have been developed and studied along with their metal counterparts. The bulk of these ligands contain an N-based moiety in their framework such as oxazolines (**E**),¹³²⁻¹⁴⁰ imidazolines (**F**),¹⁴¹⁻¹⁴³ imines (**G**),^{144, 145} and pyrrolidines (**H**) (Figure 24).¹⁴⁶⁻¹⁴⁹

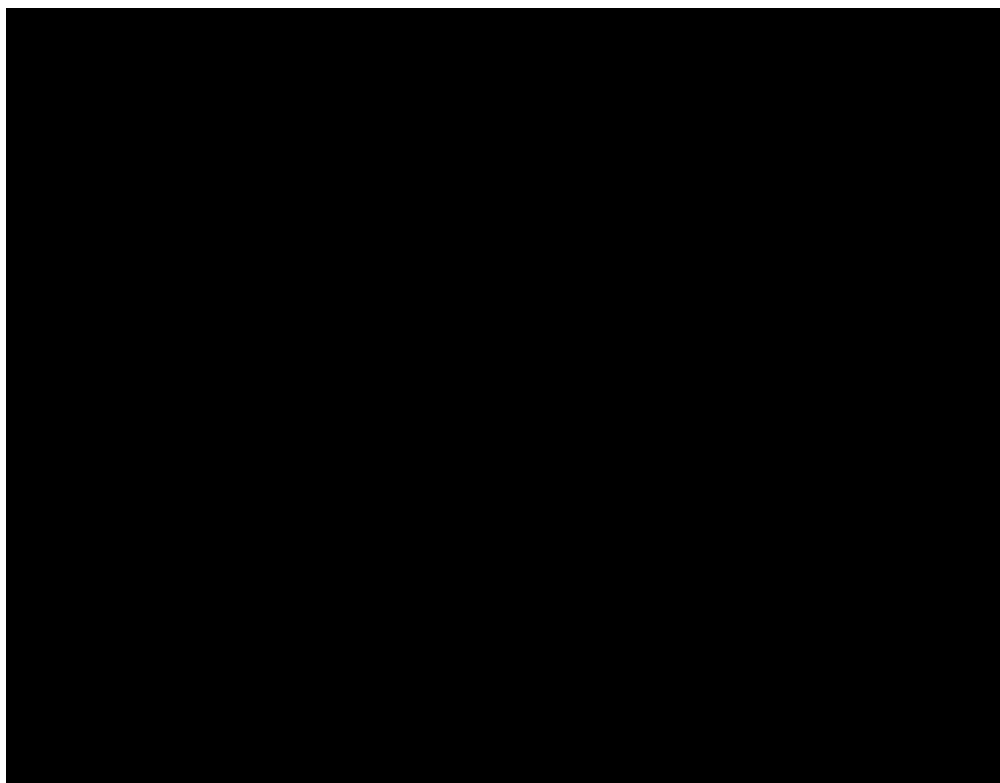


Figure 24. Examples of Chiral NCN Complexes

However, with the plethora of P-containing pincer complexes available, the study into these chiral derivatives remains scarce, most likely due to the difficulty associated with preparation and isolation. Nevertheless, a few chiral PCP-based pincer ligands (Figure 25) have been prepared that contain a chiral moiety at the benzylic methylene position (**I**, **J**),^{55, 74, 150-153} and also a phosphite PCP-based ligand that contains the chiral component in the substituents on the phosphorus atoms (**K**) has been prepared.¹⁵⁴⁻¹⁵⁶

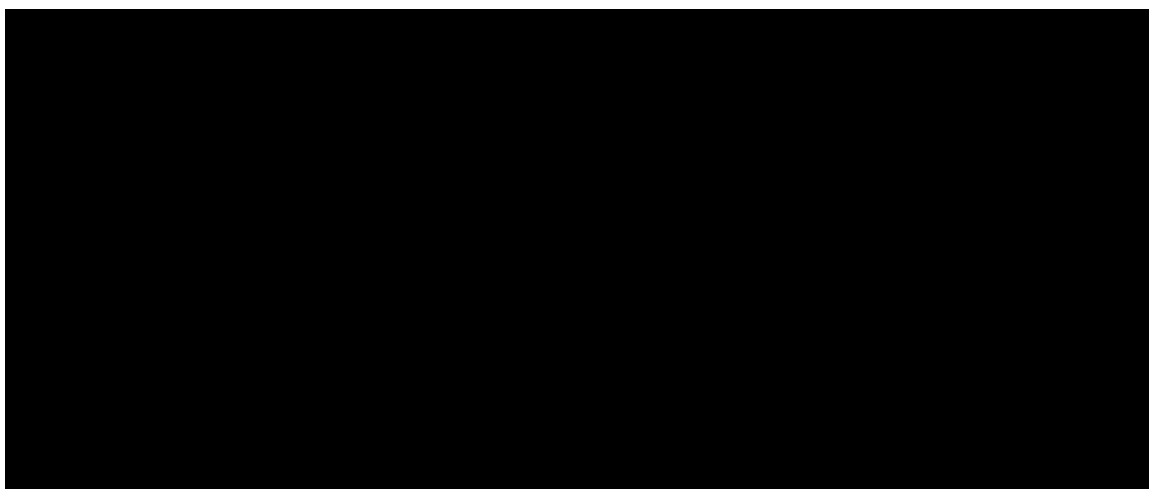
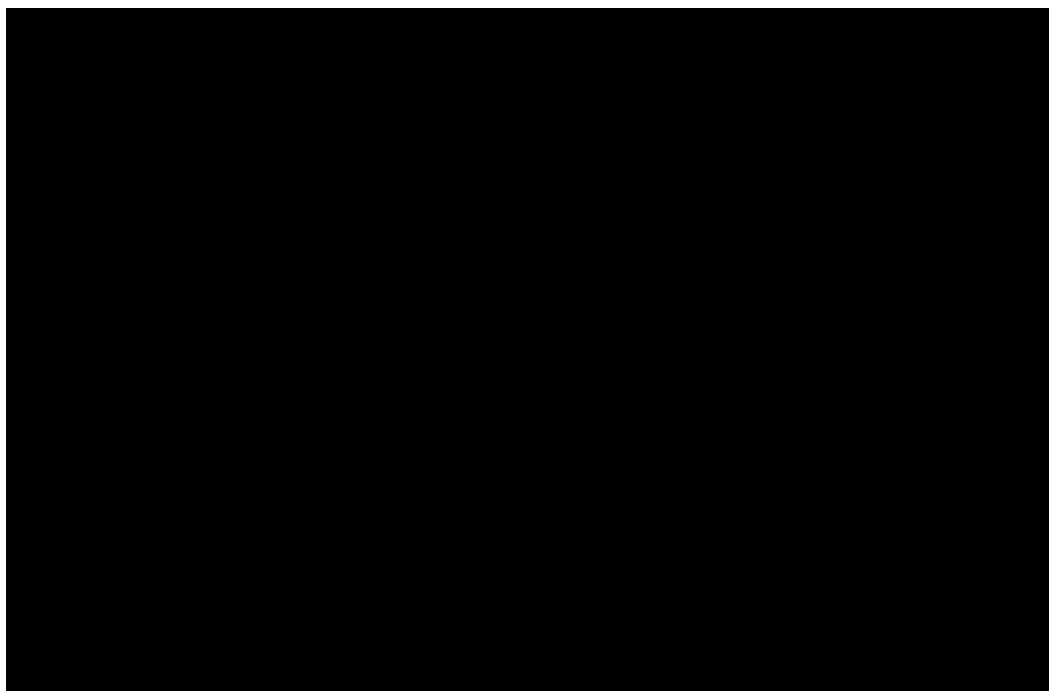


Figure 25. Examples of Chiral P-based Ligands

One particular chiral ligand (**L**) has its stereogenic position located on the phosphorus donor atoms.¹⁵⁷⁻¹⁵⁹ During the syntheses of the PNP-based free ligands, reactions were performed that generated racemic chiral PNP-based ligands. As shown below in Scheme 29, a similar protocol used for the synthesis of symmetric PNP free ligands was also employed here.



Scheme 29. Preparation of Racemic Chiral PNP Ligands

Racemic mixtures of dialkylphosphinechlorides (RR'PCI) were prepared in low yields using related literature procedure from the corresponding alkyl Grignard and dichlorophenylphosphine or dichloroalkylphosphine.^{160, 161} Reactions involving prepared phosphine chlorides, CyPhPCI **70**, CyⁱPrPCI **71**, and PhⁱPrPCI **72**, with **43** resulted in compounds ⁱPrCyPNP **73**, ^{Ph}iPrPNP **74**, and ^{Cy}PhPNP **75** in similar low yields, all obtained as pale white solids. The solid-state structures of **73**, **74**, and **75** were determined by X-ray diffraction. Single crystals of each ligand suitable for X-ray diffraction analysis were grown from a concentrated diethyl ether solution at - 30 °C. A list of selected bond lengths and bond angles of **73**, **74**, and **75** are shown in Tables 16, 17, and 18.

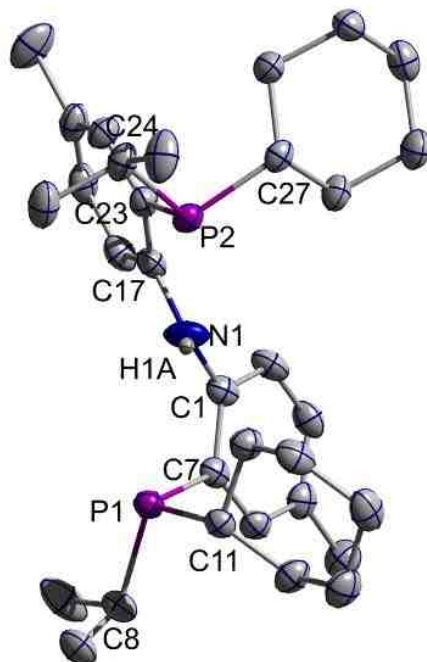


Figure 26. Thermal Ellipsoid Plot of 73 Shown at 50% Probability Level with Hydrogens Omitted for Clarity

Table 16. Selected Bond Lengths and Angles for Compound 73

Bond Lengths (Å)

Atom1	Atom2	Distance
P1	C7	1.842(4)
P1	C8	1.859(4)
P1	C11	1.861(4)
P2	C23	1.852(4)
P2	C24	1.857(4)
P2	C27	1.856(3)
N1	C1	1.401(6)
N1	C17	1.393(5)
N1	H1A	0.880(3)

Bond Angles (°)

Atom 1	Atom 2	Atom 3	Angle
C7	P1	C8	102.8(2)
C7	P1	C11	102.3(2)
C8	P1	C11	102.7(2)
P1	C7	C1	118.2(3)
C1	N1	H1A	116.4(3)
C17	N1	H1A	116.4(3)
C1	N1	C17	127.2(3)
C23	P2	C24	104.1(2)
C23	P2	C27	102.0(2)
C24	P2	C27	103.6(2)
P2	C23	C17	117.2(3)

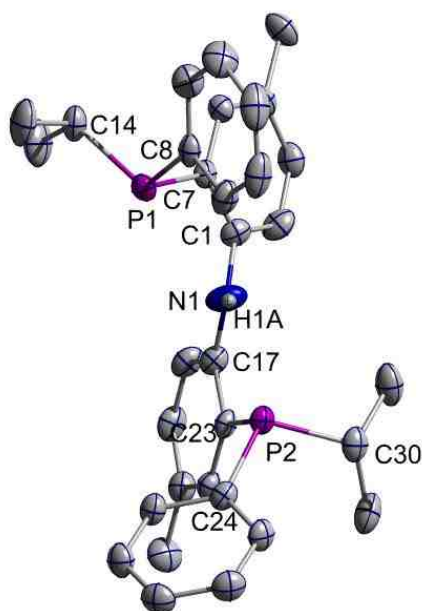


Figure 27. Thermal Ellipsoid Plot of 74 Shown at 50%Probability Level with Hydrogens Omitted for Clarity

Table 17. Selected Bond Lengths and Angles for Compound 74

Bond Lengths (Å)

Atom1	Atom2	Distance
P1	C7	1.847(3)
P1	C8	1.836(3)
P1	C14	1.848(4)
P2	C23	1.837(3)
P2	C24	1.821(3)
P2	C30	1.872(4)
N1	C1	1.395(5)
N1	C17	1.392(4)
N1	H1A	0.879(3)

Bond Angles (°)

Atom 1	Atom 2	Atom 3	Angle
C7	P1	C8	103.6(1)
C7	P1	C14	103.0(1)
C8	P1	C14	103.6(2)
P1	C7	C1	118.1(2)
C1	N1	H1A	116.5(3)
C17	N1	H1A	116.5(3)
C1	N1	C17	126.9(3)
C23	P2	C24	102.8(1)
C23	P2	C30	101.7(1)
C24	P2	C30	105.1(2)
P2	C23	C17	117.4(2)

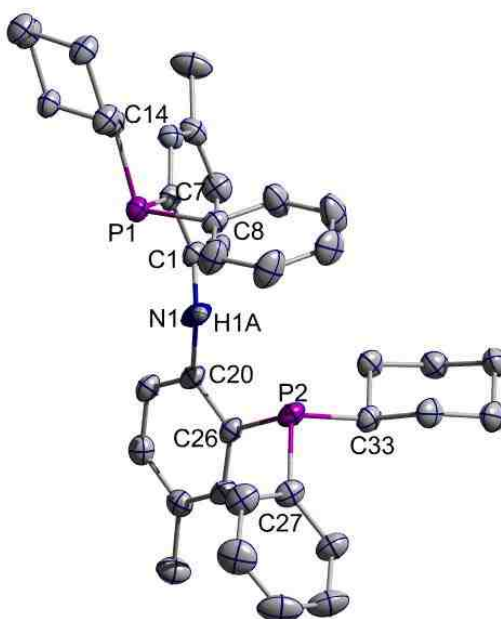


Figure 28. Thermal Ellipsoid Plot of 75 Shown at 50%Probability Level with Hydrogens Omitted for Clarity

Table 18. Selected Bond Lengths and Angles for Compound 75

Bond Lengths (Å)

Atom1	Atom2	Distance
P1	C7	1.834(2)
P1	C8	1.839(2)
P1	C14	1.860(2)
P2	C26	1.839(2)
P2	C27	1.833(2)
P2	C33	1.848(2)
N1	C1	1.411(3)
N1	C20	1.400(3)
N1	H1A	0.880(2)

Bond Angles (°)

Atom 1	Atom 2	Atom 3	Angle
C7	P1	C8	99.76(9)
C7	P1	C14	103.04(9)
C8	P1	C14	102.03(9)
P1	C7	C1	117.4(1)
C1	N1	H1A	118.0(2)
C20	N1	H1A	118.0(2)
C1	N1	C20	124.1(2)
C26	P2	C27	101.6(1)
C26	P2	C33	99.46(9)
C27	P2	C33	103.8(1)
P2	C26	C20	118.7(1)

The initial crystallization attempts resulted in surprising results. The crystal structures of **74** and **75** exhibited the substituents on the donor atoms in a *trans* fashion, while the crystal structure of **73** exhibited the *cis* mode. The second attempt at recrystallization of the pale white solids exhibited different results. The recrystallization of **74** and **75** resulted in identical results to the initial attempts; however, the recrystallization of **73** revealed the structure of the other isomer of **76** (*trans*). A third attempt at recrystallization for all ligands revealed the *trans* mode in all compounds. The crystal structures reveal that racemic mixtures of two different isomers (*cis* and *trans*) are present upon generation. Examination of the $^{31}\text{P}\{^1\text{H}\}$ NMR of the pale white solid of $^{i\text{PrCy}}\text{PNP}$ (**73** and **76**) revealed a singlet at -16.4 ppm with no other chemical shifts present. The $^{31}\text{P}\{^1\text{H}\}$ NMR spectra of **74** and **75** also revealed lone singlets.

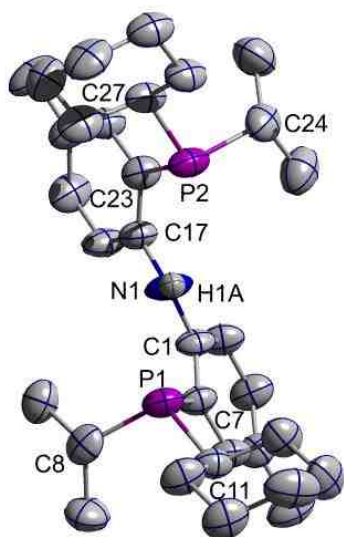


Figure 29. Thermal Ellipsoid Plot of 76 Shown at 50% Probability Level with Hydrogens Omitted for Clarity

Table 19. Selected Bond Lengths and Angles for Compound 76

Bond Lengths (Å)

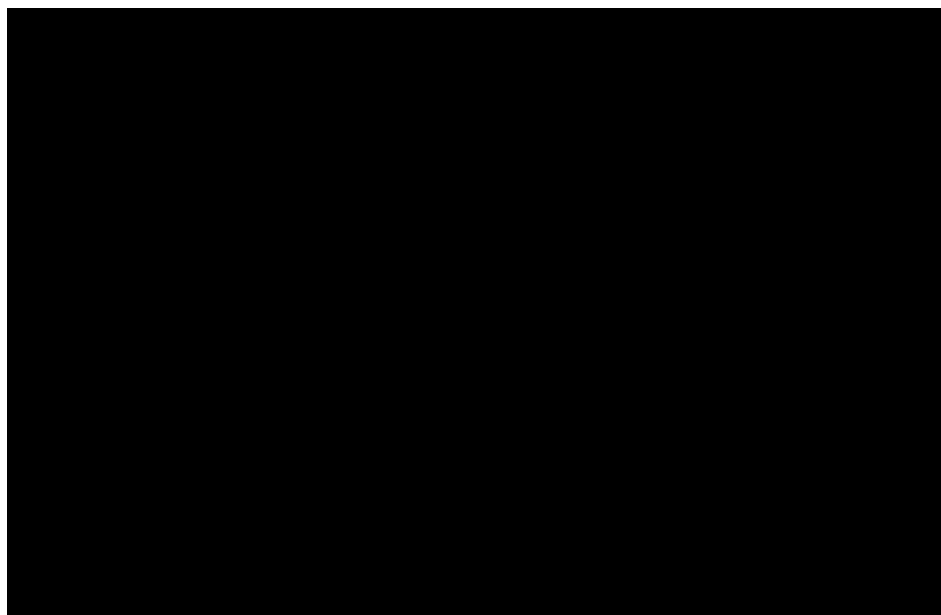
Atom1	Atom2	Distance
P1	C7	1.837(7)
P1	C8	1.851(7)
P1	C11	1.856(7)
P2	C23	1.844(7)
P2	C24	1.853(7)
P2	C27	1.842(7)
N1	C1	1.410(9)
N1	C17	1.378(9)
N1	H1A	0.861(5)

Bond Angles (°)

Atom 1	Atom 2	Atom 3	Angle
C7	P1	C8	102.0(3)
C7	P1	C11	103.7(3)
C8	P1	C11	104.5(3)
P1	C7	C1	118.2(5)
C1	N1	H1A	115.8(6)
C17	N1	H1A	115.9(6)
C1	N1	C17	128.3(6)
C23	P2	C24	101.3(3)
C23	P2	C27	103.8(3)
C24	P2	C27	104.5(3)
P2	C23	C17	117.7(5)

Each reaction that resulted in the generation of **73**, **74**, and **75** were repeated and resulted in similar yields of pale white solids. Recrystallization of each compound resulted in the identical *trans* isomer. With the assumption that the other isomer would possibly be present in the mother liquor, recrystallization of the mother liquor resulted in the *trans* isomer. The $^{31}\text{P}\{^1\text{H}\}$ NMR spectra of the repeated reactions and the mother liquors all resulted in similar results. With the repeated isolation of the *trans* isomer, it is assumed that this is the major product formed but its estimated yield is difficult to determine based on the lone singlet in the $^{31}\text{P}\{^1\text{H}\}$ NMR. An initial attempt at chiral resolution with chiral resolving agents led to difficulties and inconclusive results.

Metalation reactions involving these racemic chiral PNP-based ligands were investigated with metal precursors used previously. As shown below, a racemic mixture of the chiral ligand was refluxed with a metal precursor for a short duration and after the workup, generated similar red and yellow solids in comparable high yields.



Scheme 30. Preparation of Racemic PNP-based Metal Halides

Melattation was possible for these racemic chiral PNP-based ligands with Pd and Pt precursors. Although more examples were prepared, only two examples are presented here to confirm the presence of racemic mixtures of metal complexes. Compound $^{iPrCy}PNP-Pd-Cl$ **77** was generated as a red solid in 86% yield. The presence of the two isomers is more evident in the $^{31}P\{^1H\}$ NMR. The $^{31}P\{^1H\}$ NMR spectrum of **77** exhibits two resonances very close to each other in an approximate 2:1 ratio at 44.8 ppm and 44.6 ppm. Similarly, the $^{31}P\{^1H\}$ NMR spectrum of $^{PhCy}PNP-Pd-Cl$ **78** exhibits two close chemical shifts, one at 33.9 ppm and the other at 32.1 ppm in a 1:2 ratio. The molecular structures of **77** and **78** were determined by X-ray diffraction analysis (Figure 30 and 31). A single crystal of each compound suitable for X-ray diffraction was grown from a concentrated benzene solution at room temperature. A list of selected bond lengths and angles for **77** and **78** are shown in Table 20 and 21.

The crystal structure of **77** exhibits the *cis* orientation of the substituents on donor atoms, while the crystal structure of **78** displays the *trans* isomer of ^{PhCy}PNP-Pd-Cl. This type of behavior exhibited was expected and only reinforces the idea that the chiral ligands must be separated in order to generate pure enantiomers of the metal complexes.

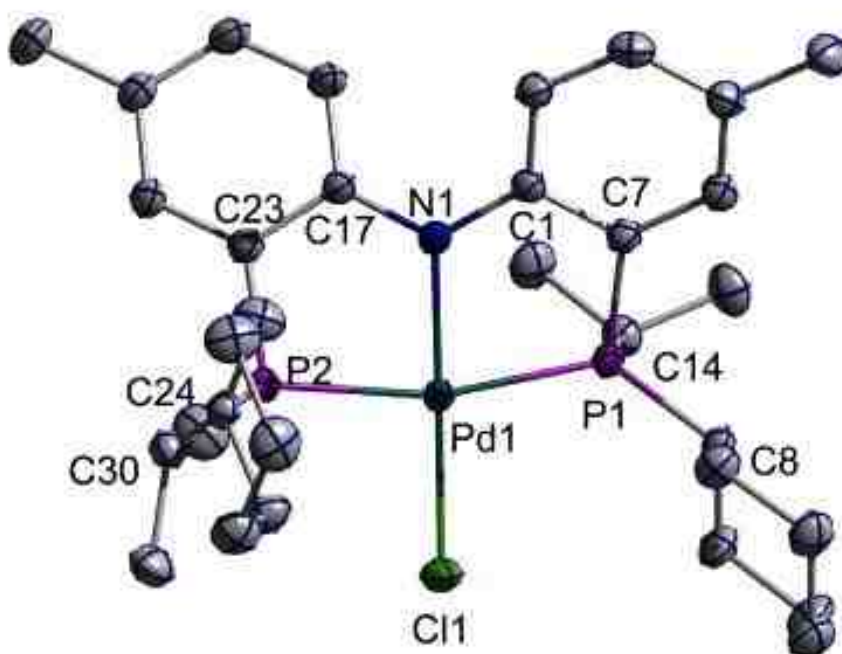


Figure 30. Thermal Ellipsoid Plot of 77 Shown at 50% Probability Level with Hydrogens Omitted for Clarity

Table 20. Selected Bond Lengths and Angles for Compound 77

Bond Lengths (Å)

Atom 1	Atom 2	Distance
Pd1	Cl1	2.301(7)
Pd1	P1	2.295(2)
Pd1	P2	2.291(6)
Pd1	N1	2.023(2)
P1	C7	1.811(3)
P1	C8	1.836(2)
P1	C14	1.844(3)
P2	C23	1.808(2)
P2	C24	1.847(2)
P2	C30	1.844(4)

Bond Angles (°)

Atom1	Atom 2	Atom3	Angle
P2	Pd1	P1	165.06(2)
N1	Pd1	Cl1	179.07(6)
Cl1	Pd1	P1	98.63(3)
Cl1	Pd1	P2	95.68(3)
N1	Pd1	P1	82.08(6)
N1	Pd1	P2	83.66(6)
Pd1	P1	C7	98.29(8)
Pd1	P1	C8	122.49(4)
Pd1	P2	C26	98.55(8)
Pd1	P2	C33	118.24(9)
C1	N1	Pd1	118.1(2)
C20	N1	Pd1	118.1(2)

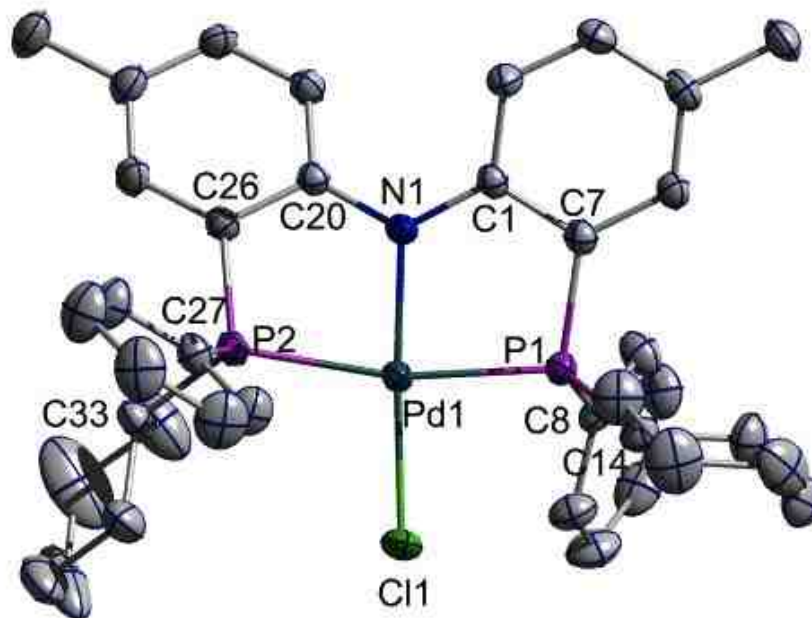


Figure 31. Thermal Ellipsoid Plot of 78 Shown at 50% Probability Level with Hydrogens Omitted for Clarity

Table 21. Selected Bond Lengths and Angles for Compound 78

Bond Lengths (Å)

Atom 1	Atom 2	Distance
Pd1	Cl1	2.319(7)
Pd1	P1	2.274(7)
Pd1	P2	2.298(7)
Pd1	N1	2.017(2)
P1	C7	1.800(3)
P1	C8	1.820(2)
P1	C14	1.831(2)
P2	C26	1.805(2)
P2	C27	1.828(2)
P2	C33	1.833(2)

Bond Angles (°)

Atom1	Atom 2	Atom3	Angle
P2	Pd1	P1	167.70(2)
N1	Pd1	Cl1	178.06(6)
Cl1	Pd1	P1	93.74(2)
Cl1	Pd1	P2	98.53(2)
N1	Pd1	P1	83.76(6)
N1	Pd1	P2	83.94(6)
Pd1	P1	C7	100.17(8)
Pd1	P1	C8	116.15(8)
Pd1	P2	C26	99.29(8)
Pd1	P2	C33	120.61(8)
C1	N1	Pd1	118.5(2)
C20	N1	Pd1	118.8(1)

3.5 Reactions with O₂ and Attempted Oxygen Transfer Reactions

The strategy used for oxygen insertion reactions in Chapter 2 was also employed in these oxygen insertion reactions. A small amount of **52** was placed into a J. Young NMR tube with a small volume of toluene-*d*₈, resulting in a dark brown solution. The system was pressurized with 5 atm of O₂ with no immediate color change apparent. After diligent monitoring for two days, the color of the reaction solution gradually changed to an orange/red solution with the ³¹P{¹H} NMR revealing the disappearance of the singlet at 59.7 ppm for **52** and the formation of two new chemical shifts at 41.9 ppm and 41.3 ppm, presumably for the –OOH and –OH species. The ¹H NMR spectrum reveals the disappearance of the hydride ligand at -10.4 ppm for **52** and the emergence of two peaks at 3.27 ppm and -2.21 ppm, presumably for the hydroperoxide proton and the hydroxide proton. In the previous reactions of our group's ^tBuPCP-Pd-H **40** species with O₂, this type of behavior was seen with the formation of two new species in the NMR

with the $^{31}\text{P}\{^1\text{H}\}$ NMR chemical shifts being very close to each other.⁸⁵ Eventually after two to three days, only one significant peak remained in the $^{31}\text{P}\{^1\text{H}\}$ NMR, presumably for the hydroxide complex. This type of behavior to generate the Pd-OH was also seen in the PCP-Pd-OOH complexes. The fate of the other oxygen atom is unknown at this time but it is likely converted to O_2 .

After several attempts, a single crystal of an O_2 insertion product suitable for X-ray diffraction was grown from a concentrated solution in deuterated toluene at -30°C . However, the quality of data was not ideal as the crystal showed decomposition during collection. However, the crystal structure (Figure 32) could be solved to establish atom connectivity of the molecule, but showed significant distortion around the bound hydroperoxide, which was expected. However, this result was significant in that it indicated O_2 insertion into PNP-Pd-H complexes could afford the desired PNP-Pd-OOH complex.

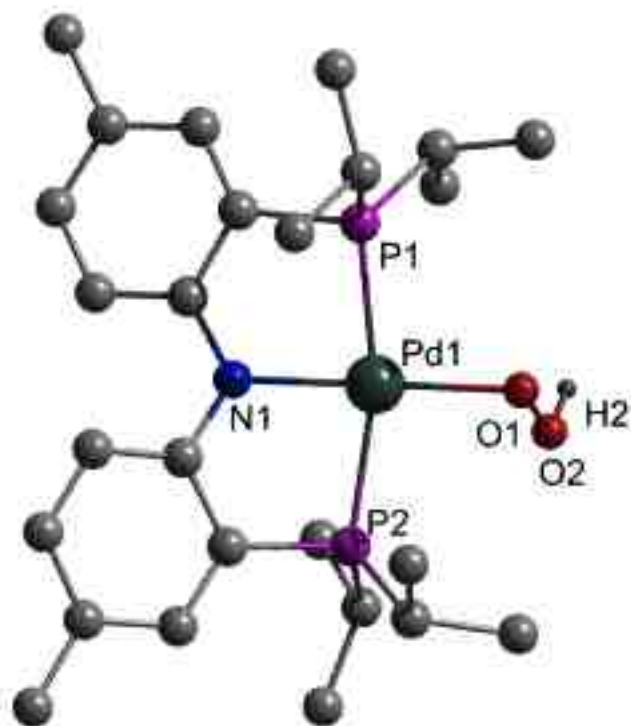


Figure 32. Ball and Stick Plot of $i\text{PrPNP-Pd-OOH}$

Two more PNP-based Pd hydrides were investigated in this oxygen insertion reaction. Prof. Oleg Ozerov, now at Texas A&M University, was generous enough to provide us with two PNP-based Pd hydrides, $^{\text{F}}\text{PNP-Pd-H}$ **78** and $^{\text{Th}}\text{PNP-Pd-H}$ **79**. Two of our new hydrides, $^{\text{Cy}}\text{PNP-Pd-H}$ and $^{\text{Ph}}\text{PNP}^{i\text{Pr}}\text{-Pd-H}$, were also examined. Compound **78** was reacted with O_2 and after a day, the reaction turned from dark brown to an orange/red solution. The $^{31}\text{P}\{^1\text{H}\}$ NMR spectrum reveals the disappearance of the singlet at 59.0 ppm for **78** and the appearance of two chemical shifts at 41.3 ppm (OOH) and 40.9 ppm (OH). The ^1H NMR spectrum reveals the disappearance of the hydride peak at -10.6 ppm for **78** and the appearance of two new chemical shifts at 3.21 ppm and -2.20

ppm. The hydroxide complex, F PNP-Pd-OH, has been synthesized by Ozerov and has a $^{31}\text{P}\{^1\text{H}\}$ NMR chemical shift at 40.4 ppm with a ^1H NMR chemical shift at -2.15 ppm (OH).¹⁶² The other PNP-based Pd hydrides exhibited similar behavior in their NMR spectra with the disappearance of their respective hydride peaks and appearance of two new chemical shifts. Unfortunately, despite much effort in this area, single crystals suitable for X-ray diffraction analysis could not be isolated for any of these hydroperoxides or hydroxides.

Platinum PNP-based hydrides were investigated in oxygen insertion reactions. Small amounts of compounds **54** and **55** were placed separately into two J. Young NMR tubes and dissolved into toluene- d_8 . The NMR tubes were then pressurized with 5 atm of O_2 with no immediate color change observed. The systems were closely monitored over several days with no change in the color in either solution, nor in the NMR chemical shifts of the hydride complexes. This was somewhat expected as insertion into Pt-H bond mentioned earlier proceeded via a radical mechanism.^{97, 98}

Nickel PNP-based hydrides were investigated in these oxygen insertion reactions. These complexes reacted faster with O_2 than Pd PNP-based metal hydrides. Compounds **65** and **66** were treated with O_2 and an immediate color change from brown to green was noted. In the $^{31}\text{P}\{^1\text{H}\}$ NMR spectra, the hydride chemical shift disappeared followed by the formation of several peaks. In the ^1H NMR spectra, the hydride peak disappears with no formation of resonances that can be assigned to the -OH and -OOH species. With no spectroscopic evidence

for the formation of –OH and-OOH species, these complexes were not further investigated in the next step of our cycle.

With the successful generation of the hydroperoxide species, the next step in the potential catalytic cycle is to examine them in oxygen transfer reactions. The ideal and cleanest case for this type of reaction would be to isolate the hydroperoxide complex and react it directly with an organic substrate without any other oxygen source. Unfortunately, isolation of the PNP-based hydroperoxides proved to be difficult, as they exhibited only a short life prior to total decomposition and conversion to a hydroxide species. Due to this reactivity, the potential oxygen transfer ability of the hydroperoxides could only be gauged by generating them *in situ* and reacting them with an organic substrate. There are two ways this could be accomplished. The first route requires the generation of our hydroperoxide *in situ* and then exposing it to an organic substrate, while the second route involves the *in situ* generation of our hydroperoxide species in the presence of an organic substrate.

Early or late transition metals have been shown to epoxidize olefins and have been well-documented with differing discussions on the mechanism of the oxygen transfer process.^{27, 163, 164} Studies of early transition metal complexes have shown that the epoxidation process occurs through the direct reaction of the olefin with the proximal oxygen atom of hydroperoxide or peroxy species.¹⁶³ Coordination of the olefin to the metal center is not necessary, with electron-rich olefins exhibiting greater reaction rates. This increase in rate indicates the electrophilic character of the transferred oxygen.^{163, 164}

On the other hand, Strukul has demonstrated that his late transition metal platinum complexes react in an opposite fashion to early transition metals. He showed that coordination of the olefin is necessary to facilitate attack of the now electrophilic olefin. This indicates that the transferred oxygen atom is now nucleophilic in nature with electron-withdrawing olefins affording greater reaction rates.¹⁶⁵⁻¹⁶⁸

With these prior results in mind, the scheme to investigate the oxygen transfer ability of our hydroperoxides is to mimic Strukul in the use of electron-withdrawing olefins such as acrylonitrile and fumaniitrile in these reactions. With the expected by-product of these O-transfer reactions being hydroxides, ^FPNP-Pd-H was first used in these reactions because of the NMR chemical shifts of ^FPNP-Pd-OH were known with certainty. However, we investigated other hydrides, including ^{iPr}PNP-Pd-H and ThPNP-Pd-H. In order to monitor any possible side reactions of O₂ with the organic substrate, this reaction in the absence of metal species was monitored over several days with no epoxide or other oxidized product identified. Initial reactions involved the direct interaction of the *in situ* generated hydroperoxide species with organic substrates. The system was monitored by ³¹P{¹H} NMR and ¹H NMR for several days. In all cases no direct epoxidation of olefins and hydroxide was identified. No NMR peaks corresponding to oxidized organics were obtained. The oxygen atom in our hydroperoxide does not seem to possess sufficient nucleophilic character to react, even with our electron-withdrawing olefins.

With the lack of success of the first method, the organic substrate was introduced with the hydride before the addition of O₂ to the system. In base-case studies the organic substrate and hydride were initially screened to rule out any insertion reaction between the two. The reactions were done in C₆D₆ and were again monitored by NMR over several days. Unfortunately, no hydroperoxide species were identified in any of the cases.

3.6 Concluding Remarks

The goal of this chapter was to prepare new ^RPNP-M-H complexes and examine their potential catalytic ability in activating molecular oxygen for the oxidation of organic substrates. Several new symmetric (^{Cy}PNP) and unsymmetric PNP free ligands (^{Ph}PNP^{iPr} and ^{Ph}PNP^{Cy}) were first synthesized in low yields, using prior literature as a synthetic guide. Reactions involving asymmetric phosphine chlorides in the generation of our free ligands resulted in a racemic mixture of chiral PNP-based ligands. Unfortunately, resolution of the two isomers could not be achieved; however, this is an interesting area for future study.

From these PNP-based free ligands, metalation with different metal precursors was successful in many cases to generate symmetric and unsymmetric PNP-based metal complexes, ^RPNP^{R'}-M-Cl (M = Pd and Pt) in high yields. Many of these species have been characterized by X-ray crystallography.

The established procedure for the generation of the PNP-based metal hydrides calls for the addition of a hydride source to the PNP-M-Cl complexes. A variety of possible hydride sources have been used, and it is a matter of trial and

error to find the optimal hydride source. In most cases, the use of a Super Hydride solution proved acceptable. Using this method, several new symmetric and unsymmetric PNP-based metal hydrides were generated.

From these generated PNP-M-H complexes, several metal hydrides have shown reactivity with molecular oxygen. Palladium hydrides have shown to react with molecular oxygen to generate palladium hydroperoxides. In one particular case, a crystal structure was obtained to confirm connectivity of the hydroperoxide moiety. Interestingly, Nickel hydrides have shown to react faster with O₂ than Pd hydrides; however, no spectroscopic evidence confirmed the formation of any –OH and-OOH species. The oxygen atom transfer ability of these complexes was investigated through the reactions with organic substrates. Base-case experiments were performed to confirm that no reactivity between the starting hydrides and organic substrates occurred. Attempted reactions to transfer O were performed by different routes. Direct reactions of pre-formed M-OOH complexes with substrates were undertaken, as were *in situ* generated M-OOH complex reactions with substrates. Unfortunately, as yet, no evidence has been observed to indicate partial oxidation of substrates via oxygen atom transfer.

3.7 Experimental

3.7.1 General Experimental

All procedures and manipulations were carried out under argon using an MBRAUN UL-03-143 glove box or by standard Schlenk techniques. All solvents used were of high purity (anhydrous) or were dried by using standard methods.

All reagents were purchased from Acros, Aldrich, Alfa Aesar, or Strem and were used as received. Bis(2-bromo-4-methylphenyl)amine **43**,¹¹⁸ bis[2-(diisopropylphosphino)-4-methylphenyl]amine (ⁱPrPNP) **44**,⁴⁶ [bis[2-(diisopropylphosphino)-4-methylphenyl]amido]chloropalladium **47**,⁴⁶ [bis[2-(diisopropylphosphino)-4-methylphenyl]amido]chloroplatinum **50**,¹²⁹ [bis[2-(diisopropylphosphino)-4-methylphenyl]amido]hydridopalladium **52**,⁴⁶ [bis[2-(diisopropylphosphino)-4-methylphenyl]amido]hydridoplatinum **54**,¹²⁹ [bis[2-(diisopropylphosphino)-4-methylphenyl]amido]hydridonickel **65**,¹²⁹ phenylisopropylchlorophosphine (PhⁱPrPCI) **72**,¹⁶⁰ cyclohexylisopropylchlorophosphine (CyiPrPCI) **71**,¹⁶⁰ cyclohexylphenylchlorophosphine (CyPhPCI) **70**,¹⁶¹ were prepared according to literature procedures.

NMR spectra were obtained at room temperature on a Bruker AMX 250 MHz spectrometer or on a Bruker AC 250 MHz spectrometer with a Tecmag MacSpect upgrade. All chemical shifts are reported in (δ) ppm with ¹H and ¹³C spectra referenced to tetramethylsilane or to their respective residual solvent peaks. ³¹P NMR spectra were referenced externally using 85% H₃PO₄ at δ 0 ppm. Elemental analyses were performed by Columbia Analytical Services of Tucson, AZ.

3.7.2 Crystallographic Determination

Data for X-ray crystallographic determination were collected and solved with the assistance of Dr. Eileen Duesler at the University of New Mexico and Dr.

Diane Dickie of the Kemp research group. Crystallographic figures shown in this dissertation were generated using Diamond 3.1d.¹⁰¹

Crystallographic data were collected on a Bruker X8 APEX CCD-based X-ray diffractometer using monochromated Mo-K α radiation ($\lambda = 0.71073 \text{ \AA}$). The single crystals were coated in oil (Paratone-NTM) and mounted on nylon cryoloops (Hampton Research). Bruker APEX2 was used to collect and process the data.¹⁰² The structures were solved by either the direct or Patterson method with XSHel and were refined by full matrix least-squares method on F² with SHELXTL.¹⁰³ All non-hydrogens were refined anisotropically and hydrogen atoms were fixed at calculated geometric positions. PLATON squeeze was used to treat disordered solvent molecules. All crystallographic data are located in the Appendix.

3.7.3 Synthesis of PNP ligands and complexes

Synthesis of Bis[2-(dicyclohexylphosphino)-4-methylphenyl]amine (CyPNP)

45

n-BuLi (12.91 mL, 32.28 mmol, 2.5 M in hexane) was added dropwise to a solution of bis(2-bromo-4-methylphenyl)amine (3.82 g, 10.76 mmol) in 25 mL of diethyl ether at $-35 \text{ }^\circ\text{C}$. The solution was stirred at RT for 3 hrs. The reaction mixture was cooled back down to $-35 \text{ }^\circ\text{C}$ and dicyclohexylchlorophosphine (5.00 g, 21.52 mmol) was added dropwise. The reaction mixture was stirred overnight. The volatiles were removed under reduced pressure resulting in a yellow residue. The yellow residue was redissolved into 30 mL of CH₂Cl₂ and 15 mL of degassed DI water was added. Separated the organic layer from the aqueous layer and

extracted the aqueous layer twice more (5 mL). The organic layers were combined and dried with MgSO₄. The mixture was filtered through Celite and the volatiles were removed under reduced pressure resulting in an off-white solid. The off-white solid was washed with cold pentane and dried under vacuum to give **45** (2.45 g, 39%). ¹H NMR (C₆D₆, 250.13 MHz): δ 8.26 (t, 1H, J_{HP} = 8.25, NH), 7.44 (dd, 2H, Ar), 7.36 (bs, 2H, Ar), 6.93 (d, 2H, Ar), 2.19 (s, 6H, Me), 2.15 - 1.97 (m, Cy), 1.85 - 0.98 (m, Cy). ³¹P{¹H} NMR (C₆D₆, 101.26 MHz): δ -20.7. ¹³C{¹H} NMR (CDCl₃, 62.91 MHz): δ 146.6 (d, J_{CP} = 16.5, C), 134.6 (s, CH), 129.9 (s, CH), 128.6 (s, CH), 123.0 (d, J_{CP} = 16.4, C), 117.1 (s, CH), 33.3 (d, J_{CP} = 11.6, CH), 30.7 (d, J_{CP} = 17.1, CH₂), 29.3 (d, J_{CP} = 8.3, CH₂), 27.2 (d, J_{CP} = 12.9, CH₂), 27.0 (d, J_{CP} = 8.6, CH₂), 26.4 (s, CH₂), 20.8 (s, Me). Anal. Calcd for C₃₈H₅₇NP₂: C, 77.38; H, 9.74; N, 2.37. Found: C, 77.10; N, 10.10; 2.27.

Synthesis of [Bis[2-(dicyclohexylphosphino)-4-methylphenyl]amido]chloropalladium (CyPNP-Pd-Cl) **48**

CyPNP (0.500 g, 0.080 mmol) and (COD)PdCl₂ (0.240 g, 0.080 mmol) were placed into a round bottom flask along with 20 mL of THF and one equiv. of NEt₃. The red solution was refluxed for one hour, filtered through Celite, and the volatiles were removed under reduced pressure resulting in a red solid. The red solid was washed with cold pentane and dried under vacuum to give **48** (0.051 g, 82%). ¹H NMR (C₆D₆, 250.13 MHz): δ 7.75 (d, 2H, J_{HP} = 8.51, Ar), 7.05 (bs, 2H, Ar), 6.79 (d, 2H, J_{HP} = 8.51 Ar), 2.15 (s, 6H, Me), 2.50 - 1.45 (m, Cy), 1.40 - 0.88 (m, Cy). ³¹P{¹H} NMR (C₆D₆, 101.26 MHz): δ 40.6. ¹³C{¹H} NMR (C₆D₆, 62.89

MHz): δ 162.5 (t, $J_{CP} = 11.1$, C), 132.7 (s, CH), 132.4 (s, CH), 125.8 (s, CH), 119.7 (t, $J_{CP} = 17.4$, C), 116.3 (t, $J_{CP} = 5.2$, CH), 34.3 (t, $J_{CP} = 11.9$, PCH), 28.6 (s, CH₂), 28.2 (s, CH₂), 27.1 (s, CH₂) 27.0 (s, CH₂), 26.1 (s, CH₂) 20.4 (s, Me).
Anal. Calcd for C₃₈H₅₆CINP₂Pd: C, 62.46; H, 7.72; N, 1.92. Found: C, 62.34; N, 8.32; 1.85.

Synthesis of [Bis[2-(dicyclohexylphosphino)-4-methylphenyl]amido]hydropalladium (^{Cy}PNP-Pd-H) 53

^{Cy}PNP-Pd-Cl (0.030 g, 0.041 mmol) was placed into a round bottom flask along with 15 mL of THF. The solution was cooled to -35 °C and Super Hydride (0.041 mL, 0.041 mmol, 1.0M in THF) was added. The solution was stirred at RT for 3.5 hrs. The volatiles were removed under reduced pressure, resulting in a brown residue. The brown residue was redissolved into pentane and filtered through Celite, resulting in a brown solution. The volatiles were removed under reduced pressure resulting in a brown solid. The brown solid was dried under vacuum to give **53** (0.021 g, 74%). ¹H NMR (C₆D₆, 250.13 MHz): δ 7.99 (d, 2H, $J_{HP} = 8.25$, Ar), 7.09 (bs, 2H, Ar), 6.94 (d, 2H, $J_{HP} = 8.00$, Ar), 2.23 (s, 6H, Me), 2.15 - 1.40 (m, Cy), 1.35 - 0.85 (m, Cy) -10.22 (t, 1H, $J_{HP} = 7.00$, Pd-H). ³¹P{¹H} NMR (C₆D₆, 101.26 MHz): δ 50.43. ¹³C{¹H} NMR (C₆D₆, 62.89 MHz): δ 161.4 (t, $J_{CP} = 10.6$, C), 133.6 (s, CH), 132.5 (s, CH), 123.6 (s, CH), 121.8 (t, $J_{CP} = 17.4$, C), 115.8 (s, CH), 33.8 (t, $J_{CP} = 12.7$, PCH), 30.0 (s, CH₂), 28.6(s, CH₂), 27.0 (s, CH₂) 26.9 (s, CH₂), 26.2 (s, CH₂) 20.6 (s, Me).

Synthesis of [Bis[2-(dicyclohexylphosphino)-4-methylphenyl]amido]chloroplatinum (^{Cy}PNP-Pt-Cl) 51

^{Cy}PNP (0.270 g, 0.470 mmol) and (COD)PtCl₂ (0.170 g, 0.470 mmol) were placed into a round bottom flask along with 20 mL of THF and one equiv. of NEt₃. The solution was refluxed for 2.5 hours, filtered through Celite, and the volatiles were removed under reduced pressure resulting in a yellow solid. The yellow solid was washed with cold pentane and dried under vacuum to give **51** (0.297 g, 78%). ¹H NMR (C₆D₆, 250.13 MHz): δ 7.82 (d, 2H, J_{HP} = 8.76, Ar), 7.10 (bs, 2H, Ar), 6.78 (d, 2H, J_{HP} = 8.25, Ar), 2.17 (s, 6H, Me), 2.59 - 1.55 (m, Cy), 1.53-0.88 (m, Cy). ³¹P{¹H} NMR (C₆D₆, 101.26 MHz): δ 33.8 (J_{Pt} = 2666.6). ¹³C{¹H} NMR (C₆D₆, 62.89 MHz): δ 162.4 (t, J_{CP} = 9.81, C), 132.7 (s, CH), 132.3 (s, CH), 126.3 (s, CH), 119.9 (t, J_{CP} = 22.6, C), 116.2 (t, J_{CP} = 5.3, CH), 34.6 (t, J_{CP} = 15.1, PCH), 28.3 (s, CH₂), 28.2 (s, CH₂), 27.1 (s, CH₂) 27.0 (s, CH₂), 26.2 (s, CH₂) 20.4 (s, Me).

Synthesis of [Bis[2-(dicyclohexylphosphino)-4-methylphenyl]amido]hydroplatinum (^{Cy}PNP-Pt-H) 55

^{Cy}PNP-Pt-Cl (0.029 g, 0.035 mmol) was placed into a round bottom flask along with 15 mL of THF. The solution was cooled to -35 °C and Super Hydride (0.035 mL, 0.035 mmol, 1.0M in THF) was added. The solution was stirred at RT for one hour. The volatiles were removed under reduced pressure, resulting in a brown residue. The brown residue was redissolved into pentane and filtered through Celite resulting in a brown/yellow solution. The volatiles were removed under

reduced pressure resulting in a yellow solid. The yellow solid was dried under vacuum to give **55** (0.022 g, 76%). ^1H NMR (C_6D_6 , 250.13 MHz): δ 8.02 (d, 2H, $J_{\text{HP}} = 8.50$, Ar), 7.09 (bs, 2H, Ar), 6.93 (d, 2H, $J_{\text{HP}} = 8.50$, Ar), 2.23 (s, 6H, Me), 2.15 - 0.98 (m, Cy), -12.04 ($J_{\text{HP}} = 14.5$ and $J_{\text{HPt}} = 1022.4$, Pt-H). $^{31}\text{P}\{^1\text{H}\}$ NMR (C_6D_6 , 101.26 MHz): δ 49.6 ($J_{\text{PPt}} = 2771.7$).

Synthesis of [2-(diisopropylphosphino)-4-methylphenyl][2-(diphenylphosphino)-4-methylphenyl]amine ($^{\text{iPr}}\text{PNP}^{\text{Ph}}$) **56**

n-BuLi (2.4 mL, 6.03 mmol, 2.5 M in hexane) was added dropwise to a solution of bis(2-bromo-4-methylphenyl)amine (1.07 g, 3.02 mmol) in diethyl ether (50 mL) at $-35\text{ }^\circ\text{C}$. The solution was stirred at RT for 3 hrs. The reaction mixture was cooled back down to $-35\text{ }^\circ\text{C}$ and a diethyl ether (5 mL) solution of diisopropylchlorophosphine (0.460 g, 3.02 mmol) was added dropwise. The reaction mixture was stirred overnight. The yellow solution was cooled back down to $-35\text{ }^\circ\text{C}$ and *n*-BuLi (0.71 mL, 1.76 mmol, 2.5 M in hexane) was added dropwise. The solution was stirred at RT for 3 hrs. The reaction mixture was cooled back down to $-35\text{ }^\circ\text{C}$ and a diethyl ether (5 mL) solution of diphenylchlorophosphine (0.390 g, 1.76 mmol) was added dropwise. The reaction mixture was stirred overnight, filtered through Celite, and evaporated to dryness under reduced pressure resulting in an orange residue. The orange residue was dissolved into diethyl ether (20 mL) and 5 mL of degassed DI water was added. The solution was then dried with MgSO_4 , filtered through Celite, and evaporated to dryness under reduced pressure resulting in an orange oil. The oil

was dissolved into a solution of diethyl ether and layered with pentane (3:1) and cooled to $-35\text{ }^{\circ}\text{C}$. This resulted in an off-white solid of **56** (0.590 g, 39%). ^1H NMR (C_6D_6 , 250.13 MHz): δ 7.66 (dd, 1H, $J_{\text{HP}} = 10.51$ and $J_{\text{HP}} = 3.25$, NH), 7.49 (dt, 4H, Ar) 7.40 (dd, 1H, Ar) 7.24 (dd, 1H, Ar), 7.09 (m, 7H, Ar), 6.90 (m, 3H, Ar), 2.16 (s, 3H, Ar-Me), 1.96 (s, 3H, Ar-Me), 1.88 (m, 2H, CHMe_2), 1.02 (dd, 6H, CHMe_2), 0.88 (dd, 6H, CHMe_2). $^{31}\text{P}\{^1\text{H}\}$ NMR (C_6D_6 , 101.26 MHz): δ -14.5 (bs, P^iPr_2), -16.5 (d, $J_{\text{PP}} = 8.10$, PPh_2). Observable $^{13}\text{C}\{^1\text{H}\}$ NMR (C_6D_6 , 62.89 MHz): δ 147.7 (d, $J_{\text{CP}} = 19.0$, C), 144.9 (d, $J_{\text{CP}} = 19.9$, C), 136.9 (d, $J_{\text{CP}} = 11.1$, C), 134.7 (s, CH), 134.3 (d, $J_{\text{CP}} = 19.9$, CH), 133.7 (s, CH), 131.3 (s, CH), 130.7 (d, $J_{\text{CP}} = 7.4$, CH), 128.8 (s, CH), 128.7 (s, CH) 122.1 (d, $J_{\text{CP}} = 15.7$, C), 119.7 (s, CH), 116.9 (s, CH), 23.6 (d, $J_{\text{CP}} = 11.1$, CHMe_2), 20.9 (s, Ar-Me), 20.8 (s, Ar-Me) 20.5 (d, $J_{\text{CP}} = 19.0$, CHMe_2), 19.3 (d, $J_{\text{CP}} = 9.2$, CHMe_2). Anal. Calcd for $\text{C}_{32}\text{H}_{37}\text{NP}_2$: C, 77.24; H, 7.49; N, 2.81. Found: C, 77.49; H, 7.85; N, 2.68.

Synthesis of [2-(dicyclohexylphosphino)-4-methylphenyl][2-(diphenylphosphino)-4-methylphenyl]amine ($^{\text{Cy}}\text{PNP}^{\text{Ph}}$) **57**

n-BuLi (8.15 mL, 20.37 mmol, 2.5 M in hexane) was added dropwise to a solution of bis(2-bromo-4-methylphenyl)amine (3.62 g, 10.19 mmol) in diethyl ether (80 mL) at $-5\text{ }^{\circ}\text{C}$. The solution was stirred at RT for 3 hrs. The reaction mixture was cooled back down to $-35\text{ }^{\circ}\text{C}$ and a diethyl ether (5 mL) solution of dicyclohexylchlorophosphine (2.37 g, 10.19 mmol) was added dropwise. The reaction mixture was stirred overnight. The yellow solution was cooled back down to $-35\text{ }^{\circ}\text{C}$ and *n*-BuLi (4.08 mL, 10.19 mmol, 2.5 M in hexane) was added

dropwise. The solution was stirred at RT for 3 hrs. The reaction mixture was cooled back down to $-35\text{ }^{\circ}\text{C}$ and a diethyl ether (5 mL) solution of diphenylchlorophosphine (2.25 g, 10.19 mmol) was added dropwise. The reaction mixture was stirred overnight, filtered through Celite, and evaporated to dryness under reduced pressure resulting in an orange residue. The orange residue was redissolved into diethyl ether (20 mL) and 5 mL of degassed DI water was added. The solution was dried with MgSO_4 , filtered through Celite, and evaporated to dryness under reduced pressure resulting in an orange oil. The orange oil was redissolved into a solution of diethyl ether and layered with pentane (1:3) and cooled to $-35\text{ }^{\circ}\text{C}$. This resulted in an off-white solid of **57** (1.92 g, 33%). ^1H NMR (C_6D_6 , 250.13 MHz): δ 7.70 (dd, 1H, $J_{\text{HP}} = 10.13$ and $J_{\text{HP}} = 3.25$, NH), 7.49 (m, 5H, Ar) 7.28 (m, 2H, Ar), 7.11 (m, 6H, Ar), 6.91 (m, 3H, Ar), 2.18 (s, 3H, Me), 1.96 (s, 3H, Me), 1.88-1.38 (m, Cy), 1.38-0.95 (m, Cy). $^{31}\text{P}\{^1\text{H}\}$ NMR (C_6D_6 , 101.26 MHz): δ -16.5 (d, $J_{\text{PP}} = 7.7$, PPh_2), -23.5 (bs, PCy_2). Observable $^{13}\text{C}\{^1\text{H}\}$ NMR (C_6D_6 , 62.89 MHz): δ 148.0 (d, $J_{\text{CP}} = 19.0$, C), 144.1 (d, $J_{\text{CP}} = 19.5$, C), 137.1 (d, $J_{\text{CP}} = 10.6$, C), 134.7 (s, CH), 134.4 (d, $J_{\text{CP}} = 19.9$, CH), 134.0 (s, CH), 131.4 (s, CH), 130.7 (d, $J_{\text{CP}} = 7.9$, CH), 128.8 (s, CH), 128.7 (s, CH) 121.8 (d, $J_{\text{CP}} = 16.2$, C), 119.5 (s, CH), 116.9 (s, CH), 33.6 (d, $J_{\text{CP}} = 11.6$, CH), 30.9 ($J_{\text{CP}} = 17.6$, CH_2), 29.2 (d, $J_{\text{CP}} = 7.4$, CH_2), 27.4 (d, $J_{\text{CP}} = 12.5$, CH_2), 27.3 (d, $J_{\text{CP}} = 7.4$, CH_2), 26.8 (s, CH_2), 21.0, (s, Ar-Me), 20.9 (s, Ar-Me). Anal. Calcd for $\text{C}_{38}\text{H}_{45}\text{NP}_2$: C, 79.00; H, 7.85; N, 2.42; Found: C, 78.82; H, 7.93; N, 2.22.

Synthesis of [2-(diisopropylphosphino)-4-methylphenyl][2-(diphenylphosphino)-4-methylphenyl]amido]chloropalladium (ⁱPrPNP^{Ph}-Pd-Cl) **58**

ⁱPrPNP^{Ph} (0.051 g, 0.180 mmol) and (COD)PdCl₂ (0.089 g, 0.180 mmol) were placed into a round bottom flask along with 20 mL of THF and one equiv. of NEt₃. The red solution was refluxed for one hour, filtered through Celite, and the volatiles were removed under reduce pressure resulting in a red solid. The red solid was washed with cold pentane and dried under vacuum to give **58** (0.110 g, 96%). ¹H NMR (C₆D₆, 250.13 MHz): δ 7.96 (m, 4H, Ar), 7.78 (dd, 1H, Ar) 7.68 (dd, 1H, Ar) 6.99 (m, 7H, Ar), 6.78 (td, 3H, Ar), 2.28 (m, 2H, CHMe₂), 2.11 (s, 3H, Ar-Me), 1.91 (s, 3H, Ar-Me), 1.43 (dd, 6H, CHMe₂), 1.07 (dd, 6H, CHMe₂).

³¹P{¹H} NMR (C₆D₆, 101.26 MHz): δ 54.0 (d, J_{PP} = 437.2, PⁱPr₂), 25.7 (d, J_{PP} = 437.2, PPh₂). Observable ¹³C{¹H} NMR (C₆D₆, 62.89 MHz): δ 161.8 (d, J_{CP} = 20.4, C), 161.5 (d, J_{CP} = 25.1, C), 135.2 (s, CH), 134.0 (d, J_{CP} = 12.1, CH), 133.1 (s, CH), 132.5 (s, CH), 131.5 (d, J_{CP} = 43.1 and J_{CP} = 3.7, C), 130.5 (s, CH), 129.0 (s, CH), 128.8 (s, CH), 126.9 (d, J_{CP} = 7.0, CH), 126.3 (d J_{CP} = 7.0, CH), 121.3 (d, J_{CP} = 46.5, C), 119.2 (d, J_{CP} = 39.4, C), 116.9 (d, J_{CP} = 13.0, CH), 116.5 (J_{CP} = 14.3, CH), 25.2 (d, J_{CP} = 21.3, CHMe₂), 20.4 (s, Ar-Me), 20.2 (s, Ar-Me), 18.8 (d, J_{CP} = 3.7, CHMe₂), 18.1 (s, CHMe₂). Anal. Calcd for C₃₂H₃₆ClNP₂Pd: C, 60.20; H, 5.68; N, 2.19; Found: C, 60.55; H, 5.69; N, 2.08.

Synthesis of [2-(dicyclohexylphosphino)-4-methylphenyl][2-(diphenylphosphino)-4-methylphenyl]amido]chloropalladium (^{Cy}PNP^{Ph}-Pd-Cl) **59**

^{Cy}PNP^{Ph} (0.191 g, 0.330 mmol) and (COD)PdCl₂ (0.094 g, 0.330 mmol) were placed into a round bottom flask along with 20 mL of THF and one equiv. of NEt₃. The red solution was refluxed for one hour, filtered through Celite, and the volatiles were removed under reduced pressure resulting in a red solid. The red solid was washed with cold pentane and dried under vacuum to give **59** (0.129 g, 84%). ¹H NMR (C₆D₆, 250.13 MHz): δ 8.00 (m, 4H, Ar), 7.83 (dd, 1H, Ar) 7.74 (dd, 1H, Ar) 6.99 (m, 8H, Ar), 6.77 (td, 2H, Ar), 2.13 (s, 3H, Ar-Me), 1.91 (s, 3H, Ar-Me), 2.48 – 0.91 (m, 22H, Cy). ³¹P{¹H} NMR (C₆D₆, 101.26 MHz): δ 46.5 (d, *J*_{PP} = 437.5, PCy₂), 25.7 (d, *J*_{PP} = 437.4, PPh₂). Observable ¹³C{¹H} NMR (C₆D₆, 62.89 MHz): δ 162.0 (d, *J*_{CP} = 20.4, C), 161.6 (d, *J*_{CP} = 25.7, C), 135.2 (s, CH), 134.0 (d, *J*_{CP} = 11.3, CH), 133.9 (d, *J*_{CP} = 30.1, CH), 132.5 (s, CH), 131.4 (dd, *J*_{CP} = 43.0 and *J*_{CP} = 3.8, C), 130.6 (s, CH), 129.0 (s, CH), 128.8 (d, *J*_{CP} = 5.0, CH), 126.9 (*J*_{CP} = 6.0, CH), 126.3 (d, *J*_{CP} = 6.8, CH), 121.3 (d, *J*_{CP} = 47.5, C), 119.5 (d, *J*_{CP} = 40.0, C), 117.0 (d, *J*_{CP} = 12.8, CH), 116.5 (*J*_{CP} = 14.3, CH), 34.4 (d, *J*_{CP} = 21.3, CH), 28.7 (s, CH₂), 28.3 (s, CH₂), 27.1 (s, CH₂), 27.0 (s, CH₂), 25.8 (s, CH₂), 20.4 (s, Ar-Me), 20.0 (s, Ar-Me). Anal. Calcd for C₃₈H₄₄ClNP₂Pd: C, 63.51; H, 6.17; N, 1.95; Found: C, 63.14; H, 6.16; N, 1.87.

Synthesis of [2-(diisopropylphosphino)-4-methylphenyl][2-

(diphenylphosphino)-4-methylphenyl]amido]chloroplatinum (ⁱPrPNP^{Ph}-Pt-Cl)

60

ⁱPrPNP^{Ph} (0.093 g, 0.190 mmol) and (COD)PtCl₂ (0.070 g, 0.190 mmol) were placed into a round bottom flask along with 20 mL of THF and one equiv. of NEt₃. The yellow solution was refluxed for 2.5 hours, filtered through Celite, and the volatiles were removed under reduced pressure resulting in a yellow solid. The yellow solid was washed with cold pentane and dried under vacuum to give **60** (0.102 g, 75%). ¹H NMR (C₆D₆, 250.13 MHz): δ 8.00 (m, 4H, Ar), 7.78 (dd, 1H, Ar) 7.68 (dd, 1H, Ar) 6.99 (m, 8H, Ar), 6.78 (td, 2H, Ar), 2.52 (m, 2H, CHMe₂), 2.13 (s, 3H, Ar-Me), 1.94 (s, 3H, Ar-Me), 1.43 (dd, 6H, CHMe₂), 1.08 (dd, 6H, CHMe₂). ³¹P{¹H} NMR (C₆D₆, 101.26 MHz): δ 45.7 (dt, $J_{\text{PPt}} = 2754.5$ and $J_{\text{PP}} = 401.6$, PⁱPr₂), 41.7 (dt, $J_{\text{PPt}} = 2754.2$ and $J_{\text{PP}} = 401.6$, PⁱPr₂) 26.7 (dt, $J_{\text{PPt}} = 2673.9$ and $J_{\text{PP}} = 401.9$, PPh₂), 22.7 (dt, $J_{\text{PPt}} = 2673.9$ and $J_{\text{PP}} = 401.9$, PPh₂). Observable ¹³C{¹H} NMR (C₆D₆, 62.89 MHz): δ 162.0 (d, $J_{\text{CP}} = 18.1$, C), 161.6 (d, $J_{\text{CP}} = 20.4$, C), 135.1 (s, CH), 134.0 (d, $J_{\text{CP}} = 10.6$, CH), 132.6 (d, $J_{\text{CP}} = 45.3$, C), 132.4 (s, CH), 131.6 (d, $J_{\text{CP}} = 52.1$ and $J_{\text{CP}} = 3.0$, C), 130.6 (s, CH), 128.9 (s, CH), 128.7 (s, CH), 127.3 (s, CH), 126.7 (d $J_{\text{CP}} = 6.8$, CH), 121.5 (d, $J_{\text{CP}} = 55.8$, C), 119.5 (d, $J_{\text{CP}} = 48.3$, C), 116.8 (d, $J_{\text{CP}} = 11.3$, CH), 116.4 ($J_{\text{CP}} = 12.1$, CH), 25.3 (d, $J_{\text{CP}} = 28.0$, CHMe₂), 20.3 (s, Ar-Me), 20.0 (s, Ar-Me), 18.4 (s, CHMe₂), 17.9 (s, CHMe₂). Anal. Calcd for C₃₂H₃₆ClNP₂Pt: C, 52.86; H, 4.99; N, 1.93; Found: C, 52.46; H, 5.14; N, 1.71.

Synthesis of [2-(dicyclohexylphosphino)-4-methylphenyl][2-(diphenylphosphino)-4-methylphenyl]amido]chloroplatinum (^{Cy}PNP^{Ph}-Pt-Cl)

61

^{Cy}PNP^{Ph} (0.056 g, 0.096 mmol) and (COD)PtCl₂ (0.036 g, 0.096 mmol) were placed into a round bottom flask along with 20 mL of THF and one equiv. of NEt₃. The yellow solution was refluxed for 2.5 hours, filtered through Celite, and the volatiles were removed under reduced pressure resulting in a yellow solid. The yellow solid was washed with cold pentane and dried under vacuum to give **61** (0.067 g, 87%). ¹H NMR (C₆D₆, 250.13 MHz): δ 8.03 (m, 4H, Ar), 7.90 (dd, 1H, Ar) 7.81 (dd, 1H, Ar) 6.97 (m, 8H, Ar), 6.75 (td, 2H, Ar), 2.15 (s, 3H, Ar-Me), 1.93 (s, 3H, Ar-Me), 2.60 – 0.99 (m, 22H, Cy). ³¹P{¹H} NMR (C₆D₆, 101.26 MHz): δ 37.8 (dt, $J_{\text{PPt}} = 2749.2$ and $J_{\text{PP}} = 402.4$, PCy₂), 34.5 (dt, $J_{\text{PPt}} = 2749.4$ and $J_{\text{PP}} = 402.4$, PCy₂) 26.2 (dt, $J_{\text{PPt}} = 2673.0$ and $J_{\text{PP}} = 402.3$, PPh₂), 22.9 (dt, $J_{\text{PPt}} = 2673.0$ and $J_{\text{PP}} = 402.3$, PPh₂). Observable ¹³C{¹H} NMR (C₆D₆, 62.89 MHz): δ 162.0 (d, $J_{\text{CP}} = 17.4$, C), 161.6 (d, $J_{\text{CP}} = 19.6$, C), 135.1 (s, CH), 134.0 (d, $J_{\text{CP}} = 10.6$, CH), 132.7 (d, $J_{\text{CP}} = 52.0$, C), 132.6 (s, CH), 132.3 (s, CH₂), 131.7 (d, $J_{\text{CP}} = 53.6$, C), 130.6 (s, CH), 128.9 (s, CH), 128.7 (s, CH), 127.3 (d, $J_{\text{CP}} = 7.5$, CH), 126.8 (d, $J_{\text{CP}} = 6.7$, C), 121.5 (d, $J_{\text{CP}} = 55.8$, C), 119.7 (d, $J_{\text{CP}} = 46.0$, C), 116.9 (d, $J_{\text{CP}} = 10.6$, CH), 116.4 ($J_{\text{CP}} = 11.3$, CH), 34.7 (d, $J_{\text{CP}} = 27.9$, CH), 28.4 (s, CH₂), 28.3 (d, $J_{\text{CP}} = 6.3$, CH₂), 27.2 (s, CH₂), 27.0 (d, $J_{\text{CP}} = 6.2$, CH₂), 26.1 (s, CH₂), 20.4 (s, Ar-Me), 20.0 (s, Ar-Me). Anal. Calcd for C₃₈H₄₄ClNP₂Pt: C, 56.54; H, 5.49; N, 1.74; Found: C, 56.98; H, 6.35; N, 1.98.

Synthesis of [2-(diisopropylphosphino)-4-methylphenyl][2-(diphenylphosphino)-4-methylphenyl]amido]Hydropalladium (^{iPr}PNP^{Ph}-Pd-H) 62

^{iPr}PNP^{Ph}-Pd-Cl (0.103 g, 0.160 mmol) and Super Hydride (0.160 mL, 0.160 mmol) were placed into a round bottom flask with 20 mL of THF and stirred at RT for 5 hours. The volatiles were removed under reduced pressure resulting in a brown residue. The brown residue was redissolved into pentane and filtered through Celite resulting in a brown solution. The volatiles were removed under reduced pressure resulting in a brown solid. The brown solid was dried under vacuum to give **62** (0.081 g, 84%). ¹H NMR (C₆D₆, 250.13 MHz): δ 7.96 (m, 2H, Ar), 7.83 (m, 4H, Ar) 6.98 (m, 8H, Ar), 2.05 (m, 2H, CHMe₂), 2.21 (s, 3H, Ar-Me), 2.00 (s, 3H, Ar-Me), , 1.22 (dd, 6H, CHMe₂), 0.90 (dd, 6H, CHMe₂) -9.97 (vt, 1H, J_{HP} = 5.25, Pd-H). ³¹P{¹H} NMR (C₆D₆, 101.26 MHz): δ 63.4 (d, J_{PP} = 354.2, PⁱPr₂), 31.4 (d, J_{PP} = 354.3, PPh₂).

Synthesis of [2-(dicyclohexylphosphino)-4-methylphenyl][2-(diphenylphosphino)-4-methylphenyl]amido]Hydropalladium (^{Cy}PNP^{Ph}-Pd-H) 63

^{Cy}PNP^{Ph}-Pd-Cl (0.100 g, 0.140 mmol) and Super Hydride (0.140 mL, 0.140 mmol) were placed into a round bottom flask along with 20 mL of THF and stirred at RT for 3 hours. The volatiles were removed under reduced pressure resulting in a brown residue. The brown residue was redissolved into pentane and filtered through Celite resulting in a brown solution. The volatiles were removed under

reduced pressure resulting in a brown solid. The brown solid was dried under vacuum to give **63** (0.083 g, 87%). ^1H NMR (C_6D_6 , 250.13 MHz): δ 7.99 (m, 4H, Ar), 7.90 – 7.75 (m, 2H, Ar), 7.14 – 6.86 (m, 10H, Ar), 2.23 (s, 3H, Ar-Me), 2.16 (s, 3H, Ar-Me), 2.01 – 0.95 (m, 22H, Cy), -9.91 (vt, 1H, $J_{\text{HP}} = 4.75$, Pd-H). $^{31}\text{P}\{^1\text{H}\}$ NMR (C_6D_6 , 101.26 MHz): δ 54.5 (d, $J_{\text{PP}} = 354.5$, PCy_2), 31.5 (d, $J_{\text{PP}} = 354.5$, PPh_2).

Synthesis of [2-(diisopropylphosphino)-4-methylphenyl][2-(diphenylphosphino)-4-methylphenyl]amido]Hydroplatinum ($^{i\text{Pr}}\text{PNP}^{\text{Ph}}\text{-Pt-H}$) **64**

$^{i\text{Pr}}\text{PNP}^{\text{Ph}}\text{-Pt-Cl}$ (0.043 g, 0.060 mmol) and Super Hydride (0.060 mL, 0.060 mmol) were placed into a round bottom flask along with 20 mL of THF and stirred at RT for 2 hours. The volatiles were removed under reduced pressure resulting in a brown residue. The brown residue was redissolved into pentane and filtered through Celite resulting in a brown solution. The volatiles were removed under reduced pressure resulting in a brown solid. The brown solid was dried under vacuum to give **64** (0.035 g, 85%). ^1H NMR (C_6D_6 , 250.13 MHz): δ 8.05 - 7.71 (m, 6H, Ar), 7.11 - 6.96 (m, 10H, Ar), 2.13 (m, 2H, CHMe_2), 2.11 (s, 3H, Ar-Me), 2.00 (s, 3H, Ar-Me), 1.18 (dd, 6H, CHMe_2), 0.93 (dd, 6H, CHMe_2), -11.6 (vtt 1H, $J_{\text{HP}} = 14.1$ and $J_{\text{HPt}} = 1031.8$, Pt-H). $^{31}\text{P}\{^1\text{H}\}$ NMR (C_6D_6 , 101.26 MHz): δ 61.6 (dt, $J_{\text{PPt}} = 2860.3$ and $J_{\text{PP}} = 361.4$, P^iPr_2), 58.0 (dt, $J_{\text{PPt}} = 2860.2$ and $J_{\text{PP}} = 361.4$, P^iPr_2), 36.3 (dt, $J_{\text{PPt}} = 2824.0$ and $J_{\text{PP}} = 361.3$, PPh_2), 32.8 (dt, $J_{\text{PPt}} = 2823.91$ and $J_{\text{PP}} = 361.38$, PPh_2).

Synthesis of [Bis[2-(dicyclohexylphosphino)-4-methylphenyl]amido]chloronickel (^{Cy}PNP-Ni-Cl) 66

^{Cy}PNP (0.500 g, 0.080 mmol) and NiCl₂ (0.240 g, 0.080 mmol) were placed into a round bottom flask along with 20 mL of THF and one equiv. of NEt₃. The green solution was refluxed for one hour, filtered through Celite, and the volatiles were removed under reduced pressure resulting in a green solid. The green solid was washed with cold pentane and dried under vacuum to give **66** (0.051 g, 82%).

¹H NMR (C₆D₆, 250.13 MHz): δ 7.58 (d, 2H, *J*_{HP} = 8.50, Ar), 7.11 (bs, 2H, Ar), 6.73 (d, 2H, *J*_{HP} = 8.51 Ar), 2.14 (s, 6H, Me), 2.69 - 1.83 (m, Cy), 1.82 - 0.95 (m, Cy). ¹³C{¹H} NMR (C₆D₆, 250.13 MHz): δ 162.5 (t, *J*_{CP} = 13.1, C), 132.2 (s, CH), 131.9 (s, CH), 125.3 (s, CH), 120.8 (t, *J*_{CP} = 18.6, C), 116.7 (t, *J*_{CP} = 5.3, CH), 34.3 (t, *J*_{CP} = 11.9, PCH), 28.7 (s, CH₂), 28.1 (s, CH₂), 27.3 (bs, CH₂) 27.2 (bs, CH₂), 26.3 (s, CH₂) 20.4 (s, Me) ³¹P{¹H} NMR (C₆D₆, 101.26 MHz): δ 26.9.

Synthesis of [Bis[2-(dicyclohexylphosphino)-4-methylphenyl]amido]hydronickel (^{Cy}PNP-Ni-H) 67

Method 1: ^{Cy}PNP-Ni-Cl (0.030 g, 0.041 mmol) was placed into a round bottom flask along with 15 mL of THF. The solution was cooled to -35 °C and Super Hydride (0.041 mL, 0.041 mmol, 1.0M in THF) was added. The solution was stirred at RT for 3.5 hrs. The volatiles were removed under reduced pressure resulting in a brown residue. The brown residue was redissolved into pentane and filtered through Celite resulting in a brown solution. The volatiles were

removed under reduced pressure, resulting in a brown solid. The brown solid was dried under vacuum to give **67** (0.021 g, 74%).

Method 2: ^{Cy}PNP (0.084 g, 0.142 mmol) and Ni(COD)₂ (0.039 g, 0.142 mmol) were placed into a round bottom flask along with 20 mL of benzene and stirred at RT for 15 minutes. The volatiles were removed under reduced pressure resulting in a brown solid. The brown solid was dried under vacuum to give **67** (0.088 g, 96%). ¹H NMR (C₆D₆, 250.13 MHz): δ 7.91 (d, 2H, J_{HP} = 8.50, Ar), 7.14 (bs, 2H, Ar), 6.93 (d, 2H, J_{HP} = 8.25, Ar), 2.24 (s, 6H, Me), 2.21 - 1.40 (m, Cy), 1.35 - 0.95 (m, Cy) -18.4 (t, 1H, J_{HP} = 63.2, Ni-H). ³¹P{¹H} NMR (C₆D₆, 101.26 MHz): δ 46.7.

Synthesis of [2-(diisopropylphosphino)-4-methylphenyl][2-

(diphenylphosphino)-4-methylphenyl]amido]Hydronickel (^{iPr}PNP^{Ph}-Ni-H) **68**

^{iPr}PNP^{Ph} (0.103 g, 0.160 mmol) and Ni(COD)₂ (0.160 mL, 0.160 mmol) were placed into a round bottom flask along with 20 mL of benzene and stirred at RT for 15 minutes. The volatiles were removed under reduced pressure, resulting in a brown residue. The brown residue was washed with cold pentane and dried under vacuum to give **68** (0.081 g, 84%). ¹H NMR (C₆D₆, 250.13 MHz): δ 7.95 - 7.75 (m, 6H, Ar), 7.10 - 6.85 (m, 10H, Ar) 2.05 (m, 2H, CHMe₂), 2.21 (s, 3H, Ar-Me), 2.02 (s, 3H, Ar-Me), 1.23 (dd, 6H, CHMe₂), 0.95 (dd, 6H, CHMe₂) -18.1 (dd, 1H, J_{HP} = 68.5 and J_{HP} = 68.2, Ni-H). ³¹P{¹H} NMR (C₆D₆, 101.26 MHz): δ 58.9 (d, J_{PP} = 244.2, PⁱPr₂), 31.4 (d, J_{PP} = 244.1, PPh₂). Observable ¹³C{¹H} NMR (C₆D₆, 62.89 MHz): δ 161.4 (dd, J_{CP} = 21.4 and J_{CP} = 3.5, C), 160.9 (dd, J_{CP} = 25.1 and J_{CP} = 2.3, C), 134.5 (s, CH), 133.8 (d, J_{CP} = 12.5, CH), 133.0 (s, CH),

132.5 (s, CH), 130.0 (s, CH), 128.6 (d, $J_{CP} = 9.9$, CH), 128.5 (s, CH), 124.6 (d, $J_{CP} = 7.0$, C), 124.5 (d, $J_{CP} = 42.3$, C), 124.1 (d, $J_{CP} = 5.4$, CH), 122.5 (d, $J_{CP} = 34.2$, C), 115.6 (d, $J_{CP} = 10.8$, CH), 115.0 ($J_{CP} = 11.1$, CH), 23.7 (d, $J_{CP} = 25.7$, $CHMe_2$), 20.5 (s, Ar-Me), 20.3 (s, Ar-Me), 19.5 (d, $J_{CP} = 5.7$, $CHMe_2$), 18.3 (s, $CHMe_2$). Anal. Calcd for $C_{32}H_{37}NP_2Ni$: C, 69.09; H, 6.70; N, 2.52; Found: C, 69.27; H, 6.88; N, 2.27.

Synthesis of [2-(dicyclohexylphosphino)-4-methylphenyl][2-

(diphenylphosphino)-4-methylphenyl]amido]Hydronickel ($CyPnP^{Ph}-Ni-H$) **69**

$CyPnP^{Ph}$ (0.100 g, 0.104 mmol) and $Ni(COD)_2$ (0.140 mL, 0.140 mmol) were placed into a round bottom flask along with 20 mL of benzene and stirred at RT for 15 minutes. The volatiles were removed under reduced pressure resulting in a brown solid. The brown solid was washed with cold pentane and dried under vacuum to give **69** (0.083 g, 87%). 1H NMR (C_6D_6 , 250.13 MHz): δ 8.00 - 7.78 (m, 6H, Ar) 7.14 - 6.85 (m, 10H, Ar), 2.22 (s, 3H, Ar-Me), 2.02 (s, 3H, Ar-Me), 2.22 - 0.85 (m, Cy), -18.1 (dd, $J_{HP} = 67.8$ and $J_{HP} = 67.8$). $^{31}P\{^1H\}$ NMR (C_6D_6 , 101.26 MHz): δ 49.6 (d, $J_{PP} = 244.9$, PCy_2), 31.8 (d, $J_{PP} = 244.2$, PPh_2). (C_6D_6 , 101.26 MHz): δ 58.9 (d, $J_{PP} = 244.2$, P^iPr_2), 31.4 (d, $J_{PP} = 244.1$, PPh_2). Observable $^{13}C\{^1H\}$ NMR (C_6D_6 , 62.89 MHz): δ 161.6 (dd, $J_{CP} = 21.9$ and $J_{CP} = 3.6$, C), 160.9 (dd, $J_{CP} = 25.3$ and $J_{CP} = 2.4$, C), 134.4 (s, CH), 133.8 (d, $J_{CP} = 12.4$, CH), 132.7 (d, $J_{CP} = 31.0$, CH), 132.4 (s, CH), 129.9 (s, CH), 128.8 (s, CH), 128.6 (s, CH), 124.6 (d, $J_{CP} = 6.1$, C), 124.6 (d, $J_{CP} = 42.0$, C), 124.2 (d, $J_{CP} = 5.4$, CH), 122.6 (d, $J_{CP} = 34.3$, C), 115.6 (d, $J_{CP} = 10.4$, CH), 115.1 ($J_{CP} = 11.7$,

CH), 33.3 (d, $J_{CP} = 26.0$, CH), 29.8 (d, $J_{CP} = 4.1$, CH₂), 28.6 (s, CH₂) 27.4 (s, CH₂), 27.0 (s, CH₂), 26.6 (s, CH₂), 20.6 (s, Ar-Me), 20.3 (s, Ar-Me).

Final Remarks

The goal of this research was to generate pincer PNP-based metal hydrides and investigate their potential catalytic ability in activating molecular oxygen for the oxidation of organic substrates. Two types of PNP-based ligands were investigated in the potential catalytic cycle shown in Scheme 4. The first type of PNP ligand exists in the neutral form and was allowed to react with a Rh precursor to generate two new $^R\text{PNP-Rh-Cl}$ species in high yields. The conversion of these PNP-Rh-Cl complexes to hydride derivatives proved to be a difficult task. The investigations revealed the synthetic difficulty in generating pincer hydrides from common hydride sources, even those that have shown successful conversion in related PCP complexes. Several hydride sources were employed in screening reactions under a variety of conditions. However, no success in preparing the metal hydrides using this direct route was realized.

An alternative method was proposed and investigated for the synthesis of new Rh hydrides. The route was a multi-step sequence that led to the preparation of the desired $^R\text{PNP-Rh-H}$ complexes. After preparation, these PNP-based Rh hydrides were investigated in oxygen insertion reactions. Each Rh hydride was allowed to react with O_2 directly using different levels of O_2 pressures; however, none showed any direct insertion of O_2 . NMR spectroscopy revealed that the Rh hydrides appear to decompose and generate an oxidized Rh(III) species and/or an unknown phosphine-containing species, rather than inserting O_2 to form a hydroperoxide.

A second family of pincer PNP-based ligands was investigated in proposed catalytic scheme. In these reactions, the pincer PNP ligand was anionic rather than neutral. From this anionic PNP-based ligand set, several modifications were performed to produce new symmetric, unsymmetric and racemic chiral ligands. The generated symmetric and unsymmetric ligands were allowed to react with Group 10 metals to form several new PNP-M-Cl complexes in high yields. These metal complexes were then treated with several hydride sources in an attempt to produce the pincer metal hydrides. Once again, the synthesis of these pincer hydrides was not straightforward and required a great deal of experimentation to find hydride sources that would work effectively. From these reactions several new symmetric and unsymmetric PNP-M-H complexes were produced and characterized. Many of the PNP-M-Cl and PNP-M-H species were characterized by X-ray crystallography. These pincer hydrides were then subjected to oxygen insertion reactions, which resulted in spectroscopic evidence for the formation of hydroperoxide species for the Pd-based complexes. One new Pd-OOH was crystallographically characterized.

With the difficulty in isolating most of the hydroperoxide species, investigation into their potential oxygen transfer capabilities was done by an *in situ* method. Upon the formation of these hydroperoxide species, several organic substrates were introduced into these attempted oxygen transfer reactions. These reactions were monitored by $^{31}\text{P}\{^1\text{H}\}$ NMR and ^1H NMR for several days. In all cases no direct oxidized species and hydroxide was identified. The oxygen

atom in our hydroperoxide species does not seem to possess sufficient nucleophilic character to react with the organic substrates.

Appendix

Compound	29	30	31
Empirical Formula	C ₁₉ H ₃₅ CINP ₂ Rh	C ₃₁ H ₅₁ CINP ₂ Rh	C ₂₄ H ₄₃ F ₃ NO ₃ P ₂ RhS
FW	477.78	638.03	647.50
Cryst Size (mm)	0.41 x 0.19 x 0.16	0.46 x 0.18 x 0.12	0.40 x 0.30 x 0.10
Cryst Syst	Triclinic	Orthorhombic	Monoclinic
Space Group	P-1	P2(1)2(1)2(1)	P2(1)/n
a, Å	16.1890(13)	12.5181(13)	10.4271(4)
b, Å	16.1903(13)	14.0828(13)	19.8855(9)
c, Å	16.2011(12)	17.629(17)	15.3683(6)
α, deg	103.985(5)	90	90
β, deg	104.050(5)	90	109.787(2)
γ, deg	103.971(5)	90	90
Volume (Å ³)	3788.7(5)	3107.9(5)	2998.4(2)
Z	8	4	4
Calc.density,g/cm ³	1.675	1.364	1.434
μ(MoKα), mm ⁻¹	1.214	0.759	0.789
Indep reflecons	16550	10386	7444
	R _(int) = 0.1556	R _(int) = 0.0358	R _(int) 0.0572
T, K	228(2)	228(2)	253(2)
R1, wR2 (all data)	0.2721, 0.3475	0.0308, 0.0737	0.0604, 0.1022
R1, wR2 [I>2σ(I)]	0.0876, 0.2447	0.0242, 0.0629	0.0343, 0.0841
GOF on F ²	0.991	1.159	1.125

Compound	34	45	48
Empirical Formula	C ₂₄ H ₄₅ F ₃ NO ₃ P ₂ RhS	C ₃₈ H ₅₇ NP ₂	C ₃₈ H ₅₆ ClNP ₂ Pd
FW	649.52	589.79	730.63
Cryst Size (mm)	0.50 x 0.40 x 0.10	0.41 x 0.25 x 0.16	0.34 x 0.23 x 0.09
Cryst Syst	Triclinic	Monoclinic	Monoclinic
Space Group	P-1	P2(1)/c	P2(1)/c
a, Å	8.507(4)	10.4046(7)	11.6085(5)
b, Å	13.111(6)	19.0459(13)	16.1951(8)
c, Å	14.899(6)	17.4212(13)	19.2677(9)
α, deg	107.63(2)	90	90
β, deg	103.21(3)	96.960(2)	95.556(2)
γ, deg	93.66(3)	90	90
Volume (Å ³)	1525.8(12)	3426.8(4)	3605.3(3)
Z	2	4	4
Cal. density, g/cm ³	1.414	1.143	1.346
μ(MoKα), mm ⁻¹	0.776	0.153	0.704
Indep reflcns	6040	8768	8603
	R _(int) = 0.0315	R _(int) = 0.0639	R _(int) = 0.0469
T, K	253(2)	183(2)	183(2)
R1, wR2 (all data)	0.0887, 0.1654	0.0868, 0.1643	0.0556, 0.1171
R1, wR2 [I > 2σ(I)]	0.0530, 0.1487	0.0518, 0.1302	0.0353, 0.0970
GOF on F ²	1.055	1.081	1.144

Compound	53	56	58
Empirical Formula	C ₃₈ H ₅₇ NP ₂ Pd	C ₃₂ H ₃₇ NP ₂	C ₃₅ H ₃₉ CINP ₂ Pd
FW	696.19	497.57	677.46
Cryst Size (mm)	0.20 x 0.20 x 0.10	0.45 x 0.19 x 0.16	0.60 x 0.43 x 0.28
Cryst Syst	Monoclinic	Orthorhombic	Monoclinic
Space Group	P2(1)/c	P n a 2 ₁	P2(1)/n
a, Å	10.7894(2)	15.4380(11)	9.6912(6)
b, Å	31.9286(6)	22.8418(16)	11.5459(7)
c, Å	13.1827(2)	8.1278(5)	28.3155(17)
α, deg	90	90	90
β, deg	113.5930(10)	90	98.821(3)
γ, deg	90	90	90
Volume (Å ³)	4161.71(13)	2866.12(3)	3130.8(3)
Z	4	4	4
Calc density, g/cm ³	1.111	1.153	1.437
μ(MoKα), mm ⁻¹	0.545	0.172	0.805
Indep reflcns	12191	5539	15154
	R _(int) = 0.1201	R _(int) = 0.0390	R _(int) = 0.0297
T, K	228(2)	228(2)	183(2)
R1, wR2 (all data)	0.1529, 0.2451	0.0579, 0.1208	0.0411, 0.0962
R1, wR2 [I > 2σ(I)]	0.0787, 0.2034	0.0373, 0.0980	0.0325, 0.0856
GOF on F ²	1.046	1.121	1.239

Compound	59	60	61
Empirical Formula	C ₄₄ H ₅₀ CINP ₂ Pd	C ₃₂ H ₃₆ CINP ₂ Pt	C ₄₄ H ₅₀ CINP ₂ Pt
FW	796.64	766.14	885.32
Cryst Size (mm)	0.50 x 0.23 x 0.11	0.06 x 0.09 x 0.21	0.32 x 0.16 x 0.09
Cryst Syst	Triclinic	Monoclinic	Triclinic
Space Group	P-1	P 21/c	P-1
a, Å	11.3446(3)	9.7018(3)	11.3219(5)
b, Å	11.7317(3)	11.5256(4)	11.7353(5)
c, Å	15.4507(4)	28.4989(10)	15.5010(6)
α, deg	93.6470(10)	90	93.810(2)
β, deg	109.9500(10)	100.733(2)	110.178(2)
γ, deg	93.1420(10)	90	92.996(2)
Volume (Å ³)	1922.61(9)	3130.97(18)	1922.65(14)
Z	2	4	2
Calc density, g/cm ³	1.376	1.625	1.529
μ(MoKα), mm ⁻¹	0.667	4.694	3.834
Indep reflcns	16083	7789	13063
	R _(int) = 0.0289	R _(int) = 0.0764	R _(int) = 0.0381
T, K	188(2)	183(2)	183(2)
R1, wR2 (all data)	0.0461, 0.1030	0.0501, 0.0656	0.0514, 0.1336
R1, wR2 [I>2σ(I)]	0.0348, 0.0929	0.0320, 0.0601	0.0411, 0.1260
GOF on F ²	1.142	1.024	1.157

Compound	63	67	68
Empirical Formula	C ₃₈ H ₄₅ NP ₂ Pd	C ₃₈ H ₅₇ NNiP ₂	C ₃₂ H ₃₇ NNiP ₂
FW	684.09	664.50	556.28
Cryst Size (mm)	0.25 x 0.12 x 0.07	0.55 x 0.28 x 0.23	0.30 x 0.15 x 0.10
Cryst Syst	Triclinic	Monoclinic	Monoclinic
Space Group	P1	P2(1)/c	P2(1)/n
a, Å	11.3866(5)	10.7370(5)	12.3808(8)
b, Å	11.4791(5)	32.0366(13)	14.9010(10)
c, Å	14.9377(7)	13.0358(5)	15.9008(10)
α, deg	91.051(2)	90	90
β, deg	108.575(2)	114.182(2)	98.497(4)
γ, deg	94.265(2)	90	90
Volume (Å ³)	1843.81(14)	4090.5(3)	2901.3(3)
Z	2	4	4
Calc density, g/cm ³	1.232	1.079	1.274
μ(MoKα), mm ⁻¹	0.614	0.578	0.800
Indep reflcns	24605	10218	3871
	R _(int) = 0.0330	R _(int) = 0.0429	R _(int) = 0.0386
T, K	183(2)	228(2)	188(2)
R1, wR2 (all data)	0.0562, 0.1184	0.0814, 0.1660	0.0553, 0.1340
R1, wR2 [<i>I</i> > 2σ(<i>I</i>)]	0.0411, 0.1030	0.0557, 0.1479	0.0449, 0.1214
GOF on F ²	1.073	1.072	1.076

Compound	73	74	75
Empirical Formula	C ₃₂ H ₄₉ NP ₂	C ₃₂ H ₃₇ NP ₂	C ₃₈ H ₄₅ NP ₂
FW	509.66	497.57	577.69
Cryst Size (mm)	0.28 x 0.14 x 0.07	0.30 x 0.25 x 0.20	0.41 x 0.16 x 0.12
Cryst Syst	Monoclinic	Triclinic	Monoclinic
Space Group	P2(1)	P-1	P2(1)/c
a, Å	9.6527(7)	11.0836(4)	9.3673(3)
b, Å	13.2866(8)	11.4178(4)	10.0674(3)
c, Å	12.3847(9)	12.0810(5)	35.0069
α, deg	90	94.103(2)	90
β, deg	105.793(3)	110.913(2)	95.796
γ, deg	90	97.635(2)	90
Volume (Å ³)	1528.40(18)	1403.74(9)	3284.43
Z	2	2	4
Calc density, g/cm ³	1.107	1.177	1.168
μ(MoKα), mm ⁻¹	0.162	0.175	0.159
Indep reflcns	5467	2919	9975
	R _(int) = 0.0474	R _(int) = 0.0359	R _(int) = 0.0459
T, K	173(2)	228(2)	183(2)
R1, wR2 (all data)	0.0679, 0.1649	0.0533, 0.1430	0.0919, 0.1685
R1, wR2 [I > 2σ(I)]	0.0467, 0.1198	0.0398, 0.1140	0.0670, 0.1537
GOF on F ²	1.148	1.148	1.171

Compound	76	77	78
Empirical Formula	C ₃₂ H ₄₉ NP ₂	C ₃₂ H ₅₁ CINP ₂ Pd	C ₄₄ H ₅₀ CINP ₂ Pd
FW	509.66	653.53	796.64
Cryst Size (mm)	0.22 x 0.12 x 0.10	0.09 x 0.07 x 0.03	0.32 x 0.14 x 0.07
Cryst Syst	Triclinic	Triclinic	Monoclinic
Space Group	P-1	P-1	P2(1)/c
a, Å	7.3952(11)	10.4623(2)	12.0905(4)
b, Å	13.208(2)	11.2348(3)	14.2808(5)
c, Å	15.9357(19)	16.0039(4)	23.2861(8)
α, deg	87.017(10)	69.6510(10)	90
β, deg	87.634(11)	76.6380(10)	104.766(2)
γ, deg	80.624(9)	62.2780(10)	90
Volume (Å ³)	1532.8(4)	155.82(6)	3887.8(2)
Z	2	2	4
Calc density, g/cm ³	1.104	1.395	1.361
μ(MoKα), mm ⁻¹	0.162	0.807	0.660
Indep reflcns	5568	11436	11890
	R _(int) = 0.1377	R _(int) = 0.0277	R _(int) = 0.0590
T, K	188(2)	183(2)	183(2)
R1, wR2 (all data)	0.2338, 0.3340	0.0531, 0.1180	0.0615, 0.1154
R1, wR2 [I > 2σ(I)]	0.0921, 0.2253	0.0415, 0.1055	0.0378, 0.0962
GOF on F ²	0.946	1.088	1.103

References and Notes

1. *Stud. Surf. Sci. Catal.* **1999**, *123*, 3-28.
2. <http://www.climatetechnology.gov/library/2005/tech-options/tor2005-143.pdf>.
3. <http://www.sriconsulting.com/WP/Public/Reports/eo/>.
4. <http://www.sriconsulting.com/WP/Public/Reports/po/>.
5. Monnier, J. R., *Applied Catalysis A: General* **2001**, *221* (1-2), 73-91.
6. Matar, S.; Hatch, L., *Chemistry of Petrochemical Processes*. 2nd ed.; Gulf Publishing Company: 2001.
7. Linic, S.; Barteau, M. A., *J. Am. Chem. Soc.* **2003**, *125* (14), 4034-4035.
8. Linic, S.; Barteau, M. A., *J. Catal.* **2003**, *214* (2), 200-212.
9. Linic, S.; Barteau, M. A., *J. Am. Chem. Soc.* **2004**, *126* (26), 8086-8087.
10. Linic, S.; Jankowiak, J.; Barteau, M. A., *J. Catal.* **2004**, *224* (2), 489-493.
11. Linic, S.; Piao, H.; Adib, K.; Barteau, M. A., *Angew Chem Int Ed Engl* **2004**, *43* (22), 2918-2921.
12. van Santen, R. A.; de Groot, C. P. M., *J. Catal.* **1986**, *98* (2), 530-539.
13. Sachtler, W. M. H.; Backx, C.; van Santen, R. A., *Cat. Rev. - Sci. Eng.* **1981**, *23* (1 & 2), 127-149.
14. Osugi, J.; Kubota, H., *The Review of Physical Chemistry of Japan* **1964**, *34* (1), 19-29.
15. Beran, S.; Jiru, P.; Wichterlova, B.; Zahrandik, R., *React. Kinet. Catal. Lett.* **1976**, *5* (2), 131-134.

16. Oyama, S. T., *Mechanisms in Homogeneous and Heterogeneous Epoxidation Catalysts*. Elsevier: 2008.
17. Yamamoto, J.; Tsuji, J., *Stud. Surf. Sci. Catal.* **2007**, *172*, 553-554.
18. Bennett, M. A.; Robertson, G. B.; Rokicki, A.; Wickramasinghe, W. A., *J. Am. Chem. Soc.* **1988**, *110* (21), 7098-7105.
19. Campora, J.; Palma, P.; del Rio, D.; Alvarez, E., *Organometallics* **2004**, *23* (8), 1652-1655.
20. Catellani, M.; Halpern, J., *Inorg. Chem.* **1980**, *19* (2), 566-568.
21. Gibson, D. H., *Coord. Chem. Rev.* **1999**, *185-186*, 335-355.
22. Thompson, J. S.; Randall, S. L.; Atwood, J. D., *Organometallics* **1991**, *10* (11), 3906-3910.
23. Blum, O.; Milstein, D., *J. Am. Chem. Soc.* **1995**, *117* (16), 4582-4594.
24. Yoshida, T.; Matsuda, T.; Okano, T.; Kitani, T.; Otsuka, S., *J. Am. Chem. Soc.* **1979**, *101* (8), 2027-2038.
25. Yoshida, T.; Okano, T.; Saito, K.; Otsuka, S., *Inorg. Chim. Acta* **1980**, *44*, L135-L136.
26. Fulmer, G. R.; Muller, R. P.; Kemp, R. A.; Goldberg, K., I., *J. Am. Chem. Soc.* **2009**, *131* (4), 1346-1347.
27. Jorgensen, K. A., *Chem. Rev.* **1989**, *89* (3), 431-458.
28. Moulton, C. J.; Shaw, B. L., *J. Chem. Soc., Dalton Trans.* **1976**, (11), 1020-4.
29. van Koten, G.; Timmer, K.; Noltes, J. G.; Spek, A. L., *J. Chem. Soc., Chem. Commun.* **1978**, (6), 250-252.

30. van Koten, G.; Jastrzebski, J. T. B. H.; Noltes, J. G.; Spek, A. L.; Schoone, J. C., *J. Organomet. Chem.* **1978**, *148* (3), 233-245.
31. Creaser, C. S.; Kaska, W. C., *Inorg. Chim. Acta* **1978**, *30*, L325-L326.
32. Crabtree, R. H., *The Organometallic Chemistry of the Transition Metals*. Third ed.; John Wiley & Sons: 2001.
33. Meijere, A. d.; Meyer, F. E., *Angew Chem Int Ed Engl* **1995**, *33* (23-24), 2379-2411.
34. Beletskaya, I. P.; Cheprakov, A. V., *Chem. Rev.* **2000**, *100* (8), 3009-3066.
35. Heck, R. F., *Organic Reactions* **1982**, *27*, 345-390.
36. Grushin, V. V.; Alper, H., *Chem. Rev.* **1994**, *95* (4), 1047-1062.
37. Cabri, W.; Candiani, I., *Acc Chem Res* **1995**, *28* (1), 2-7.
38. http://nobelprize.org/nobel_prizes/chemistry/laureates/2010/.
39. Kurti, L.; Czaki, B., *Strategic Applications of Named Reactions in Organic Synthesis*. Elsevier: 2005.
40. Ohff, M.; Ohff, A.; van der Boom, M. E.; Milstein, D., *J. Am. Chem. Soc.* **1997**, *119* (48), 11687-11688.
41. Beller, M.; Zapf, A., *Synlett* **1998**, *7*, 792-793.
42. Morales-Morales, D.; Redon, R.; Yung, C.; Jensen, C. M., *Chem. Commun.* **2000**, (17), 1619-1620.
43. Morales-Morales, D.; Grause, C.; Kasaoka, K.; Redon, R.; Cramer, R. E.; Jensen, C. M., *Inorg. Chim. Acta* **2000**, *300-302*, 958-963.

44. Miyazaki, F.; Yamaguchi, K.; Shibasaki, M., *Tetrahedron Lett.* **1999**, *40* (41), 7379-7383.
45. Bergbreiter, D. E.; Osburn, P. L.; Liu, Y.-S., *J. Am. Chem. Soc.* **1999**, *121* (41), 9531-9538.
46. Fan, L.; Foxman, B. M.; Ozerov, O. V., *Organometallics* **2004**, *23* (3), 326-328.
47. Liang, L.-C.; Huang, M.-H., *Organometallics* **2004**, *23* (11), 2813-2816.
48. Suzuki, A., *Pure Appl. Chem.* **1991**, *63* (3), 419-422.
49. Miyaura, N.; Suzuki, A., *Chem. Rev.* **1995**, *95* (7), 2457-2483.
50. Suzuki, A., *J. Organomet. Chem.* **1999**, *576* (1-2), 147-168.
51. Singleton, J. T., *Tetrahedron* **2003**, *59* (11), 1837-1857.
52. Bedford, R. B.; Draper, S. M.; Noelle Scully, P.; Welch, S. L., *New J. Chem.* **2000**, *24* (10), 745-747.
53. Zim, D.; Gruber, A. S.; Ebeling, G.; Dupont, J.; Monteiro, A. L., *Org. Lett.* **2000**, *2* (18), 2881-2884.
54. Dani, P.; Karlen, T.; Gossage, R. A.; Gladiali, S.; van Koten, G., *Angew Chem Int Ed Engl* **2000**, *39* (4), 743-745.
55. Dani, P.; Albrecht, M.; van Klink, G. P. M.; van Koten, G., *Organometallics* **2000**, *19* (22), 4468-4476.
56. Albrecht, M.; Kocks, B. M.; Spek, A. L.; van Koten, G., *J. Organomet. Chem.* **2001**, *624* (1-2), 271-286.
57. Crabtree, R. H.; Mihelcic, J. M.; Quirk, J. M., *J. Am. Chem. Soc.* **1979**, *101* (26), 7738-7740.

58. Crabtree, R. H.; Parnell, C. P.; Uriarte, R. J., *Organometallics* **1987**, 6 (4), 696-699.
59. Gupta, M.; Hagen, C.; Flesher, R. J.; Kaska, W. C.; Jensen, C. M., *Chem. Commun.* **1996**, (17), 2083-2084.
60. Wang, K.; Goldman, M. E.; Emge, T. J.; Goldman, A. S., *J. Organomet. Chem.* **1996**, 518 (1-2), 55-68.
61. Leitner, W.; Six, C., *Eur. J. Inorg. Chem.* **1997**, 130 (5), 555-558.
62. Lee, D. W.; Kaska, W. C.; Jensen, C. M., *Organometallics* **1998**, 17 (1), 1-3.
63. Gupta, M.; Hagen, C.; Kaska, W. C.; Cramer, R. E.; Jensen, C. M., *J. Am. Chem. Soc.* **1997**, 119 (4), 840-841.
64. Gupta, M.; Kaska, W. C.; Jensen, C. M., *Chem. Commun.* **1997**, (5), 461-462.
65. Gomez-Benitez, V.; Redon, R.; Morales-Morales, D., *Revista de la Sociedad Quimica de Mexico* **2003**, 47 (2), 124-126.
66. Albrecht, M.; van Koten, G., *Angew. Chem. Int. Ed.* **2001**, 40, 3750-3781.
67. Liu, F.; Pak, E. B.; Singh, B.; Jensen, C. M.; Goldman, A. S., *J. Am. Chem. Soc.* **1999**, 121 (16), 4086-4087.
68. Xu, W.-W.; Rosini, G. P.; Jespersen, K. K.; Goldman, A. S.; Gupta, M.; Jensen, C. M.; Kaska, W. C., *Chem. Commun.* **1997**, (23), 2273-2274.
69. Liu, F.; Goldman, A. S., *Chem. Commun.* **1999**, (7), 655-656.
70. Jensen, C. M., *Chem. Commun.* **1999**, (24), 2443-2449.

71. Haenel, M. W.; Oevers, S.; Angermund, K.; Kaska, W. C.; Fan, H.-J.; Hall, M. B., *Angew Chem Int Ed Engl* **2001**, *40* (19), 3596-3600.
72. Takaya, H.; Mashima, K.; Koyano, K.; Yagi, M.; Kumobayashi, H.; Taketomi, T.; Akutagawa, S., *J. Org. Chem.* **1986**, *51* (5), 629-635.
73. Burk, M. J., *J. Am. Chem. Soc.* **1991**, *113*, 8518-8519.
74. Longmire, J. M.; Zhang, X., *Tetrahedron Lett.* **1997**, *38* (10), 1725-1728.
75. van der Boom, M. E.; Milstein, D., *Chem. Rev.* **2003**, *103* (5), 1759-1792.
76. Hermann, D.; Gandelman, M.; Rozenberg, H.; Shimon, L. J. W.; Milstein, D., *Organometallics* **2002**, *21* (5), 812-818.
77. Katayama, H.; Wada, C.; Taniguchi, K.; Ozawa, F., *Organometallics* **2002**, *21* (15), 3285-3291.
78. Ziesel, R., *Tetrahedron Lett.* **1989**, *30* (4), 463-6.
79. Leung, W.-P.; Ip, Q. W.-Y.; Wong, S.-Y.; Mak, T. C. W., *Organometallics* **2003**, *22* (22), 4604-4609.
80. van de Kuil, L. A.; Luitjes, H.; Grove, D. M.; Zwikker, J. W.; van der Linden, J. G. M.; Roelofsen, A. M.; Jenneskens, L. W.; Drenth, W.; van Koten, G., *Organometallics* **1994**, *13* (2), 468-477.
81. Grove, D. M.; van Koten, G.; Ubbels, H. J. C.; R., Z.; Spek, A. L., *Organometallics* **1984**, *3* (7), 1003-1009.
82. van Beek, J. A. M.; van Koten, G.; Ramp, M. J.; Coenjaarts, N. C.; Grove, D. M.; Goubitz, K.; Zoutberg, M. C.; Stam, C. H.; Smeets, W. J. J.; Spek, A. L., *Inorg. Chem.* **1991**, *30* (15), 3059-3068.

83. Albrecht, M.; Dani, P.; Lutz, M.; Spek, A. L.; van Koten, G., *J. Am. Chem. Soc.* **2000**, *122* (48), 11822-11833.
84. Feller, M.; Ben-Ari, E.; Gupta, T.; Shimon, L. J. W.; Leitus, G.; Diskin-Posner, Y.; Weiner, L.; Milstein, D., *Inorg. Chem.* **2007**, *46* (25), 10479-10490.
85. Denney, M. C.; Smythe, N. A.; Cetto, K. L.; Kemp, R. A.; Goldberg, K. I., *J. Am. Chem. Soc.* **2006**, *128* (8), 2508-2509.
86. Marder, T. B.; Lin, Z., *Contemporary Metal Boron Chemistry I: Borylenes, Boryls, Borane o-Complexes, and Borohydrides*. Springer: 2008; Vol. 130.
87. Boro, B. J.; Duesler, E. N.; Goldberg, K. I.; Kemp, R. A., *Inorg. Chem.* **2009**, *48* (12), 5081-5087.
88. Hanson, S. K.; Heinekey, D. M.; Goldberg Karen, I., *Organometallics* **2008**, *27* (7), 1454-1463.
89. Strukul, G., *Catalytic Oxidations with Hydrogen Peroxide as Oxidant*. Kluwer Academic Publishers: 1992.
90. Bayston, J. H.; Winfield, M. E., *J. Catal.* **1964**, *3* (2), 123-128.
91. Thyagarajan, S.; Incarvito, C. D.; Rheingold, A. L.; Theopold, K. H., *Chem. Commun.* **2001**, (21), 2198-2199.
92. Johnston, L. E.; Page, J. A., *Can. J. Chem.* **1969**, *47* (22), 4241-4246.
93. Endicott, J. F.; Wong, C.-L.; Inoue, T.; Natarajan, P., *Inorg. Chem.* **1979**, *18* (2), 450-454.
94. Gillard, R. D.; Heaton, B. T.; Vaughn, D. H., *J. Chem. Soc. A* **1970**, 3126-3130.

95. Roberts, H. L.; Symes, W. R., *J. Chem. Soc. A* **1968**, 1450-1453.
96. Atlay, M. T.; Preece, M.; Strukul, G.; James, B. R., *Can. J. Chem.* **1983**, *61* (6), 1332-1338.
97. Wenzel, T. T., *Stud. Surf. Sci. Catal.* **1991**, *66*, 545-554.
98. Wick, D. D.; Goldberg Karen, I., *J. Am. Chem. Soc.* **1999**, *121* (50), 11900-11901.
99. Konnick, M. M.; Gandhi, B. A.; Guzei, I. A.; Stahl, S. S., *Angew Chem Int Ed Engl* **2006**, *45* (18), 2904-2907.
100. van der Ent, A.; Onderdelinden, A. L., *Inorganic Syntheses*. 1990.
101. Diamond; Crystal Impact GbR: Bonn, Germany, 1999.
102. Bruker APEX2; Bruker AXS, I. Madison, WI, 2007.
103. Sheldrick, G. M., *Acta Crystallographica Section A: Foundations of Crystallography* **2008**, *A64*, 112.
104. Fryzuk, M. D.; Haddad, T. S.; Rettig, S. J., *Organometallics* **1992**, *11* (9), 2967-9.
105. Fryzuk, M. D.; Leznoff, D. B.; Rettig, S. J.; Thompson, R. C., *Inorg. Chem.* **1994**, *33* (24), 5528-34.
106. Fryzuk, M. D.; Giesbrecht, G.; Rettig, S. J., *Organometallics* **1996**, *15* (15), 3329-3336.
107. Fryzuk, M. D.; Giesbrecht, G. R.; Olovsson, G.; Rettig, S. J., *Organometallics* **1996**, *15* (22), 4832-4841.
108. Fryzuk, M. D.; Mylvaganam, M.; Zaworotko, M. J.; MacGillivray, L. R., *Organometallics* **1996**, *15* (4), 1134-8.

109. Fryzuk, M. D.; Giesbrecht, G. R.; Rettig, S. J., *Organometallics* **1997**, *16* (4), 725-736.
110. Fryzuk, M. D.; Leznoff, D. B.; Ma, E. S. F.; Rettig, S. J.; Young, V. G., Jr., *Organometallics* **1998**, *17* (11), 2313-2323.
111. Fryzuk, M. D.; Leznoff, D. B.; Thompson, R. C.; Rettig, S. J., *J. Am. Chem. Soc.* **1998**, *120* (39), 10126-10135.
112. Winter, A. M.; Eichele, K.; Mack, H.-G.; Potuznik, S.; Mayer, H. A.; Kaska, W. C., *J. Organomet. Chem.* **2003**, *682* (1-2), 149-154.
113. Liang, L.-C.; Lin, J.-M.; Hung, C.-H., *Organometallics* **2003**, *22* (15), 3007-3009.
114. Ozerov, O. V.; Gerard, H. F.; Watson, L. A.; Huffman, J. C.; Caulton, K. G., *Inorg. Chem.* **2002**, *41* (21), 5615-5625.
115. Fryzuk, M. D.; Haddad, T. S.; Rettig, S. J., *Organometallics* **1991**, *10* (6), 2026-36.
116. Fryzuk, M. D.; MacNeil, P. A., *J. Am. Chem. Soc.* **1984**, *106* (23), 6993-6999.
117. Fryzuk, M. D.; Carter, A.; Rettig, S. J., *Organometallics* **1992**, *11* (1), 469-72.
118. Gilman, H.; Zuech, E. A., *J. Org. Chem.* **1961**, *26*, 3481-3484.
119. Masuda, J. D.; Jantunen, K. C.; Ozerov, O. V.; Noonan, K. J. T.; Gates, D. P.; Scott, B. L.; Kiplinger, J. L., *J. Am. Chem. Soc.* **2008**, *130* (8), 2408-2409.

120. Sjovall, S.; Wendt, O. F.; Andersson, C., *J. Chem. Soc., Dalton Trans.* **2002**, 1396-1400.
121. Shaw, B. L., *Chem. Commun.* **1998**, (13), 1361-1362.
122. Shaw, B. L., *New J. Chem.* **1998**, 22 (2), 77-79.
123. Rimmi, H.; Venanzi, L. M., *J. Organomet. Chem.* **1983**, 259 (1), C6-C7.
124. Gusev, D. G.; Madott, M.; Dolgushin, F. M.; Lyssenko, K. A.; Antipin, M. Y., *Organometallics* **2000**, 19 (9), 1734-1739.
125. Haenel, M. W.; Jakubik, D.; Kruger, C.; Betz, P., *Chem. Ber.* **1991**, 124 (2), 333-336.
126. Fryzuk, M. D.; MacNeil, P. A.; Rettig, S. J.; Secco, A. S.; Trotter, J., *Organometallics* **1982**, 1 (7), 918-30.
127. Garcia-Seijo, M. I.; Habtemariam, A.; Fernandez-Anca, D.; Parsons, S.; Garcia-Fernandez, M. E., *Z. Anorg. Allg. Chem.* **2002**, 628 (5), 1075-1084.
128. Garcia-Seijo, M. I.; Habtemariam, A.; Parsons, S.; Gould, R. O.; Garcia-Fernandez, M. E., *New J. Chem.* **2002**, 26 (5), 636-644.
129. Ozerov, O. V.; Guo, C.; Fan, L.; Foxman, B. M., *Organometallics* **2004**, 23 (23), 5573-5580.
130. Liang, L.-C.; Chien, P.-S.; Lee, P.-Y., *Organometallics* **2008**, 27 (13), 3082-3093.
131. Liang, L.-C.; Chien, P.-S.; Huang, Y.-L., *J. Am. Chem. Soc.* **2006**, 128 (49), 15562-15563.
132. Nishiyama, H., *Chem. Soc. Rev.* **2007**, 36 (7), 1133-1141.

133. Motoyama, Y.; Narusawa, H.; Nishiyama, H., *Chem. Commun.* **1999**, (2), 131-132.
134. Ito, J.-i.; Ujiie, S.; Nishiyama, H., *Chem. Commun.* **2008**, (16), 1923-1925.
135. Nishiyama, H.; Ito, J.-i., *Chem. Commun.* **2010**, 46 (2), 203-212.
136. Denmark, S. E.; Stavenger, R. A.; Faucher, A.-M.; Edwards, J. P., *J. Org. Chem.* **1997**, 62 (10), 3375-3389.
137. Stol, M.; Snelders, D. J. M.; Godbole, M. D.; Havenith, R. W. A.; Haddleton, D.; Clarkson, G.; Lutz, M.; Spek, A. L.; van Klink, G. P. M.; van Koten, G., *Organometallics* **2007**, 26 (16), 3985-3994.
138. Kimura, T.; Uozumi, Y., *Organometallics* **2008**, 27 (19), 5159-5162.
139. Stark, M. A.; Richards, C. J., *Tetrahedron Lett.* **1997**, 38 (33), 5881-5884.
140. Ito, J.-i.; Ujiie, S.; Nishiyama, H., *Organometallics* **2009**, 28 (2), 630-638.
141. Hao, X.-Q.; Gong, J.-F.; Du, C.-X.; Wu, L.-Y.; Wu, Y.-J.; Song, M.-P., *Tetrahedron Lett.* **2006**, 47 (29), 5033-5036.
142. Takenaka, K.; Minakawa, M.; Uozumi, Y., *J. Am. Chem. Soc.* **2005**, (127), 12273-12281.
143. Wu, L.-Y.; Hao, X.-Q.; Xu, Y.-X.; Jia, M.-Q.; Wang, Y.-N.; Gong, J.-F.; Song, M.-P., *Organometallics* **2009**, 28 (12), 3369-3380.
144. Fossey, J. S.; Richards, C. J., *Organometallics* **2002**, 21 (24), 5259-5264.
145. Fossey, J. S.; Russell, M. L.; Malik, K. M. A.; Richards, C. J., *J. Organomet. Chem.* **2007**, 692 (22), 4843-4848.

146. van de Kuil, L. A.; Veldhuizen, Y. S. J.; Grove, D. M.; Zwikker, J. W.; Jenneskens, L. W.; Drenth, W.; Smeets, W. J. J.; Spek, A. L.; van Koten, G., *Recl. Trav. Chim. Pays-Bas* **1994**, 113 (5), 267-277.
147. Gosiewska, S.; Herreras, S. M.; Lutz, M.; Spek, A. L.; van Koten, G.; Gebbink, R. J. M. K., *Eur. J. Inorg. Chem.* **2006**, (22), 4600-4607.
148. Gosiewska, S.; Herreras, S. M.; Lutz, M.; Spek, A. L.; Havenith, R. W. A.; van Klink, G. P. M.; van Koten, G.; Gebbink, R. J. M. K., *Organometallics* **2008**, 27 (11), 2549-2559.
149. Gosiewska, S.; in't Veld, M. H.; de Pater, J. J. M.; Bruijninx, P. C. A.; Lutz, M.; Spek, A. L.; van Koten, G.; Gebbink, R. J. M. K., *Tetrahedron: Asymmetry* **2006**, 17 (4), 674-686.
150. Gorla, F.; Togni, A.; Venanzi, L. M.; Albinati, A.; Lianza, F., *Organometallics* **1994**, 13 (5), 1607-1616.
151. Gorla, F.; Venanzi, L. M.; Albinati, A., *Organometallics* **1994**, 13 (1), 43-54.
152. Longmire, J. M.; Zhang, X.; Shang, M., *Organometallics* **1998**, 17 (20), 4374-4379.
153. Kuznetsov, V. F.; Lough, A. J.; Gusev, D. G., *Inorg. Chim. Acta* **2006**, 359 (9), 2806-2811.
154. Wallner, O. A.; Olsson, V. J.; Eriksson, L.; Szabo, K. J., *Inorg. Chim. Acta* **2006**, 359 (6), 1767-1772.

155. Baber, R. A.; Bedford, R. B.; Betham, M.; Blake, M. E.; Coles, S. J.; Haddow, M. F.; Hursthouse, M. B.; Orpen, A. G.; Pilarski, L. T.; Pringle, P. G.; Wingad, R. L., *Chem. Commun.* **2006**, (37), 3880-2.
156. Aydin, J.; Kumar, K. S.; Sayah, M. J.; Wallner, O. A.; Szabo, K. J., *J. Org. Chem.* **2007**, 72 (13), 4689-4697.
157. Williams, B. S.; Dani, P.; Lutz, M.; Spek, A. L.; van Koten, G., *Helv. Chim. Acta* **2001**, 84 (11), 3519-3530.
158. Morales-Morales, D.; Cramer, R. E.; Jensen, C. M., *J. Organomet. Chem.* **2002**, 654 (1-2), 44-50.
159. Medici, S.; Gagliardo, M.; Williams, B. S.; Chase, P. A.; Gladiali, S.; Lutz, M.; Spek, A. L.; van Klink, G. P. M.; van Koten, G., *Helv. Chim. Acta* **2005**, 88 (3), 694-705.
160. Han, J. S.; Wolfsberger, W., *Z. Naturforsch., B: Chem. Sci.* **1989**, 44 (4), 502-4.
161. Bornand, M.; Torker, S.; Chen, P., *Organometallics* **2007**, 26 (14), 3585-3596.
162. Fafard, C. M.; Ozerov Oleg, V., *Inorg. Chim. Acta* **2007**, 360, 286-292.
163. Deubel, D. V.; Sundermeyer, J.; Frenking, G., *Eur. J. Inorg. Chem.* **2001**, 2001 (7), 1819-1827.
164. Deubel, D. V.; Frenking, G.; Gisdakis, P.; Herrmann, W. A.; Rosch, N.; Sundermeyer, J., *Acc Chem Res* **2004**, 37 (9), 645-652.
165. Zanardo, A.; Pinna, F.; Michelin, R. A.; Strukul, G., *Inorg. Chem.* **1988**, 27 (11), 1966-1973.

166. Zanardo, A.; Michelin, R. A.; Pinna, F.; Strukul, G., *Inorg. Chem.* **1989**, *28* (9), 1648-1653.
167. Pizzo, E.; Sgarbossa, P.; Scarso, A.; Michelin, R. A.; Strukul, G., *Organometallics* **2006**, *25* (12), 3056-3062.
168. Colladon, M.; Scarso, A.; Sgarbossa, P.; Michelin, R. A.; Strukul, G., *J. Am. Chem. Soc.* **2007**, *129* (24), 7680-7689.